Epstein Barr Virus Encoded MicroRNAs Impact Proliferation and Autophagy in Transfected Cells *in vitro*

A Thesis submitted by

Nicole Castagnozzi

in partial fulfillment of the requirements for the degree of

Masters of Science

in

Immunology

Tufts University

Sackler School of Graduate Biomedical Sciences

August, 2018

Advisor: David Thorley-Lawson, PhD

Abstract

Epstein Barr Virus infects greater than 95% of the adult population and remains latent in memory B cells for the life of the host. EBV is associated with a number of cancers including Burkitt's lymphoma (BL), nasopharyngeal carcinoma (NPC), gastric carcinoma (GC), Hodgkin Lymphoma (HL) and others. Investigations into the causes of this association are necessary to improve outcomes for patients.

The EBV viral genome encodes a number of genes that are transcribed during the course on infection, including proteins and microRNAs. Each transcription program is associated with a different stage in B cell differentiation, for example Latency III during the activated lymphoblast stage, Latency II during germinal center differentiation, and Latency I/0 during memory. EBV associated cancers can be characterized based on the infection stage of the cells they arose from. For example, NPC is Latency II, while BL is Latency I. Of the EBV encoded microRNAs, a subset of BARTs are only expressed during the proliferative Latency III phase, and are also found to be expressed in EBV associated cancers that otherwise characterized as EBV Latency II or I/0 cancers. Therefore, these microRNAs are expressed during rapid proliferation and are dysregulated in tumor samples, suggesting there may be a link between tumorigenesis and expression of this subset of microRNAs due to their common expression during period of cell cycle disregulation.

Thus, I aimed to further elucidate the role of one or more BART microRNAs that are highly expressed during Latency III as well as in a number of EBV associated tumor samples. I sought to characterize the impact on host cell processes, including proliferation, growth, and survival. I was able to identify and validate a target for miR-BART10, ATP6V0e, which encodes a subunit of a V-Type ATPase that is involved in pH maintenance and autophagy. I also observed an increase in proliferation of relevant cell lines *in vitro* when transfected with miR-BART10, as well as miR-BART 14* and 18-5p.

Acknowledgements

I would like to acknowledge my parents, Dan and Eva, who have supported me even in ways they aren't aware. I have never doubted for a second that they have my back and want the best for me. They lead by example by being models of how human beings should behave and treat others, and have forged inspiring and impressive paths in their lives. I was basically born incredibly lucky with a giant leg up in life by virtue of being their child and I would certainly not be anywhere near where I am today without them. I also want to acknowledge my husband, Steve, who has been a day-in-day-out listener and therapist (though a pragmatic one!) through the ups and downs of graduate school, and before graduate school, in life. Although we're very different, I could never have hoped to find a better match. Whatever virtues I most lack (patience) he has in spades and I am a better, stronger person for being married to him. I also want to acknowledge my 4-legged family; Harley (<3), Rocket, Peanut, Dasha, Lili, and Felix (another therapist!) These animals have provided me with escape and relief from stress, and being with them has fed my soul and kept me sane.

Besides my family, I want to acknowledge Raka Basu, Danish Saleh, and Alex Histed, who were supportive friends and scientific sounding boards, as well as resources for general counsel and guidance in handling the various responsibilities and challenges graduate school presents. Friends outside of Tufts, including Carolyn Chyu, Emily Stone, Emily Cotran, Manneh Ghazarians, and my friend and sister-in-law Sarah Farnsworth have also provided great support to me. Albert Tai has been an extremely helpful resource at Tufts, and although he was not technically a committee member, I would seek

his guidance with basically anything I could not figure out myself and he either had the expertise to help me or knew who to refer me to. He never said he was too busy and would not help, and always made an effort to provide assistance even though it's not really his job. Ananda Roy was also a helpful resource for me scientifically, and his enthusiasm for both scientific inquiry as well as for helping students was obvious. Steve Kwok and Allan Parmalee were helpful resources as well for questions about flow cytometry, which I used frequently for my work. Dr. Daniel Cox in the neuroscience department helped me with statistics for the work shown here.

Table of Contents

Title Page i
Abstract ii
Acknowledgements iv
Table of Contents vi
List of Tables ix
List of Figures x
List of Copyrighted Materials xii
List of Abbreviations xiii

Chapter 1. Introduction 2
1.1. Epstein Barr Virus 3
1.1.1. History of EBV 3
1.1.2. Epidemiology of EBV and Associated Diseases 4
1.1.3. EBV Structure and Genome 6
1.1.4. EBV Life Cycle 8
1.2. MicroRNAs 12
1.2.1 MicroRNA Structure and Processing 12
1.2.2. MicroRNAs in Cancer 13
1.3. EBV encoded microRNAs 16
1.3.1. EBV MicroRNAs 16
1.3.2. Proliferation Associated miR-BARTs 19
1.3.3. EBV-MicroRNA-BART10-3p 24
1.4. V-Type ATPase 25
1.4.1. Structure of V-type ATPases 25
1.4.2. V-Type ATPases in Cancer 26
1.4.3. Intersection of V-Type ATPases with EBV 28
1.4.4. ATPases in Autophagy and Host Response to Viral Infection 28
1.5. Proliferation 29
1.5.1. EBV infected host cells are driven to proliferate and exhibit dysregulated cell cycle control mechanisms 30
1.5.2. Possible role of EBV driven proliferation in EBV associated malignancies 31
1.6. Autophagy 32
1.6.1. Role of Autophagy in the Cell 33
1.6.2. Role of Autophagy in Immunity 34
1.6.3. V-Type ATPases in Autophagy 36
1.7. Summary 37

Chapter 2. Materials and Methods 38
2.1. RNA Microarray Assay 39

2.1.1. Microarray Assay cell preparation 39
2.1.2. Microarray Analysis 39
2.2. Cell Culture and Transfection 40
2.2.1 Cell Culture 40
2.2.2. Transfection 40
2.3. PCR protocols 41
2.3.1 RNA Extraction 41
2.3.2. cDNA synthesis 42
2.3.3. MicroRNA RT-qPCR 42
2.3.4. mRNA RT-qPCR 43
2.4. pH/Acidification Assay 43
2.4.1. Bafilomycin A1 Treatment 43
2.4.2. Lysosensor Stain 43
2.5. Western Blot 44
2.5.1 Preparation of lysates 44
2.5.2. Western Blot Procedure 44
2.5.3. Antibodies 45
2.6. Luciferase Assay 45
2.6.1 Cloning 45
2.6.2. Luciferase Assay Protocol 46
2.7. Cell Proliferation 46
2.7.1 Cell proliferation assay – Cell Trace Violet 46
2.7.2. Cell proliferation assay – cell counting 47
2.8. Statistical Analysis 47

Chapter 3. Results 48
3.1. Finding a Target for EBV-miR-BART10 in vitro 49
3.2 Transfection of miR-BART 10 increases rate of proliferation in vitro 61
3.3. Transfection of other proliferation associated BARTS, including miR-BART10, increases rate of proliferation in vitro 67
3.4. Transfection of miR-BART10 increases presence of acidic vessicles, implying reduction in autophagic flux 72
3.5. Transfection of miR-BART10 increases accumulation of LCB3, a marker for autophagosomes 79
3.6. Accumulation of acidic vessicles and LCB3 is also observable in EBV infected cells compared to control cells 87
3.7. Conclusions and Future Directions 90

Chapter 4. Discussion 92
4.1. Evidence that numerous Herpes viruses may inhibit autophagy 93
4.2. Previous work shows that EBV modulates autophagy through a number of mechanisms 94
4.3. Evidence that EBV benefits from inhibition

of autophagy 95
4.4. Deregulation of Proliferation and cell death
in cancer 96
4.5. Importance of this work 97
4.6. Future Directions 100

Chapter 5. Appendix 102
5.1. Optimization of Electroporation 103
5.2. Sequences of oligos that were inserted into the
Pcheck2 Vector for the Luciferase Assay 104
5.3. PSIcheck2 Vector Sequence 104
5.4. Primer Sequences 107
5.5. Picture of transfected cells.....109

Chapter 6. Bibliography 110

List of Tables

TABLE 1.1. Malignancies associated with EBV infection 5
TABLE 1.2. Summary of EBV encoded proteins and their effects..... 7
TABLE 1.3. List of circulating microRNAs
implicated in different types of cancer 15
TABLE 3.1. Statistical analysis of change in proliferation rate
in transfected HEK293 cells 66
TABLE 3.2. Statistical analysis of change in proliferation rate
in transfected AGS cells 67

List of Figures

FIGURE 1.1. Illustration of EBV EBNA gene transcription during different latency types 9
FIGURE 1.2. Overview of EBV life cycle 11
FIGURE 1.3. Linear Representation of EBV viral genome showing genomic origin of latent EBV transcripts, including EBV noncoding RNAs 16
FIGURE 1.4. Profile of EBV BART miRNAs in vivo and in spontaneous lymphoblastoid cell lines (LCL) expressing latency III 18
FIGURE 1.5. Profile of EBV BART miRNAs in tumor samples and in GCB and MemB cells expressing Latency II and I/0, respectively 21
FIGURE 1.6. Tumors from AGS-EBNA1-BART and AGS-EBNA1-EMPTY (A) groups on day 60 and day 74 23
FIGURE 1.7. Model of V-Type H+ ATPase 26
FIGURE 1.8. Process of Autophagy 33
FIGURE 3.1. Heat map from microarray 49
FIGURE 3.2. Akata cells transfected with miR-BART10 or miR-MC show insignificant downregulation in FBXW7 mRNA expression 52
FIGURE 3.3. Akata cells transfected with miR-BART10 or miR-MC show insignificant downregulation in ATG5 mRNA expression 54
FIGURE 3.4. Akata cells transfected with miR-BART10 or miR-MC show significant downregulation in ATP6V0e mRNA expression 55
FIGURE 3.5. ATP6V0e mRNA in transfected HEK293 cells 57
FIGURE 3.6. Quantification of western blot using antibody against ATP6V1A 58
FIGURE 3.7. Luciferase assay confirms miR-BART10 direct targeting of ATP6V0e mRNA 60
FIGURE 3.8. HEK293 cells transfected with miR-BART10 proliferate more rapidly than control transfected cells 62
FIGURE 3.9. HEK293 cells transfected with siRNA-ATP6V0e proliferate more rapidly than control transfected cells 63
FIGURE 3.10. HEK293 cells transfected with miR-BART10 or siRNA-ATP6V0e proliferate more rapidly than control transfected cells 65
FIGURE 3.11. AGS cells transfected with miR-BART10 or siRNA-ATP6V0e proliferate more rapidly than control transfected cells 66
FIGURE 3.12. HEK293 cells transfected with miR-BARTs proliferate more rapidly than control transfected cells 69

FIGURE 3.13. HEK293 cells transfected with miR-BARTs proliferate more rapidly than control transfected cells except miR-BART15 71
FIGURE 3.14. Acidic vessicles/lysosomes accumulate in HEK293 cells treated with Bafilomycin A1, or transfected with miR-BART10 or siRNA-ATP6V0e 75-76
FIGURE 3.15. Acidic vessicles/lysosomes accumulate in AGS cells treated with Bafilomycin A1, or transfected with miR-BART10 or siRNA-ATP6V0e 77-78
FIGURE 3.16. HEK293 cells transfected with miR-BART10 or siRNA against ATP6V0e accumulate LCB3 81
FIGURE 3.17. AGS cells transfected with miR-BART10 or siRNA against ATP6V0e accumulate LCB3 82
FIGURE 3.18. HEK293 cells transfected with miR-BART10 or siRNA against ATP6V0e accumulate LCB3 83
FIGURE 3.19. HEK293 cells transfected with miR-BART10 or siRNA against ATP6V0e accumulate LCB3 84
FIGURE 3.20. AGS cells transfected with miR-BART10 or siRNA against ATP6V0e accumulate LCB3 85
FIGURE 3.21. AGS cells transfected with miR-BART10 or siRNA against ATP6V0e accumulate LCB3 86
FIGURE 3.22. AGS.BX1 cells (infected with EBV) accumulate lysosomes and autophagosomes compared to uninfected counterpart (AGS cells) 89
FIGURE 4.1. Brief Schematic illustrating the main findings of this project 99
FIGURE 5.1 Flow Cytometry Plots 103
FIGURE 5.2. Sequences of oligos that were inserted into the Pcheck2 Vector for the Luciferase Assay 104
FIGURE 5.3. PSIcheck2 Vector Sequence 104
FIGURE 5.4. Primer Sequences 107
FIGURE 5.5. Picture of transfected cells 109

List of Copyrighted Material

Permissions available in Supplementary Files Section

Forgac M. Vacuolar ATPases: rotary proton pumps in physiology and pathophysiology. 2007.Nat Rev Mol Cell Biol. 8: 917-92. 26

Nakahira K, Choi AM. Autophagy: a potential therapeutic target in lung diseases. Am J Physiol Lung Cell Mol Physiol. 2013;305(2):L93-107..... 34

Paulson EJ, Speck SH. Differential methylation of Epstein-Barr virus latency promoters facilitates viral persistence in healthy seropositive individuals. J Virol. 1999;73(12):9959-68..... 9

Qiu, J., 2014, 'Epstein-Barr Virus microRNA Expression and Function in Persistent Infection and Oncogenesis', Doctor of Philosophy, Tufts University Sackler School of Graduate Biomedical Sciences, Boston, Massachusetts..... 11

Qiu J, Cosmopoulos K, Pegtel M, et al. A novel persistence associated EBV miRNA expression profile is disrupted in neoplasia. PLoS Pathog. 2011;7(8):e1002193..... 8, 21

Skalsky RL, Cullen BR. EBV Noncoding RNAs. Curr Top Microbiol Immunol. 2015;391:181-217..... 16

List of Abbreviations

AIDS	auto-immune deficiency syndrome
APC	Antigen presenting cell
BART	BamHI-A rightward transcripts
BC	breast cancer
Bcl-2	B-cell lymphoma protein 2
BHRF1	BamHI right forward 1
BL	Burkitt's lymphoma
bp	base pair
CD-21	Cluster of differentiation 21
CRC	colorectal cancer
CRC	colorectal cancer
CTL	cytotoxic T lymphocyte
DC	Dendritic cell
DC	dendritic cell
DLBCL	diffuse large B cell lymphoma
DLBCL	diffuse large B cell lymphoma
DMEM	Dulbecco's modified Eagle's medium
DNA	deoxyribonucleic acid
eBL	endemic Burkitt's lymphoma
EBNA	Epstein Barr virus nuclear antigen
EBV	Epstein Barr virus
FACS	fluorescence-activated cell sorter
FBS	fetal bovine serum
GAPDH	glyceraldehyde-3-phosphate dehydrogenase
GC	gastric carcinoma
GC	germinal centre
GCB	germinal center B
GFP	green flourescent protein
Gp	glycoprotein
HD	Hodgkin's disease
HEK 293	cell Human embryonic kidney 293 cell
HHV-4	human herpes virus 4
HLA-DR	Human Leukocyte Antigen - antigen D Related
IFN	Interferon
Ig	immunoglobulin
IL	interleukin
JNK	Jun amino terminal kinase
LCL	lymphoblastoid cell line
LCL	lymphoblastoid cell line
LMP	latent membrane protein 1
MAPK	mitogen activated protein kinases
miRNA	micro-ribonucleic acid

miRNA	microRNA
ml	milliliter
mM	millimolar
NF-kB	nuclear factor kappa-light-chain-enhancer of activated B cells
NSCLC	non small cell lung cancer
NSCLC	non-small cell lung cancer
PAMP	pathogen associated molecular pattern
PBL	plasmablastic lymphoma
PBS	phosphate buffer saline
pDC	plasmacytoid dendritic cell
PL	promyelocytic luekemia
pmol	picomolar
PTLD	post transplant lymphoploliferative disorder
PTLD	post-transplant lymphoproliferative disorder
RISC	RNA induced silencing complex
RISC	RNA induced silencing complex
RNA	ribonucleic acid
RNA	ribonucleic acid
RT-PCR	reverse transcribed polymerase chain reaction
RT-qPCR	quantitative real time polymerase chain reaction
siRNA	small interfering ribonucleic acid
T-ALL	T-cell acute lymphoblastic luekemia
TNF-a	tumor necrosis factor –alpha
WB	Western Blot

Epstein Barr Virus Encoded MicroRNAs Impact Proliferation and Autophagy in Transfected Cells *in vitro*

Chapter 1. Introduction

1.1 Epstein Barr Virus

1.1.1. History of EBV

Epstein Barr Virus is named for Anthony Epstein and Yvonne Barr, two scientists who together with Burt Achong published an article in the journal the Lancet in 1964 identifying the first human herpesvirus that they believed could cause cancer (Epstein, Achong, Barr, 1964). Anthony Epstein began studying the virus after listening to a lecture by a Doctor, Denis Burkitt, on March 22, 1961. Dr. Burkitt was describing a particular type of cancer prevalent in rainy and temperate regions in Africa in children. Dr. Burkitt believed the cancer, now known as Burkitt Lymphoma, was caused by a virus carried by insects, due to it's geographical distribution overlapping with another insect borne disease, malaria. Epstein began studying tumor samples supplied to him by Dr. Burkitt, and after a few years he and his colleage Yvonne Barr were finally able to find evidence of virus particles in the tumor cells using an electron microscope. After the virus was discovered, it took many more years to confirm Burkitt's hypothesis that a virus, which turned out to be EBV, was the cause of the childhood Burkitt Lymphoma he observed in Africa (called endemic Burkitt Lymphoma, or eBL). Initially the studies were epidemiological in nature, observing tens of thousands of children and noting that those who developed eBL had high EBV titers long before the cancer developed, and later, when the chromosomal translocation that characterizes BL was discovered, a mechanism involving EBV was able to be investigated and described. This led to more investigations into the role of EBV in development other cancers, and we now know that EBV plays a

role in a number of human cancers. The impact of these diseases on human health is significant, and therefore efforts to understand the effects of EBV on infected cells, and how these effects may impact malignant transformation, is of great interest and importance to the medical and scientific communities.

1.1.2. Epidemiology of EBV and Associated Diseases

The oncogenic Epstein Barr Virus infects over 95% of the adult population although is asymptomatic in many individuals. EBV remains latent in memory B cells for the life of the host (Donati et al, 2006), although infection can result in infectious mononucleosis in adolescents. As discussed above EBV is associated with a number of cancers including Burkitt's lymphoma (Neri et al, 1991), nasopharyngeal carcinoma (Andersson-anvret et al, 1977), Hodgkin Lymphoma (Mernard et al, 2008), Post-transplant Lymphoproliferative Disorder (Capello et al, 2006) and several others. Infection with EBV causes rapid proliferation of host B cells, which causes replication of the genome as a normal part of cell division (Kilger E., et al, 1998; Mosialos G., et al, 1995). At the same time, EBV encoded proteins reduce genome stability (Gruhne B., et al, 2009), resulting in an increase in genetic mutations and dysregulation of the systems that normally repair those mistakes. Logically, these effects of infection promote the development of cancer.

EBV-associated cancers can be categorized according to the cell type/latency they arise from. Type I latency is observed in Burkett's lymphoma and gastric carcinoma (GC). Type II latency occurs in the course of Hodgkins lymphoma (HL) and nasopharyngeal

carcinoma (NPC). In EBV associated cancers arising in an immunocompromised state, such as PTLD and AIDS-related lymphomas, the virus expresses the Latency III transcription profile. These categorizations are summarized in introductory table 1.

Malignancy	**Latency Type**
Burkitt's Lymphoma, blasmaplastic lymphoma, primary effusion lymphoma, gastric carcinoma	I
Classic Hodgkin's lymphoma, post transplant lymphproliferative disorder (subset), lymphomatoid granulomatosis (subset), nasopharyngeal carcinoma	II
PTLD-like Lymphoma (subset), Infectious mononucleosis	III

TABLE 1.1. **Malignancies associated with EBV infection.** Data for percentage of tumors that are EBV positive is a range because percentage varies with geographic location (OK and Young, 2015; Price and Luftig, 2014).

In addition to the above mentioned diseseases, EBV is the causative agent of infectious mononucleosis (IM). IM is a clinical syndrome in which the symptoms are a manifestation of the innate immune system response to primary EBV infection, usually in adolescence (Luzuiaga et al, 2000).

1.1.3. EBV Structure and Genome

EBV is a gamma retrovirus also classified as human herpes virus 4 (HHV-4). It's genome is a circular double stranded DNA molecule 172 Kbp in length (Rickensen AB et al, 2007), encoding about 100 viral proteins (Given D, et al) which is covered by a protective glycoprotein-rich envelope when it is outside of the host cell. The glycoproteins on the surface of the envelope, particularly gp350/220, allow the virus to bind the surface of host cells by interacting with CD21 (Figeroth J., et al, 1984) or CD35 (Ogembo J., et al, 2013). Other glycoproteins including gp42, gH, gL and gB, also assist in allowing the virus to enter host cells by fusing to complementary proteins on the surface of target cells (Chen J., et al, 2016). Most importantly, gp 42 binds HLA-DR on B lymphocytes (Li, et al, 1997). The viral envelope fuses to the membrane of the host cell, dumping the viral contents inside. During different stages of infection, EBV expresses subsets of genes encoded in its genome, including but not limited to proteins and microRNAs, under different promoters (Kieff E et al, 2007). The effects of some virally encoded proteins during infection have already been characterized. For example, LMP-1, a virally encoded protein that is expressed on the surface of infected B cells during Latency types II and III, mimics the activity of CD40 (Uchida et al., 1999; Cahir-McFarland, 2004) while LMP-2 mimics a constitutively active BCR (Mancao et al, 2007). These signals together induce proliferation of the infected cells (Cesarman, et al., 2011; Gires, et al., 1997). Furthermore, LMP-1 promotes cell survival by activating anti-apoptotic and pro-proliferation pathways JNK, p38, AP-1 and NF-κB pathways (Soni et al, 2007;). EBNA-1 is expressed during all viral life stages and is crucial for maintaining

viral episomal maintenance and replication, and has been shown to induce genome instability (Gruhne B., et al, 2009). EBNA-2 deregulates c-myc, an important oncogene that promotes proliferation (Saridakis V., et al, 2005). BZLF1 down-regulates pro-inflammatory TNF-α by binding its promoter and preventing NF-κB activation (Li, et al, 2015). These and other functions of EBV encoded proteins are summarized in introductory table 2. Through expression of it's own virally encoded proteins, EBV is able to manipulate host cell processes to promote its own survival and drive infected B cells to become activated and differentiate.

EBV Encoded Protein	**Cellular Effect**
LMP-1	Mimics CD-40 Activates JNK, p38, AP-1 and NF-κB
LMP-2	Mimics low-level constitutive BCR
EBNA-1	Ensures viral persistence during Latency Destabilizes host genome
EBNA-2	Deregulates c-myc
BZLF1	Down-regulates TNF-α

TABLE 1.2. **Summary of EBV encoded proteins and their effects**. As mentioned in the text.

1.1.4. EBV Life Cycle

EBV is transmitted via saliva containing virions, which enter through the epithelium of the Waldeyers ring (circular arrangement of tonsils) in the back of the mouth. It is believed that the epithelial cells of the oral cavity serve as replication sites for the virus, which then leaves the cells to return to the saliva to be transmitted to another host (Lemon et al, 1977 and 1978). The shed visions can also infect nearby resting B cells. Infection of a naive B cell with EBV drives the infected cell to become a rapidly proliferating activated lympoblastoid cell (Babcock et al, 1998; Joseph et al, 2000), through expression of nine EBV encoded proteins, including six EBV nuclear antigens (EBNAs 1-6) and three latent membrane proteins (LMPs 1-3), as well as the viral non-coding RNAs (EBERs and miRNAs) under the transcription factor EBNA-2 (Price and Luftig, 2014). Inside the host cell, EBV's life cycle is characterized by different transcription programs (expression profiles of microRNAs and proteins under different promoters), which control the viral expression profile during different stages of the host cell's differentiation (Sixby et al, 1984). During the lymphoblastoid stage, EBV's gene expression profile referred to as immortalizing or type III Latency. (Rickenson, et al, 1996; Paulson and Speck, 1999). The transcription of EBV genes is driven by the Wp and/or Cp promoters during the type III Latency phase of EBV infection (Figure 1; Paulson and Speck, 1999). The infected lymphoblastoid cell migrates to the germinal center through the normal mechanisms, where it differentiates as any other lymphoblastoid cell would into a germinal center B cell. At this stage the virus' genetic expression is controlled by the more restricted Latency II program, and the genes

expressed include proteins EBNA1, LMP1 and LMP2, as well as the EBERs and BARTs RNAs. Transcription in this phase is driven by the Qp promoter (Price and Luftig, 2014; Paulson and Speck, 1999). A linear representation of the EBV viral genome with locations of the promoters is shown in introductory figure 1.

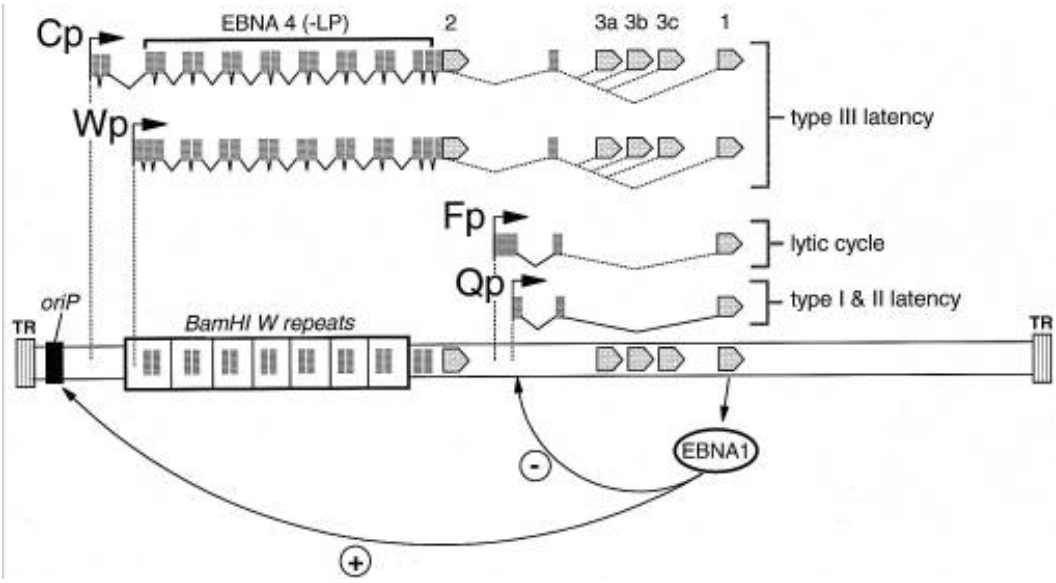

FIGURE 1.1. **Illustration of EBV EBNA gene transcription during different latency types**. Linear representation of the EBV genome showing promoters active during immortalizing (Latency III) and restricted (Latency II/I) transcription programs. Reprinted with permission from Paulson EJ, Speck SH. Differential methylation of Epstein-Barr virus latency promoters facilitates viral persistence in healthy seropositive individuals. J Virol. 1999;73(12):9959-68.

When the infected B cell differentiates into a memory cell and leaves the germinal center, the virus expresses no proteins and is immunologically silent. The viral protein EBNA-1 is expressed during S phase in memory B cells (Latency I), and plays a crucial role in EBV persistence by ensuring it's genome is replicated along with the host genome and that a copy ends up in each daughter cell. If the EBV infected cell terminally

differentiates into a plasma cell, the virus reactivates its lytic cycle genes, under the Fp promoter, results in expression of immediate early transcription factors Zta and Rta, and immediate early transactivation factors BZLF1 and BRLF1 (Li et al., 2015). BZLF1 is a viral homologue of the cellular c-jun and c-fos transcription factor that can interact with AP-l-like sequences in both the viral and host genome (Adamson et al, 2005). The lytic program results in an "expression cascade" of genes that allow EBV to produce progeny which can exit the cell (Sun et al, 2007; Shimizu and Takada, 1993). The lytic stage of infection is distinct from latency and a stimulus is required to reactivate the lytic gene expression. During the lytic stage of infection, EBV expresses all of its proteins and may infect epithelial cells of the pharynx as well as B cells. This is in contrast to the Latency stage, during which EBV is found only in B cells (Babcock et al, 1998; Miyashita et al, 1997). A diagram of the life cycle of EBV is shown in introductory figure 2.

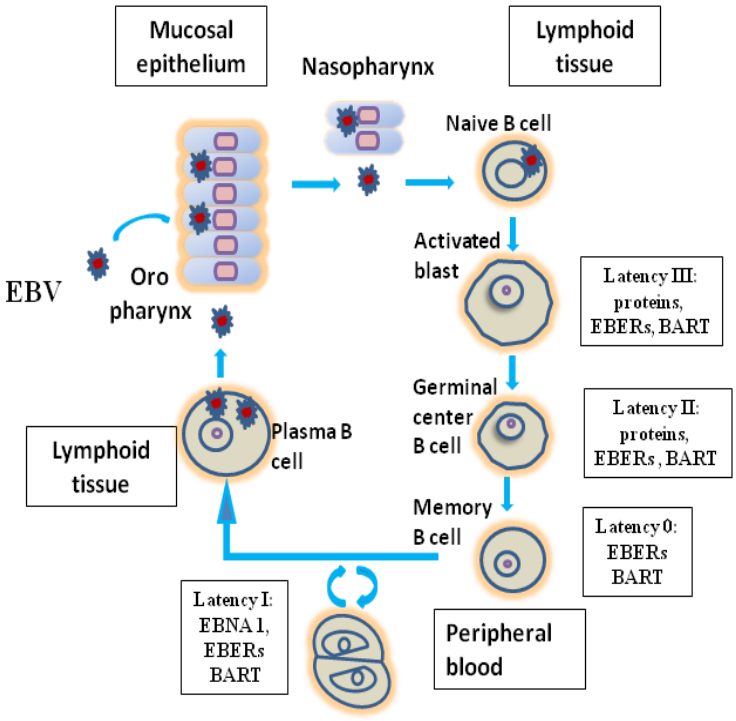

FIGURE 1.2. **Overview of EBV life cycle**. Primary infection occurs in epithelial cells of the nasopharyngeal mucosa. Viruses replicate and are released from EBV-infected epithelial cells, thus spreading the virus to other host cells. The virus can also be transmitted from host to host via saliva. Soon after primary infection, EBV-infected infiltrating B-cells will migrate back into circulation in the mucosal lymphoid tissues, express the Latency III program and proliferate. Subsequently these cells migrate to a germinal center (GC), where they express the Latency II program and LMP1 and LMP2 expression is observed. The cells undergo a GC reaction and leave the GC, generating resting memory B cells with the Latency 0 pattern of viral gene expression. EBV-infected plasma cells arising from the GC reaction can replicate EBV near the epithelium in the mucosa and provide a source of infectious virions for other B-cells or epithelial cells. EBV- specific T cells will respond and control the proliferation of EBV-infected B-cells, but not infected memory B-cells since they lack immunogenic EBV antigens. Reprinted with permission from Qiu, J., 2014, Epstein-Barr Virus microRNA Expression and Function in Persistent Infection and Oncogenesis, Doctor of Philosophy, Tufts University Sackler School of Graduate Biomedical Sciences, Boston, Massachusetts.

1.2 MicroRNAs

Investigations have begun into the function of a few of the EBV encoded microRNAs, but more work remains to be done to more fully understand how they may also be contributing to the transformation of infected cells.

1.2.1 MicroRNA Structure and Processing

MicroRNAs are a class of small, non-coding RNA sequences about 22 nucleotides in length when mature, although they are generally processed from a larger precursor RNA with multiple stem-loop structures (Bartel, 2004). MicroRNA genes are conserved through evolution and are found in mammals, fish, worms and flies (Lagos-Quintana et al, 2002, 2003; Mourelatos et al., 2002, Aravin et al., 2003, Houbaviy et al., 2003). Pri-miRNAs are transcribed by polymerase II or III and processed by the Drosha endonuclease II and DGCR2 complex (Lee Y, et al., 2003), resulting in a single stem-loop intermediate called the pre-miRNA. The pre-miRNA is then transported from the nucleus to the cytoplasm by Ran-GTP and the nuclear exporter Exportin 5 (Yi et al., 2003; Lund et al., 2005). In the cytoplasm, Dicer further processes the pre-miRNA (Lee et al., 2003). This double stranded species eventually becomes incorporated as a single stranded miRNA (after losing one strand, which is degraded, usually the miRNA* sequence) into a microRNA ribonucleoprotein complex, which is similar to the RNA-

induced Silencing Complex (RISC) that contains siRNAs except that it contains different proteins, such as eIF2C2 and Gemin-3 (Mourelatos, 2002; Hammond et al., 2000). Target mRNA have complementary sequences in their 3' UTRs to the miRNA, and are bound by the miRNA containing RISC. Bound mRNA expression is repressed through one of two mechanisms; cleavage (degradation) or repression of transcription or translation (Hutvagner and Zamore, 2002). Some microRNAs are stable and can be detected in circulating bodily fluids. These microRNAs are termed "circulating microRNAs". Interestingly, circulating microRNAs can exist even in the presence of RNAse enzymes in the serum and saliva, either inside of vesicles or out of them (Mitchell et al., 2008; Sourvinou et al., 2013). Circulating microRNAs can establish communication between cells and impact gene expression of target cells.

1.2.2. MicroRNAs in Cancer

MicroRNAs have previously been implicated in many cancer types including breast and colorectal (Bahrami A., et al, 2017; Moridikia A., et al, 2017), and luekemia (Fernandes Q, 2016). Circulating microRNAs as biomarkers for disease is an area of research that has garnered a lot of attention. Recent work measuring concentrations of circulating microRNAs as a potential method for cancer diagnosis, staging, and treatment prognostication have shown a lot of promise. For diffuse large B cell lymphoma (DLBCL), miR-155, miR-21, and miR-210 have differential expression in patients (Lawrie et al, 2008). MiR-25 and miR-223 were shown in studies to be increased in patients with non small cell lung cancer (NSCLC), indicating these microRNAs could

serve as blood-based biomarkers for the disease (Chen et al., 2008 and 2012). Additional microRNAs (miR-20a, miR-24, miR-145, miR-152, miR-199a-5p, miR-221, miR-222, and miR-320) were found to have altered expression in patients with NSCLC, and using these 8 as well as the aforementioned miR-223 and -25, NSCLC diagnosis was possible with a lead time of over 33 months, which demonstrates the value of this diagnostic method (Cui et al., 2013). The concentrations of particular microRNAs can also help predict NSCLC response to specific chemotherapuetics. For example, serum concentration of miR-125b has been shown to be predictive of response to cisplatin-based chemotherapy (Cui et al., 2013). MiR-22 is correlated with lack of response to pemetrexed-based treatment of NSCLC patients (Franchina et al., 2014). There is also evidence in the literature to support use of microRNAs in staging prostate cancer. One study found miR-107 and miR-574-3p were upregulated in nonmetastatic cancer patients compared with healthy subjects, and miR-141 and miR-375 were differentially expressed compared with nonmetastatic PC cases. (Bryant et al, 2012). Studies correlating microRNAs with breast cancer (BC) show that they may prove useful in improving diagnosis and treatment. In the literature, circulating microRNAS miR-21 (Asaga et al., 2011), miR-376c, miR-148b, miR-801, and miR-409-3p (Cuk et al., 2013), miR-133b (Chan et al., 2013); and miR-92a, miR-133a, and miR-1 (Chan et al., 2013) were associated with BC diagnosis. On study found miR-10b and miR-373 were associated with lymph node metastasis of BC (Chen et at, 2013). Circulating microRNAs have also been studied as a tool to aid in diagnosis of colorectal cancer (CRC). Ng et al. (2009) found overexpression of miR-95p, miR-222, miR-92, miR-135b, and miR-17-3 in plasma and tissue of CRC patients, indicating these microRNAs could serve as biomarkers.

Another study found miR-409-3p, miR-7, and miR-93 to be useful in distinguishing between patients with CRC and healthy controls (Wang et al., 2015). The traditional screening methods for CRC in particular present a good market for improvement, as colonoscopies are unpleasant and tedious for patients. In terms of proving information about treatment and prognosis, one study found a significant increase of miR-106a, miR-484, and miR-130b in CRC patients who failed to respond to 5-FU/oxaliplatin treatment, while miR-326 was correlated with reduced overall survival (Kjersem et al., 2014). These studies are summarized in introductory table 3.

Cancer Type	**Circulating MicroRNAs implicated**
DLBCL	miR-155, miR-21, miR-210
NSCLC	miR-25, miR-223, miR-20a, miR-24, miR-145, miR-152, miR-199a-5p, miR-221, miR-222, miR-320, miR-22, miR-125b
PC	miR-107, miR-574-3p, miR-141, miR-375
BC	miR-376c, miR-148b, miR-801, and miR-409-3p, miR-21, miR-133b, miR-92a, miR-133a, miR-1, miR-10b, miR-373
CRC	miR-95p, miR-222, miR-92, miR-135b, miR-17-3, miR-409-3p, miR-7, miR-93, miR-106a, miR-484, miR-130b, miR-326

TABLE 1.3. **List of circulating microRNAs implicated in different types of cancer**. As mentioned in the text.

1.3 EBV Encoded MicroRNAs

1.3.1. EBV MicroRNAs

The microRNAs encoded by Epstein Barr Virus are localized into two different regions of the viral genome, and therefore belong to two distinct families; BARTs and BHRFs (introductory figure 3).

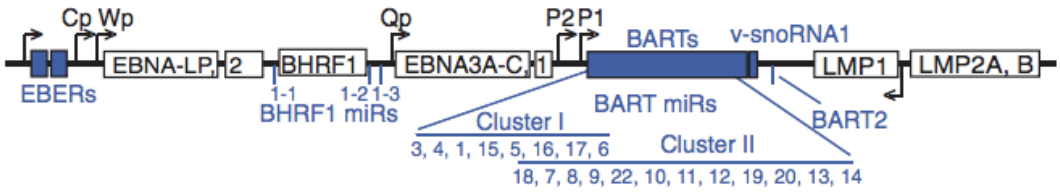

FIGURE 1.3. **Linear Representation of EBV viral genome showing genomic origin of latent EBV transcripts, including EBV noncoding RNAs.** The noncoding RNAs include the EBERs, miRNAs, BART transcripts, and an EBV snoRNA. The 25 EBV precursor miRNAs are clustered in the BHRF1 and BART regions of the genome. Reprinted with permission from Skalsky RL, Cullen BR. EBV Noncoding RNAs. Curr Top Microbiol Immunol. 2015;391:181-217.

The entire BART locus is around 20 Kbp and contains a total of seven exons. Because all BART microRNAs contain exon IIV, they have the same 3' end (Edwards et al. 2008; Al-Mozaini et al. 2009; Chen et al. 2005). Although some of the EBV encoded microRNAs have been characterized in recent literature, the function of others remains to

be defined. Previous work in our lab indicates that miR-BART-185p is involved in latency (Qiu J, 2014), while work by others indicates a role for other EBV microRNAs in cancer progression, by targeting and repressing host cellular genes (Chen et al, 2013; Wong et al 2012). Profiling work in our lab has revealed that at least some of the BART family microRNAs are expressed during all stages of viral infection including true latency (memory cell, latency I/0), but all are expressed during the proliferative stage of infection (lymphoblastoid, latency III) (Amoroso et al, 2011). This is shown in introductory figure 4.

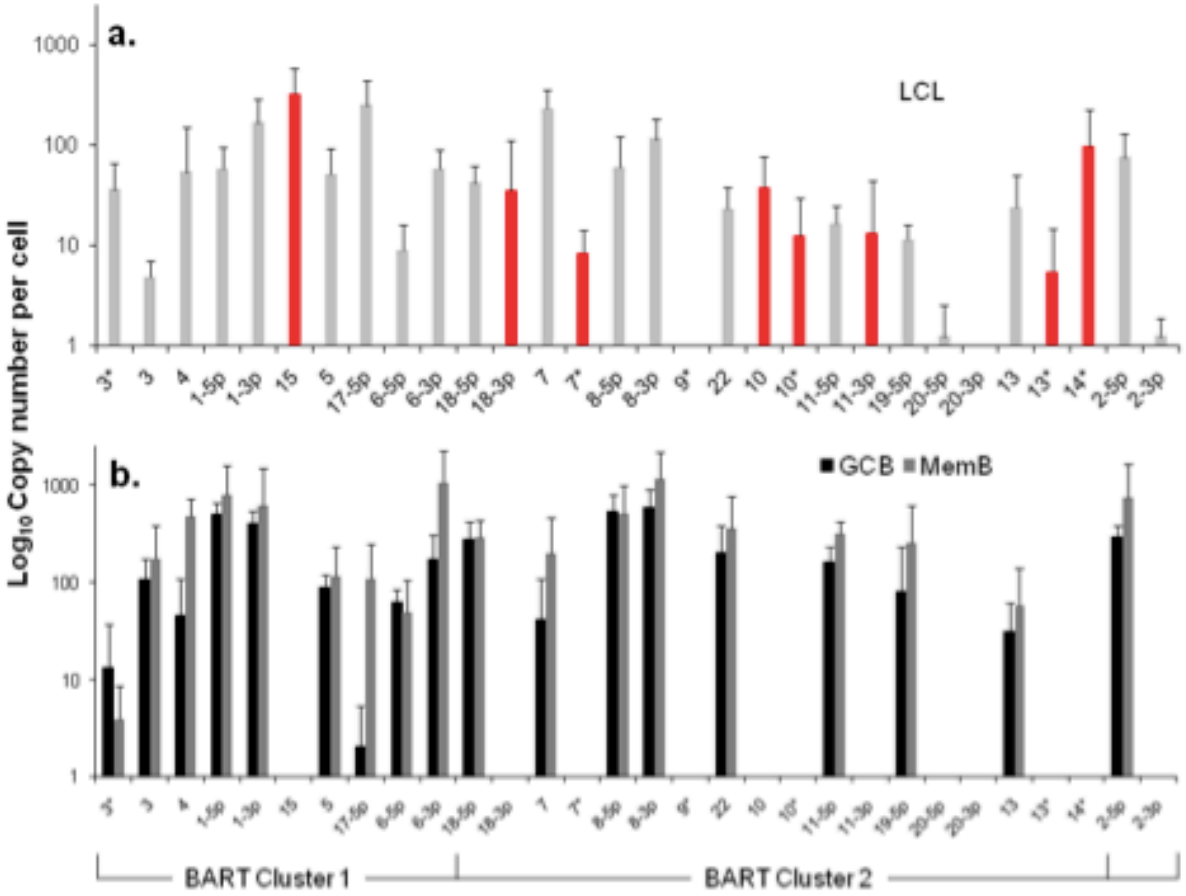

FIGURE 1.4. **Profile of EBV BART miRNAs in vivo and in spontaneous lymphoblastoid cell lines (LCL) expressing latency III**.
The data is expressed as copy number of each miRNA per infected cell. Values are normalized to U6. A. Spontaneous LCL (n=6). miRNAs that are significantly expressed in LCL but not GCB and MemB are highlighted in red. B. Normal infected tissue. Grey – GCB (n=5), black – MemB (n=4). This is the same data set as Figure 2B, expressed as copy number /cell. The y intercept is an approximation to the sensitivity of detection based on the following. The maximum number of infected cells tested for GCB and MemB was 4-6x103. Reprinted with permission from Qiu J, Cosmopoulos K, Pegtel M, et al. A novel persistence associated EBV miRNA expression profile is disrupted in neoplasia. PLoS Pathog. 2011;7(8):e1002193.

Evidence in the literature supports our results, and the BARTs are have been detected during lytic infection and latent infection, in the peripheral blood of EBV-infected individuals, in B and T cell lymphomas, in B cell lines infected in vitro, and in epithelial carcinomas (Edwards et al. 2008; Al-Mozaini et al. 2009; Chen et al. 2005). Additionally, recent literature has shown various miR-EBV-Barts to have effects on host cells and/or roles in EBV associated cancers. MiR-BART9 has been shown to have a role in metastatic NPC, possibly by targeting E-cadherin (Hsu et al, 2014), and miR-BART 20-5p/miR-BART-8 in tumor growth by indirectly inhibiting p53 (Huang et al, 2014). Other studies have revealed targets for BART family microRNAs involved in cell cycle suppression and apoptosis (Wong et all, 2012) as well as regulators of signaling such as PTEN (Cai et al, 2015).

1.3.2. Proliferation Associated miR-BARTs

Previous work by Kat Cosmopolous and Jin Qiu in our lab has shown that specific BART-miRNAs were more highly expressed in lymphoblastoid cell lines than in latently infected memory B cells (introductory figure 4, above). As discussed earlier, when the EBV infected cell is in the lymphoblast stage of differentiation, EBV's Latency III transcription program controls which viral genes are expressed. Therefore, the profile shown in Figure 4 represents the normal expression levels of the EBV-BART-miRNAs during each Latency program (LCL - Latency III, GC – Latency II, and MemB – Latency 1/0). Further profiling of EBV-miRNA expression in tissue samples from various EBV

positive tumors revealed a surprising finding with regard to EBV-miRNA expression. Tissue samples were taken from a number of EBV positive tumors, including BL (which is positive for EBV- Latency type I), HD (Latency II), GC (Latency II) and NPC (Latency III). A number of miRNAs profiled were expressed at much higher levels than would be expected based on the miRNA expression profile in normal, non-neoplastic EBV infected GC (Latency II) and MemB (Latency I/0) cells. These microRNA profiles are shown in introductory figure 4 (profiling done in normal cells) and introductory figure 5 (Profiling for EBV positive tumor samples show in the upper panel). This finding suggests that these irregularly expressed miRNAs are disregulated in the tumors. The tumors and the normal cells that highly express these miRNAs (the LCLs) share one characteristic: rapid proliferation. Therefore, we hypothesize that those miRNAs specifically may be involved in the development of cancer by contributing to deregulation of the cell cycle. In vitro, we hypothesize that they assist in the continued rapid proliferation and immortalization of the lymphoblastoid cell lines (LCL), while in vivo, the promote tumor formation by similarly contributing to an unregulated state of rapid proliferation. Therefore, we refer to this set of miRNAs as the “proliferation associated BARTs”.

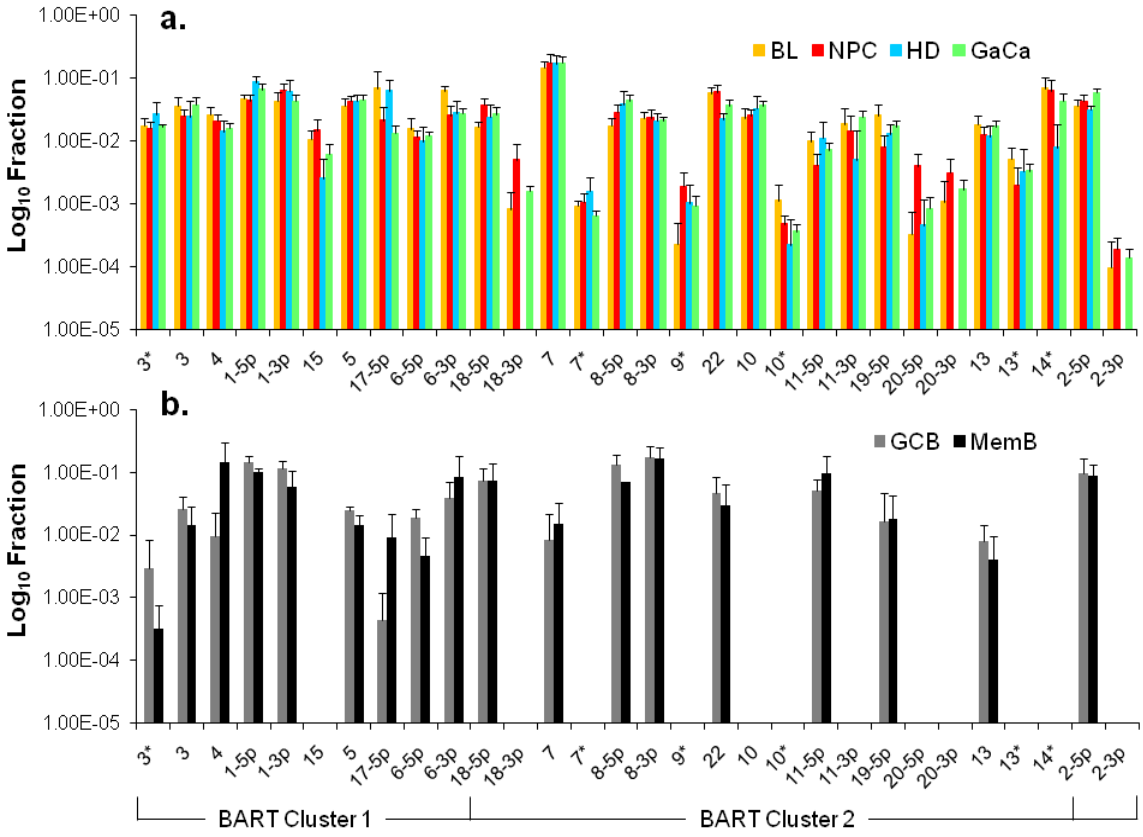

FIGURE 1.5. **Profile of EBV BART miRNAs in tumor samples and in GCB and MemB cells expressing Latency II and I/0, respectively**. The data is expressed as average and standard deviation of the fraction that each miRNA constitutes of the total of all EBV miRNAs. A. The four tumor types tested. Blue - Hodgkin's disease (n=3): yellow - Burkitt's lymphoma (n=6): green - gastric carcinoma (n=6): red - nasopharyngeal carcinoma (n=6). B. Normal infected tissue. Grey – GCB (n=5), black – MemB (n=4). The y intercept is a conservative approximation to the sensitivity of the assay (this will vary according to the input number of infected cells). It represents the fraction for a miRNA present at 10 copies, the lower limit of sensitivity for detection of all the miRNAs. The miRNAs are presented on the x-axis from left to right in the order that they appear in the viral genome. Reprinted with permission from Qiu J, Cosmopoulos K, Pegtel M, et al. A novel persistence associated EBV miRNA expression profile is disrupted in neoplasia. PLoS Pathog. 2011;7(8):e1002193.

To further investigate the role of BART microRNAs in proliferation, previous members of the lab performed an experiment to determine if expression of the BARTs in tumors would promote growth and metastasis of the tumors, leading to worse health outcomes in the host. In the experiment, mice were injected with mock tumors made from cells derived from an EBV associated tumor with or without BART microRNAs. The mock tumors were created using oriP/EBNA1 based vectors with or without the BART microRNAs. The vectors were stably transfected via lentivirus into a gastric adenocarcinoma cell line (AGS) that was derived from an EBV positive tumor but has lost the virus through passage in culture. These AGS cells were selected with antibiotic to ensure they were uniformly transfected, and then injected into the mice. The mice that received the BART microRNA positive cells grew larger tumors, and died more rapidly and more frequently (introductory figure 6).

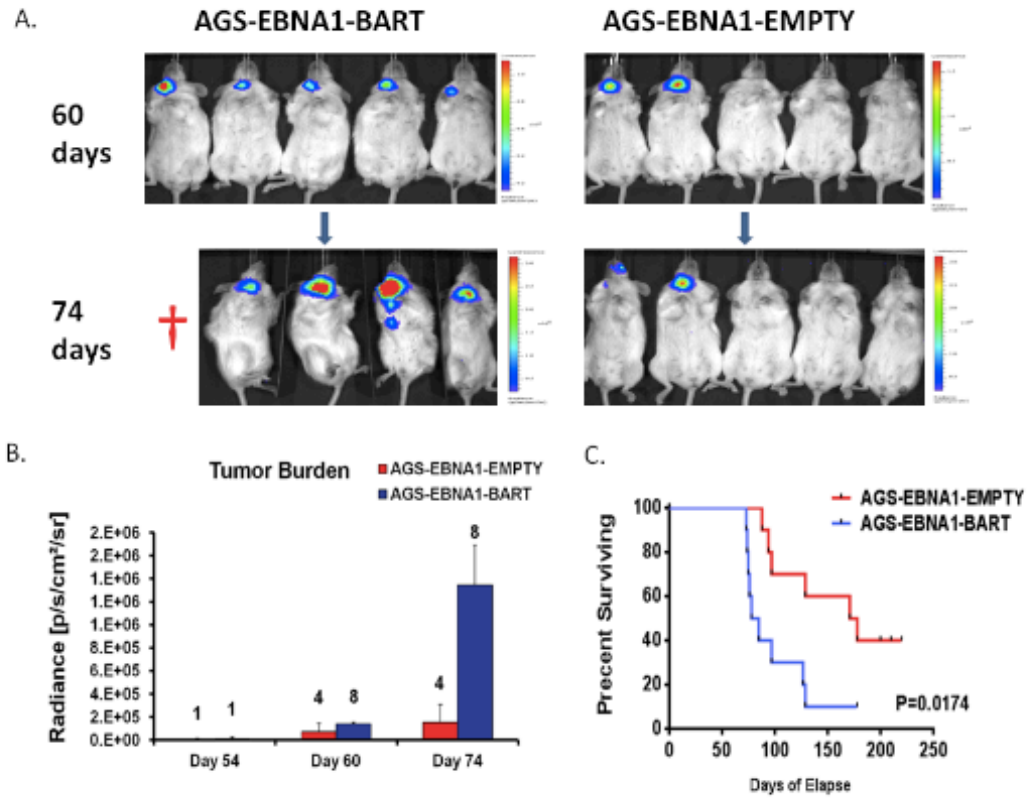

FIGURE 1.6. **Tumors from AGS-EBNA1-BART and AGS-EBNA1-EMPTY (A) groups on day 60 and day 74**. AGS-EBNA1-BART tumors grew more often, faster and larger than AGS-EBNA1-EMPTY in vivo. The red cross represents a mouse that died prior to imaging. C. Tumor burden (numerical representations of tumor size) was presented as Radiance (p/s/cm2/sr). The number of mice with detectable signals was shown above the bar. D. Kaplan-Meier analysis of survival in mice revealed that AGS-EBNA1-BART mice have a higher death rate p = 0.017). Reprinted with permission from Qiu, J., 2014, Epstein-Barr Virus microRNA Expression and Function in Persistent Infection and Oncogenesis, Doctor of Philosophy, Tufts University Sackler School of Graduate Biomedical Sciences, Boston, Massachusetts.

These findings solidified our interest in investigating the BART microRNAs, because in addition to believing that these micoRNAs are dysregulated in tissue samples from EBV positive tumor samples taken from human patients (Figure 5), the results shown in Figure 6 show that they may be increasing the growth rate of EBV positive tumors in the host. In our expression profile miR-BART-10, miR-BART-14*, and miR-BART-15, among others, are highly expressed in tumor cell lines but undetectable in resting memory B cells (introductory figure 5). Therefore we have performed a microarray assay on these genes and have list of potential genes these miRNAs may target. A number of these genes are known to be involved in apoptosis and autophagy, and a few are have been characterized as tumor suppressors.

1.3.3. EBV-MicroRNA-BART10-3p

EBV-miR-Bart10-3p (miR-BART10) is a member of the BART family of EBV-encoded microRNAs. In addition, it is one of the microRNAs of particular interest to us, since it is one of the most highly expressed "proliferation associated BARTs" (discussed in the section above). Previous work in the lab showed miR-BART10 is one of the BART microRNAs that is highly expressed in 4 EBV-associated tumor samples as well as in proliferating spontaneous lymphoblastoid cell lines (LCL) but not in germinal center (GC) or memory B (MemB) cells in vivo. These observations suggest that it may be doing something to predispose cells towards tumorigenesis, and therefore further investigation into potential targets is warranted. In this work, I have found that miR-

BART10 targets the ATP6V0e gene, which encodes the 0e subunit of V-Type H+ ATPases that are found ubiquitously in cells.

1.4 V-Type ATPase

1.4.1. Structure of V-type ATPases

The 0e protein is part of the V0 subunit of the V-type ATPase (introductory figure 7), which is embedded in the plasma membrane. The V1 subunit can be found in the cytoplasm or can assemble with the V0 subunit, which renders the ATPase operational. A reduction in translation of any part of either subunit will reduce protein expression of all of the other parts as well, since each subunit is unstable and will be degraded without all of its parts (Mauzevin, et al, 2015).

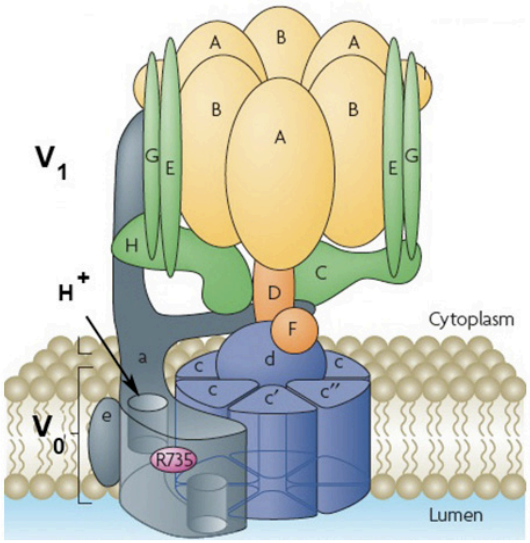

FIGURE 1.7. **Model of V-Type H+ ATPase**. Vacuolar ATPases: rotary proton pumps in physiology and pathophysiology. Reprinted with permission from Forgac M. Vacuolar ATPases: rotary proton pumps in physiology and pathophysiology. 2007. Nat Rev Mol Cell Biol. 8: 917-92

1.4.2. V-Type ATPases in Cancer

The role of ATPases in cancer is unknown, but a number of hypotheses exist and investigations into ATPase inhibitors as cancer treatments are being conducted. For example, cancer cells secrete proteolytic proteins in order to invade tissues, and inhibition of ATPases is hypothesized to affect the secretion profile of cancer cells and therefore abrogate their metastatic properties. Archazolid is a V-type ATPase inhibitor shown in the literature to reduce metastasis of cancers in vivo and reduce invasiveness in vitro (Weidmann et al, 2012). In the literature, treatment with archazolid decreases activity of cathepsin B, a prometastatic lysosomal protein (Kubisch et al, 2014).

Another hypothesis is based on the observation that malignant tumors preferentially utilize glycolysis and subsequent lactic acid fermentation for energy production (Wahrburg effect) and therefore must increase protein efflux as a consequence, as well as the fact that cancers frequently thrive in a hypoxic environment with a low extracellular pH. Therefore, a tumor would benefit from increasing it's expression of plasma membrane V-ATPases, because it could stabilize its cellular pH even in the presence of a highly acidic extracellular environment, as well as rid itself of excess hydrogen atoms generated by it's metabolic processes. Indeed, it has been observed that expression of V-ATPase correlates with invasiveness of breast cancer cells (Sennoune et al, 2004). Evidence in the literature has shown increased expression of ATP6V1C1, a regulator of ATPase complex assembly, in metastatic oral tumors, and silencing of ATP6V1C1 by RNAi inhibited cancer cell growth, maturation, and invasion in vitro (Feng, et al. 2013). Work by other labs at Tufts has shown that treatment of highly invasive MDA-MB-231 breast cancer cells with Bafilomycin A1, another V-ATPase inhibitor, reduces their invasiveness in vitro, and treatment with a plasma membrane specific V-ATPase inhibitor does not diminish this effect, further implicating plasma membrane V-ATPases in cancer cell metastasis (Cotter et al, 2014). These studies indicate that ATPases play a role in cancer growth and metastasis, and inhibition of ATPases reduces growth and metastasis of cancer.

1.4.3. Intersection of V-Type ATPases with EBV

This evidence seems to contradict the idea that EBV promotes tumorigenesis, if in fact an EBV encoded microRNA reduces expression of V-type ATPase duing infection. Simply, if V-ATPases are important for cancer growth and metastasis, and EBV encoded miRNA-BART10 reduces expression of V-ATPase, infection with EBV would not be expected to encourage cancer development. However, the effect of individual and combinations of microRNAs can be difficult to predict, because they often target hundreds of genes, so identifying a single target does not tell the whole story of how EBV encoded microRNAs may impact host cell processes. Additionally, ATPases are involved in a diverse range of cellular processes. Therefore reduction in ATPase expression may have multiple and possibly conflicting impacts on host cells.

1.4.4. ATPases in Autophagy and Host Response to Viral Infection

Separate from their effect on cancer, V-ATPases are also necessary for autophagy. During autophagy, the autolysosome must reach a crucial acidity in order to activate the lysosomal proteases that degrade autophagosomal cargo. If the autolysosomes cannot reach sufficiently low pH to allow for protease activity, they will accumulate, disrupting the usual process where degraded contents are released into the cytosol and membranes are recycled. If miR-BART10, which is aberrantly expressed in EBV positive tumors, reduces the rate of autophagy through targeting of the ATP6V0e gene, this effect may predispose non-malignant cells to transform and become tumorigenic. While this effect

may have evolved to benefit EBV during latent infection, as autophagy is an antiviral process, it may also promote malignant transformation of host cells as a side effect. Epstein Barr Virus Nuclear Antigen 1 (EBNA-1), the sole protein antigen expressed during latency and the dominant CD4+ T cell antigen, has been shown to be digested and presented on MHC-II through the autophagic pathway, and that inhibition of autophagy decreases it's presentation in vitro (Paludan, et al, 2005). Response to this antigen is crucial for immune system control of the virus (Moorman AM, et al, 2007). Therefore, during latent infection, EBV may subvert the adaptive immune response by downregulating autophagy through expression of miR-BART10, reducing expression of EBNA-1 on MHC molecules on the surface of the host cell. However, during malignant transformation, autophagy seems to suppress tumor formation by neutralizing damaged oxidative organelles, thereby reducing accumulation of reactive oxygen radicals and preventing genome instability (Matthew R, et al, 2007). Therefore, while the virus may have evolved the ability to suppress autophagy during latency in order to evade recognition by immune cells, it may also predispose latently infected cells to become malignant. Further investigations are necessary to determine if inhibition of autophagy contributes to the link between EBV infection and tumorigenesis.

1.5. Proliferation

One of the most important characteristics of EBV is it's capacity for transformation of host cells, most significantly it's ability to drive proliferation in infected B cells. Although mentioned briefly in section 1.1., the fact that EBV drives B cell proliferation

should be emphasized due to its crucial role in development of EBV-associated malignant tumors in it's human hosts.

1.5.1. EBV infected host cells are driven to proliferate and exhibit dysregulated cell cycle control mechanisms.

It is well accepted that infection of a naive B cell with EBV drives the infected cell to become activated and rapidly proliferate (Babcock et al, 1998; Joseph et al, 2000). At this stage, the virus express its Latency III transcription program, which causes expression of nine EBV encoded proteins, including six EBV nuclear antigens (EBNAs 1-6) and three latent membrane proteins (LMPs 1-3), as well as the viral non-coding RNAs (EBERs and miRNAs) under the transcription factor EBNA-2 (Price and Luftig, 2014). Although the exact mechanism for how EBV drives differentiation of the host cells is not fully characterized, a number of EBV encoded proteins expressed during Latency III are known to participate in activating and driving proliferation. LMP-1, a virally encoded protein that is expressed on the surface of infected B cells during Latency types II and III, mimics the activity of CD40 (Uchida et al., 1999; Cahir-McFarland, 2004) and LMP-2 mimics a constitutively active BCR (Mancao et al, 2007). These signals together provide activating and co-stimulatory signals to the resting B cell and thus induce proliferation (Cesarman, et al., 2011; Gires, et al., 1997). LMP-1 also promotes cell survival by activating anti-apoptotic and pro-proliferation pathways JNK, p38, AP-1 and NF-κB pathways (Soni et al, 2007). LMP- 2A has been shown to potentiate MYC expression to overcome a cell cycle checkpoint (Fish et al, 2014). EBV latent antigen 3C (EBNA3C),

which is essential for EBV-induced immortalization of B-cells in vitro, has been shown to stabilize Pim-1 through abrogation of the proteasome/Ubiquitin pathway by physically associated with Pim-1 through its amino-terminal domain. Pim-1, or Proto-oncogene serine/threonine-protein kinase, is linked to several cellular functions involving cell survival, proliferation, differentiation, and apoptosis. EBNAC3C was shown to significantly induce Pim-1 mediated proteosomal degradation of p21, a potent regulator of cell cycle progression at G1 and S phase (Gartel and Radhakrishnan, 2005; Banerjee et al, 2014). Furthermore, a significant reduction in cell proliferation of EBV-transformed LCLs was observed upon stable knockdown of Pim-1 (Banerjee et al, 2014).

1.5.2. Possible role of EBV driven proliferation in EBV associated malignancies.

EBV has been associated with a number of malignancies, yet an explanation for how the virus promotes host cell transformation only exists for some of the associated diseases. More specifically, eBL has been clearly linked to EBV infection, as all eBL tumors are infected with EBV, and evidence in the literature exists to show EBV creates an environment in which the characteristic myc translocation occurs (Goldstein and Bernstein, 1990). While more work remains to determine exactly how EBV promotes other associated diseases, there is plenty of evidence already that EBV encoded proteins and microRNAs are involved in disregulating the cell cycle, which is a common trait of all tumors. As discussed above, EBV encoded proteins impact a number of important cell cycle regulators including Myc (Fish et al, 2014), p21 (Banerjee et al, 2014), p38 (Soni et al, 2007). Elevated expression of MYC is a shared property of many human cancers,

including DLBCL (Yamato, 2001), PBL - notably, Myc was found to be more commonly mutated in EBER positive tumors (OK et al, 2014), and of course, Burkitt Lymphoma (Leoncini et al, 2008).

More work remains to be done to mechanistically connect EBV infection to development of various EBV associated tumors.

1.6. Autophagy

By reducing expression of the H+ ATP-ase involved in this process, miR-BART10 may reduce digestion of intracellular debris and pathogens by the autophagic pathway. Autophagy was initially categorized as a survival mechanism, and in many cases induction of autophagy increases survival especially during time of stress or nutrient deprivation (Yang et al, 2015; Xie WY et al, 2015). However, in some instances autophagy is required for caspase-dependent cell death and as a result, blocking autophagy prevents apoptosis and promotes survival (Espert L et al, 2006). The role of autophagy is cancer is also controversial, as in some contexts upregulation is oncogenic while in others it is tumor-suppressing (Zhi et al, 2015). During infection, autophagy is important for host defense against intracellular pathogens, as they are degraded in autolysosomes and the degraded particles activate innate immune responses when they are loaded onto endosomal TLRs, or adaptive immune responses when loaded onto MHC molecules (Palaudin et al, 2005).

1.6.1. Role of Autophagy in the Cell

Autophagy is a cellular process that provides a mechanism for removing misfolded or damaged proteins, clearing damaged organelles, and eliminating extracellular pathogens, as well as balancing nutrients by recycling amino acids during times of cellular stress. During autophagy, a phagophore derived from cellular membranes engulfs intracellular material, forming an autophagosome. The autophagosome then fuses with cellular lysosomes, which are acidic and contain proteases, and the contents are degraded in the resulting autophagolysosome. This process is represented in introductory figure 8. For reference the steps that are impacted by Bafilomycin A1, a drug used in my experiments, as well as several other drugs that impact autophagy, are also illustrated in the figure.

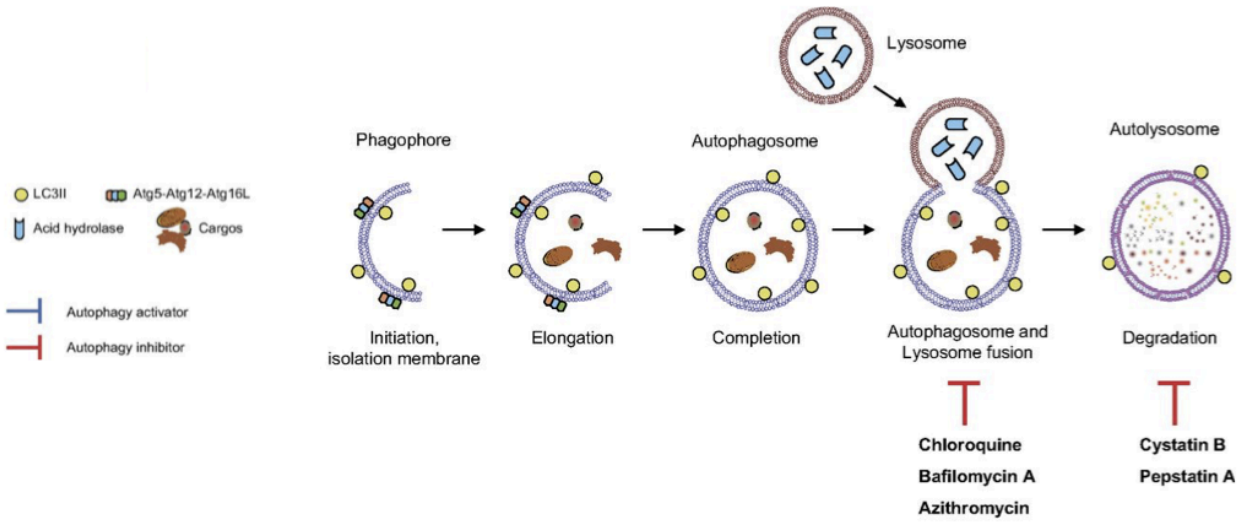

FIGURE 1.8. **Process of Autophagy.** A portion of cytoplasm, which may include organelles, misfolded proteins, or invading pathogens, is enclosed by a phagophore or isolation membrane to form an autophagosome. The outer membrane of the autophagosome subsequently fuses with the lysosome, and the internal material is degraded. Adapted with permission from Nakahira K, Choi AM. Autophagy: a potential therapeutic target in lung diseases. Am J Physiol Lung Cell Mol Physiol. 2013;305(2):L93-107. Changes include cropping and removing labels.

Autophagy is upregulated in vivo in response to stressors such as rapid proliferation, infection with virus (specifically in response to IFN-y), or cellular damage. While excessive autophagy results in cell death, it is usually characterized as a pro-survival adaptation to stress (Xie WY, et al, 2015). Therefore, the relationship between autophagy and cell survival is complicated and not well understood. In contrast, the role of autophagy in cellular defense against pathogens is well characterized.

1.6.2. Role of Autophagy in Immunity

Autophagy participates in innate immunity by engulfing and digesting invading microorganisms. This both contributes to the destruction of the pathogen, and promotes adaptive immune response by providing peptides which can be loaded onto MHC molecules on APCs (Munz C, 2009). Evidence in the literature points to autophagy being crucial for immune control of bacteria including Group A *Streptoccus* (Nakagawa et al, 2004), *Rikettsia conorii* (Walker et al, 1997), and *Listeria monocytogenes* (Rich and Burkett, 2003), and others. The pathogen *Legionella pneumophila* has been shown to target autophagy as a strategy for immunoevasion (Horenkamp, et al, 2015). There is even evidence that selection of substrates for degradation via the autophagic pathway, while non-specific at baseline and/or during times of general stress (i.e. starvation), becomes specific and targeted to promote capture of pathogens during an inflammatory response (Munz C, 2009; Rich et al, 2003). Viral particles of another herpesvirus, herpes simplex virus 1 (HSV-1), have been observed in autophagosomes of infected cells (Liang et al, 1998).

Invading pathogens including bacteria and viruses can stimulate autophagy by binding to TLRs on the surface of cells. The pathogens are subsequently ingested and degraded via the autophagic pathway in a process called xenophagy (Tattoli I, et al, 2012; Shelly S, et al, 2009). Xenophagy augments immune control of pathogens by two mechanisms. First, this process delivers cytoplasmic pathogen-associated molecular patterns (PAMPs) to endocytic TLRs and can thus stimulate their signaling activity (Shi C. et al, 2010). Secondly, MHC class II antigen presentation of viral antigens is augmented by autophagy, similarly to the mechanism by which self-antigens are processed (Paludan, et al, 2005). Therefore, autophagy participates in immunity by targeting and digesting pathogens, as well as augmenting immune responses in other cells.

Evidence in the literature has shown that numerous viruses of the Herpesviridae family inhibit autophagy. Herpes simplex virus (HSV-1) encodes a virulence protein ICP34.5 which has been shown to inhibit autophagy through interactions with Beclin-1, and HSV-1 mutants lacking this protein are substantially attenuated (Lieb D, et al, 2009). Viral homologues of Bcl-2 encoded by Kaposi sarcoma virus (HHV8), murine gammaherpesvirus 68 (γHV-68), and EBV (HHV-4) have also been shown to inhibit autophagy through interactions with Beclin 1 (Orvedahl A, et al, 2007; Pattingre S , et al, 2005; Sinha S, et al, 2008; Kelly GL, et al, 2009). Studies have been done with EVS as well. It has been shown that autophagic vessicles are stabilized during lytic EBV replication and that these autophagic membranes become incorporated into EBV viral envelopes, suggesting that EBV subverts antiviral xenophagy processes and recruits autophagic membranes to its viral envelope for efficient viral packaging during lytic infection (Nowag H, et al, 2013). Others have shown that inhibition of autophagy by Bafilomycin A1 increased EBV lytic genes expression and viral

progeny yield, and furthermore observed a decrease in autophagy correlating with increased expression of EBV early antigens, suggesting that EBV inhibits autophagy early after reactivation from latency (De Leo A, et al, 2015)

1.6.3. V-Type ATPases in Autophagy

V-Type ATPases play a crucual role in maintaining lysosomal, and consequently autophagosomal, pH. Through this action they participate in the regulation of autophagy and V-ATPase activiy is necessary for autophagy to proceed. Recent work has shown that the transcription factor E2F1 impacts autophagy through regulation of V-type ATPase activiy (Meo-evoli et al, 2015). Interestingly, E2F1 has been shown to be overexpressed in sporadic BL (Molina-Privado, et al, 2009). V-ATPase activity and inhibition of v-ATPase activity reduced lysosomal trafficking and mTORC1 activation, thus negatively impacting autophagic flux. In this study, the authors found that E2F1 was able to regulating lysosomal biology and autophagy through impacts on v-ATPases. EBV could be impacting autophagy through regulation of the same target, V-type ATPase (Meo-evoli et al, 2015). Additionally, Bafilomycin A1, the drug used as a control in my experiments, is a well characterized inhibitor of autophagy. The drug's repressive action on autophagy works partially by inhibiting V-Type ATPases (Mauvezin and Neufeld, 2015).

1.7. Summary

Although literature strongly points to EBV being able to reprogram host cells and drive differentiation, the exact mechanism of this push through each maturation state is not completely understood. Further investigations into EBV encoded regulatory genes including microRNAs are necessary to understand the mechanisms. Our initial observation that EBV encoded BART microRNAs seemed to increase proliferation (Figures 1.4, 1.5, and 1.6) made us interested in investigating individual BART microRNAs to identify and very targets that could provide a mechanism for the associated proliferation of host cells expressing the microRNAs. In this work, that initial investigation lead to the identification of a subunit of V-type ATPase (V0e subunit) as a target for one of the proliferation associated BART microRNAs, BART10. Although the role of V-type ATPases in proliferation isn't well characterized or understood, in my study, targeting of that same subunit by siRNA also seems to impact proliferation in vitro, although less significantly. The role of the V-type ATPase in autophagy, on the other hand, is well described. I therefore began explorations into whether the miR-BART10 impacts autophagy via targeting of the V-type ATPase. In this project, I have produced data to support the idea that miR-BART10 impacts autophagy, and to some degree also proliferation, in vitro in relevant EBV-associated cancer cell lines.

Chapter 2. Materials and Methods

2.1. RNA Microarray Assay

2.1.1. Microarray Assay cell preparation

2x106 EBV-negative B cells (BL2 and BJAB) were transfected with 100 pmol EBV miRNA mimics or control microRNAs. MiRNA mimics are synthetic double-strand duplexes with the unwanted strand chemically modified to avoid its off-target activity. The miRNA mimic control (MC) sequence is taken from a non-physiological C. elegans-derived miRNA that has no mammalian gene target. Microarray analysis was performed using Affymetrix human HGU133 plus 2.0 array (Board Institute). HGU133 plus 2.0 contains 55,000 probe sets, representing nearly 40,000 genes. Each miRNA was transfected in duplicate in both cell lines.

2.1.2. Microarray Analysis

For data analysis, the dChip software was applied to normalize the arrays and extract gene expression values. The mean expression value was obtained from duplicate experiments and the fold change ratio of averaged EBV mir-transfected experiment over averaged MC was calculated. A ratio of 1 refers to no change; below 1 reflects a down regulation while a ratio above 1 indicates up regulation.

2.2. Cell Culture and Transfection

2.2.1 Cell Culture

Akata cells were cultured in RPMI supplemented with 10% FBS, 1mM L-glutamine, 2mM sodium pyruvate, 100units/mL penicillin, 100ug/mL streptomycin, and 5ug/mL ciprofloxacin. HEK293 cells were cultured in DMEM supplemented with 10% FBS, 1mM L-glutamine, 2mM sodium pyruvate, 100units/mL penicillin, 100ug/mL streptomycin, and 5ug/mL ciprofloxacin. AGS.BX1 and AGS cells were cultures in FK-12 supplemented with 10% FBS, 1mM L-glutamine, 2mM sodium pyruvate, 100units/mL penicillin, 100ug/mL streptomycin, and 5ug/mL ciprofloxacin.
Cells were maintained in Sanyo incubator at $37^{o}C$ with 5% CO_2.

2.2.2. Transfection

Akata cells were transfected using Nucleofector 2B device from Lonza and Cell line nucelofector kit V from Lonza. 2.5 x 10^6 cells were pelleted and resuspended in 100uL Lonza transfection solution, 400pmol microRNA was added, and this mixture was transfected in a cuvette on program C-09. 500uL warm media was added for 10 minutes to allow cells to recover, then cells were plated in 75mL flasks. Synthetic miRNA mimics were purchased from Thermo scientific. Mimic negative control #1 (MC) is based on C. elegan's cel-miR-67 and the mature sequence is 5'-UCACAACCUCCUAGAAAGAGUAGA-3'. Mimic miRNAs are custom products.

BART10 sequence is 5'-UACAUAACCAUGGAGUUGGCUGU-3'. HEK293 and AGS cells were transfected using siRNA x-treme gene transfection reagent (Roche) according to product manual at 40% confluency in 10cm plates. 40uM siRNA was used for each transfection.

2.3. PCR protocols

2.3.1 RNA Extraction

Cells were pelleted in an eppendorf tube by spinning in a microcentrifuge for 5 minutes at 7,000 rpm. Media was removed, washed by resuspending the pellet in 1x PBS (Thermofisher) and centrifuged again. PBS was carefully aspirated off and the cells were lysed in TRIZOL reagent (Life Technologies) by pipetting. 1mL of TRIZOL reagent was used for each 5-10x10^6 cells. I then incubated the samples for 5 minutes at 15-30oC to permit the complet dissociation of nucleoprotein complexes. I then added 200uL of chloroform per 1mL of TRIZOL reagent and shook vigourously by hand for 15 seconds, then incubated at 15-30^{o}C for 10 minutes. I then centrifuged the samples at 4oC and 14,000 rpm for 15 minutes to ensure phase separation. I then removed the upper, aqueous phase which contains the RNA and moved to a new eppendorf tube, discarding the old tubes containing the interphase and the lower, TRIZOL phase. Then to precipitate the RNA, I added 2.5uL of glycogen and then filled the rest of the tube with 100% ethanol, and incubated the samples at -20^{o}C overnight. The following day, I spun the samples in a microcentrifuge at 4^{o}C for 30 minutes at 14,000 rpm. I then carefully aspirated the

supernatant off the RNA pellet. Then I washed the RNA in 500uL 85% ethanol and spun again at 14,000 rpm for 5 minutes at 4^{o}C. Again I carefully removed the supernatant and let the pellet dry in the inverted tube. Then I resuspended the pellet in 50uL of deionized water.

2.3.2. cDNA synthesis

I extracted total RNA using trizol/chloroform from transfected cells and synthesized cDNA as follows. 5uL total RNA (dilute with dH_20 if necessary) plus 3uL 5x RT primers from AB Biosystems reverse transcription kit were incubated at 85^{o}C for 5 minutes, then 60^{o}C for 5 minutes to denature the template RNA, then placed on ice. I added 7uL "master mix", and spun for 5 min at 5,000 RPM. I let the plate rest for 5 more minutes on ice and then put the plate on a thermocycler with the following program; 30 minutes at 16^{o}C, 30 minutes at 42^{o}C, 5 minutes at 85^{o}C, and 4^{o}C hold.
Recipe for the mastermix referenced above is as follows (all from AB Biosystems reverse transcription kit): 1ul 100mM dNTPs, 6uL multiscribe reverse transcriptase, 10uL 10x RT buffer, 1.1uL 20U/uL RNAse inhibitor, 25uL H_2O.

2.3.3. MicroRNA RT-qPCR

To obtain information about microRNA with the cDNA obtained by the above procedure, 1uL of cDNA was combined with 5ul IQ supermix (Biorad), 1uL of 100uM custom forward primer for miRNA-BART10 and 1uL 100uM universal reverse primer for all

microRNAs (both synthesized by Tufts Core Facilities – Integrated DNA Technologies, Inc) as well as 100uM custom Taqman prove for miRNA BART10 (ThermoFisher). The sample was analyzed by the BioRad My IQ rt PCR machine with the following program: 3 minutes at 95^{o}C for 1 cycle, then 35 cycles of 10 seconds at 95^{o}C followed by 30 seconds at 60^{o}C, then finally a hold at 4^{o}C.

2.3.4. mRNA RT-qPCR

I combined 4uL cDNA, 5uL Evagreen (ThermoFisher), 2uL each F and R primer at 100uM and 7uL deionized water. Samples were analyzed on a BioRad My IQ rt PCR machine with the following program: 1 cycle of 95^{o}C for 1 minute, 40 cycles of 95^{o}C for 15 seconds followed by 65^{o}C for 45 seconds, ending with 95^{o}C.

2.4. pH/Acidification Assay

2.4.1. Bafilomycin A1 Treatment

Cells were treated with 60uM Bafilomycin in media for 1.5-2 hours.

2.4.2. Lysosensor Stain

Transfected cells were stained 48 hours after transfection, or immediately after Bafilomycin A1 treatment, with Lysosensor green DND-189 (lifetechnologies). 1mL stock dye was diluted to a concentration of 1uM into prewarmed media and added to

cells. Cells were incubated in dark at 37^{o}C for 20 minutes. Media was then aspirated and cells were resuspended in PBS prior analysis by flow cytometry.

2.5. Western Blot

2.5.1 Preparation of lysates

Cells were washed In PBS and lysed in SDS Red loading buffer +DTT (Cell Signaling Technology), sonicated for 3 rounds of 15 seconds on ice, and boiled for 5 minutes before being centrifuged briefly and incubated on Ice.

2.5.2. Western Blot Procedure

Lysates were run in invitrogen Bolt 12% bis-tris plus gels for 90 minutes at 130 volts In 1x MOPS SDS running buffer (Novex NUPAGE). Gels were then transferred using 1x tris-glycine transfer buffer with methanol (Novex) for 70 minutes at 90 volts onto PVDF membrane. After transfer, the membranes were washed 3 times for 5-10 minutes each In TBST, and blocked In 5% milk in TBST for 1 hour. Membranes were again washed and then incubated overnight In primary antibodIes at specified concentrations In 5% BSA In TBST. The following day, the membranes were washed, incubated in secondary anibody at specified concentration in 5%BSA In TBST for 1-2 hours. After this the membranes were washed again and incubated briefly in freshly prepared 1x Lumiglo reagent A+B (Cell Signaling Technology)

2.5.3. Antibodies

Primary antibodies used include GAPDH (Cell Signaling Technology #5174) at 1:10,000 and LC3B (Cell Signaling Technology #2775) at 1:000. Secondary antibody used is anti-rabbit IgG HRP linked antibody (Cell Signaling Technology #7074) at 1:2000.

2.6. Luciferase Assay

2.6.1 Cloning

Oligos for insertion were synthesized by Integrated DNA Technologies, Inc. and sequences are provided in the appendix. 1.5ug of Pcheck 2 vector was cut with Not1-HF restriction enzyme (New England Biolabs) in 5uL cutsmart buffer + 42ul water (37^{o}C for 1 hour followed by 65^{o}C for 20 minutes) and run on 1.5% Agarose gel in TAE buffer. Linearized vector was gel purified using Qiagen kit and according to manufacturer protocols. Gibson Assemby (New England Biolabs) was used to clone synthesized oligos and linearlized Pcheck2 vector into competent E.Coli (New England Biolabs - NEB) according to protocols from NEB. Sequence for Pcheck2 vector is available in the appendix. E.Coli were grown on Agarose gels containing ampicillin overnight. Colonies were selected, grown for one hour in SOC media (life technologies) and then expanded into 4mL cultures with 5% ampicillin overnight. Minipreps were prepared using Qiagen kit and according to manufacturer protocols.

Cloning was verified by sequencing reactions performed by Tufts Core Facilities - Integrated DNA Technologies, Inc.

2.6.2. Luciferase Assay Protocol

HEK293 cells were cotransfected with Pcheck2 vector and si/miRNA in a 96 well plate using Xtremegene 9 (Roche) according to manufacturer's protocol, then luciferase and renilla activity were measured sequentially using Dual-glow luciferase kit (Promega) according to manufacturer protocol.

2.7. Cell Proliferation

2.7.1 Cell proliferation assay – Cell Trace Violet

HEK293 and AGS cells were transfected as described above. Cells were stained with Cell Trace Violet (ThermoFisher/Life Technologies) 24 after transfection. To stain, I diluted 1mM probe stock lysosensor dye to 1uM in warm media, added to cells for 20 minutes, and immediately analyzed using flow cytometry on a Beckman-Dickson LSR-II machine using the PacBlue channel.

2.7.2. Cell proliferation assay – cell counting

HEK293 and AGS cells were transfected as described above. Cell counting was performed using Sceptor 2.0 cell counter (EMD millipore) at indicated day intervals. Number of cells at day 0 was an estimate based on confluency of starting culture. Subsequent number of cell totals were calculated based on dilution factor of the sample that was counted and factoring in cell splits performed prior to count.

2.8. Statistical Analysis

QPCR results from Akata cells shown in figures 2, 3, and 4 were analyzed using unpaired t-test with Welch's correction (not assuming equivalent SD).

Q-PCR results from transfected 293 and AGS cells over time (figure 5) were analyzed using 2 way ANOVA with sidek correction for comparison of mimic control transfected cells with miR-BART10 transfected cells over time.

Proliferation results P values were obtained by doing t test on the slope of the of the proliferation curves, using the exponential equation $y=Ae^{kt}$ where K is the curve (tables 1 and 2).

Changes in MFI (figures 14 and 15) were analyzed using a one-way ANOVA with bonferoni test to compare selected pairs of control/treatment conditions.

Statistics in figure 22 were done using unpaired t-test.

Chapter 3. Results

3.1. Finding a Target for EBV-miR-BART10 *in vitro.*

In order to begin investigations into how the proliferation associated BARTs may be impacting host cells, a previous student in our lab commissioned a microarray analysis of multiple cell lines and tumor samples in which various levels of EBV-miR-BARTs are detectable. This left us with a list of potential mRNA targets for each microRNA in each sample, and we were able to create a "consensus list" from the results of groups of samples. This consensus list is shown in the heat map in Figure 1.

	Fold Change	Significance [-log10 (p value)]
ATP6V0e1	-1.91	1.28
RAB35	-1.70	1.79
ATP6V0e1	-1.65	2.59
ATG5	-1.59	1.54
CDC2L6	-1.52	0.94
EIF2S1	-1.42	2.01
FYN	-1.35	2.06
UNG	-1.32	1.63
DICER1	-1.29	0.68
CARD8	-1.28	1.47
NOD9	-1.27	0.93
ELL2	-1.25	0.18
FBXW7	-1.24	1.19
LITAF	-1.22	1.02
MLLT10	1.21	1.4
CEND1	1.23	0.93
ATP6V1C1	1.24	1.99

FIGURE 3.1. **Heat map from microarray.** A subset of the data from the microarray assay is displayed with color indicating up or downregulation (green for upregulation, red for downregulation).

From this data I begun investigating several promising targets to confirm that miR-BART10 could reduce target mRNA expression in vitro. I was initially interested in FBXW7, due to it's implicated role in development of cancer. FBXW7 is an "F-box" protein, which is the variable part of the SCF E3 ligase complex. The F-box portion of the complex determines target specificity through recognition and binding of target proteins for ubiquitination and degradation (Welcker and Clurman, 2008). The human FBXW7 gene is encoded on chromosome 4 and encodes three isoforms α, β, γ. The isoforms localize to different locations (nucleoplasm, cytoplasm, nucleolus, respectively) but are conserved at the interaction domain in the C terminus (Spruck et al, 2004). Studies have shown that FBXW7 targets substrates including Cyclin E (Hao et al, 2007; Welcker and Clurman 2007), c-Myc (Yada et al, 2004), c-Jun (Nateri et al, 2004), Mcl-1 (Ren, et al, 2013), SREBP (Sundqvist et al, 2005), the Notch pathway (Oberg et al, 2001; Wu et al, 2001; Gupta-Rossi et al, 2001) mTOR (Mao et al, 2008), and HIF-1α (Flugel et al, 2012).

FBXW7 is targeted by human micro-RNAs miR-32 (Xia et al, 2017), miR-223 (Deiuliis et al, 2016), miR-27b (Sun et al, 2016), miR-155-3p (Tang et al, 2016) and is upregulated by miR-25 (Zhang Y. et al, 2016). It is frequently mutated in many different cancer types including endometrial, breast, and colorectal cancers, and is mutated in 30% of a T-cell acute lymphoblastic leukemias (T-ALL).

In nasopharyngeal carcinoma, the PI3-K/Akt-GSK3beta-FBW7 signaling axis is dysregulated as a result of the expression of LMP1, an EBV encoded protein (Xiao et al, 2014). Additionally, in 45.5% of gastric carcinoma samples, one copy of FBXW7 has

been shown to be deleted, and mRNA expression of FBXW7 was reduced in the more severe cases (Calcagno, Freitas et al. 2013). The microarray data suggested that FBXW7 is downregulated by miR-BART-10 by about 20% (Figure 1). These studies led me to believe that FBXW7 was a crucial target to investigate. I hypothesized that the combined effect of mir-BART-10 and LMP1 might cause significant downregulation of FBXW7, thereby causing an increased expression of c-Myc and contributing to dysregulation of the cell cycle and the development of cancer.

I transfected Burkitt Lymphoma cells that were EBV positive but have lost the virus through passage in culture (Akata EBV -) with a mimic control microRNA or mature miR-BART10 (Dharmacon) via electroporation, waited approximately 24 hours, and extracted RNA from the cells using trizol and chloroform. I then made cDNA and performed qPCR to determine expression of FBXW7 mRNA in miR-BART10 transfected cells compared to controls (Figure 2, A.). I also did reverse-transcribed PCR (rt-PCR) to obtain the microRNA expression so I could measure miR-BART10 levels in transfected cells, to ensure the transfection was successful (Figure 2, B.)

A.

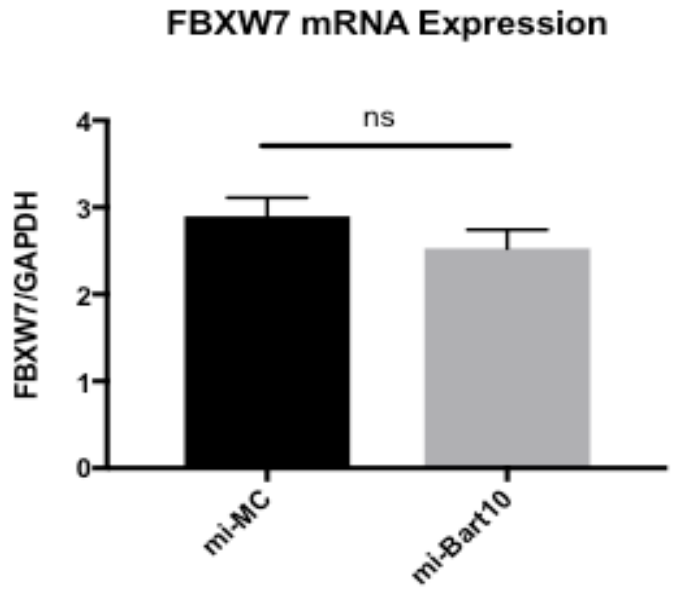

B.

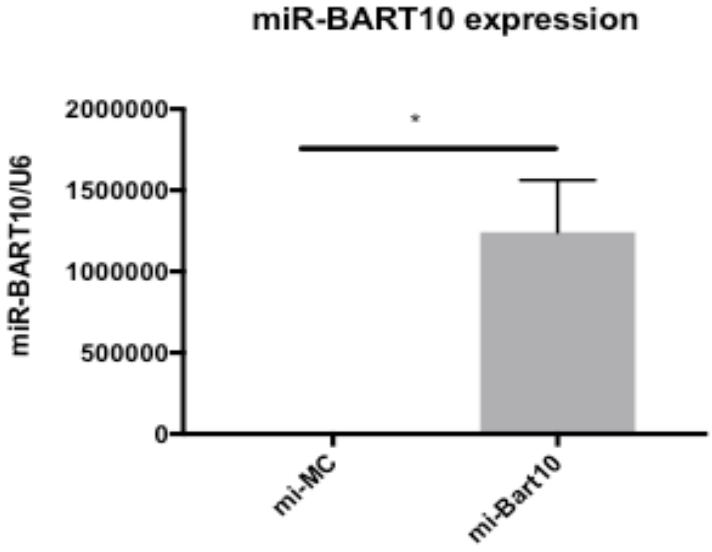

FIGURE 3.2. **Akata cells transfected with miR-BART10 or miR-MC show insignificant downregulation in FBXW7 mRNA expression.** A. Akata EBV (–) cells were transfected via electroporation with a mimic control (MC) or miR-BART10 (B10) and values were normalized to GAPDH. Representative results shown. N=4. B. Relative expression of miR-BART10 in samples of Akata EBV (–) cells transfected via electroporation with a mimic control (MC) or miR-BART10 (B10) normalized to endogenous U6 microRNA. N=3. ns indicates no statistical significance. * indicates $P<.01$.

Unfortunately, I did not see a significant downregulation of FBXW7 by miR-BART10, although a small insignificant reduction in mRNA expression was consistently observable. Due to this discouraging result, I did not continue experiments with FBXW7, although it remains an interesting target that may merit further investigations with more sensitive technologies.

I also measured mRNA expression of ATG5, an autophagy related protein that also looks to be downregulated based on the microarray data. I observed no down-regulation of ATG5 mRNA at all, so also abandoned investigations into this target (Figure 3).

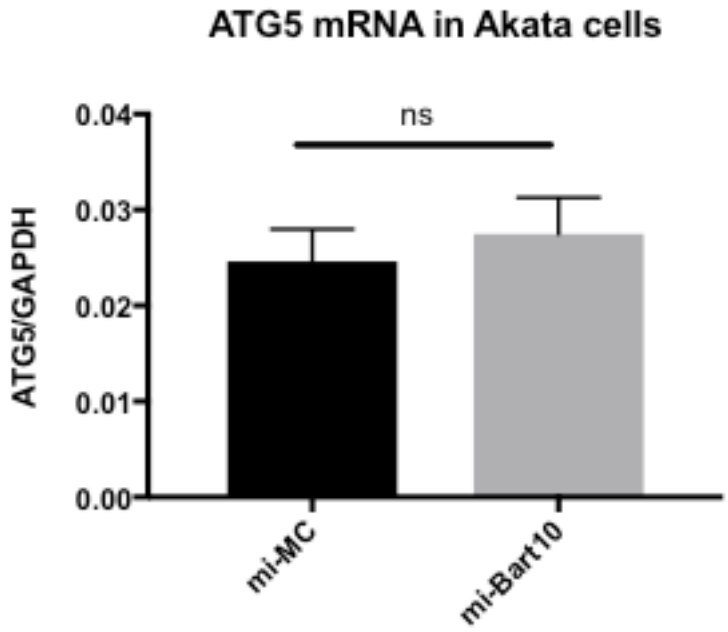

FIGURE 3.3. **Akata cells transfected with miR-BART10 or miR-MC show insignificant downregulation in ATG5 mRNA expression.** Akata EBV (–) cells were transfected via electroporation with a mimic control (MC) or miR-BART10 (B10) and values were normalized to GAPDH. Average of 3 separate transfection episodes and standard deviations shown. N=3. ns indicates no statistical significance.

Finally, I investigated ATP6V0e1. I observed a reproducible ~30% reduction in ATP6V0e miRNA in the BART10 transfected cells compared to the mimic control transfected cells (Figure 4).

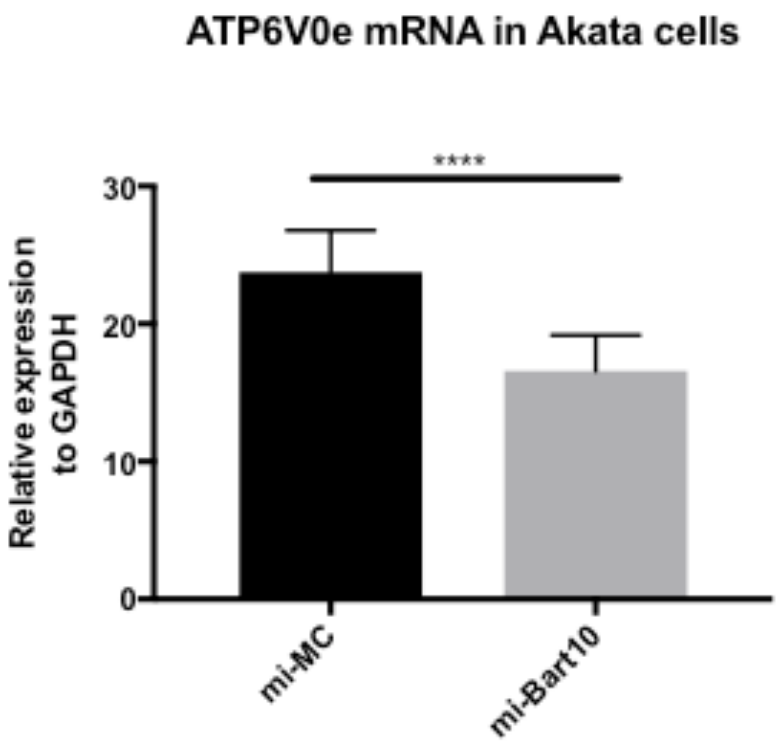

FIGURE 3.4. **Akata cells transfected with miR-BART10 or miR-MC show significant downregulation in ATP6V0e mRNA expression.** Akata EBV (–) cells were transfected via electroporation with a mimic control (MC) or miR-BART10 (B10) and values were normalized to GAPDH. Average of 9 separate transfection episodes and standard deviations shown . N=9. **** indicates P<.0001

I also transfected HEK293 cells with miR-BART10 and analyzed expression of ATP6V0e mRNA on days indicated (Figure 5, A). Reduction in ATP6V0e1 mRNA was more effective than in Akata cells at approximately 60% (Figures 4 and 5), possibly due to low viability in nucleofected Akata cells (Figure 4) and differences in transfection reagents.

As an additional control, I purchased a validated siRNA against ATP6V0e analyzed mRNA expression in transfected HEK293 cells over time in parallel (Figure 5, B). In both conditions I found a reliable reduction in ATP6V0e mRNA continuing out to day 5 (Figure 5, A and B). This work confirms that miR-BART10 targets and reduces the expression of ATP6V0e in two different cell lines, and that the siRNA I purchased is working as advertised. Therefore, I continued to use the siRNA as an additional control in future experiments.

A.

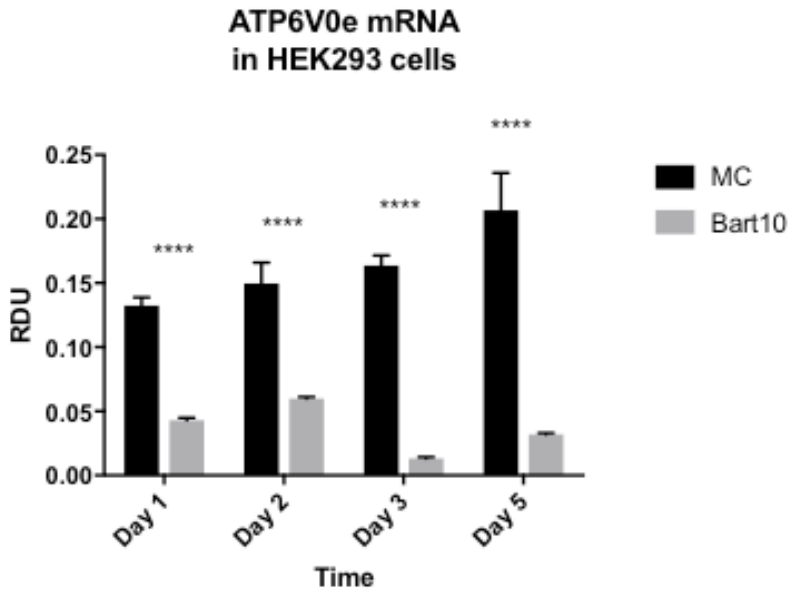

B.

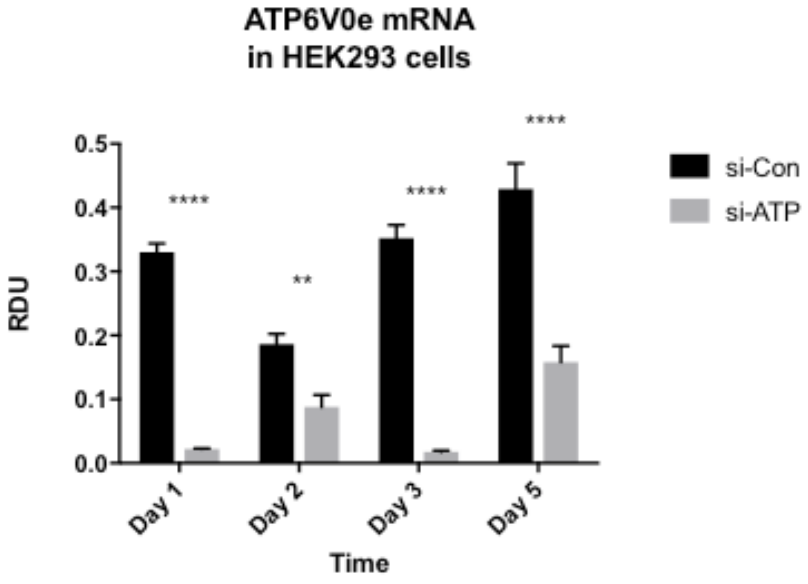

FIGURE 3.5. **ATP6V0e mRNA in transfected HEK293 cells.** Results of RT-qPCR showing expression of ATP6V0e mRNA in samples of HEK293 cells transfected via electroporation with a mimic control (MC), miR-BART10 (B10), siRNA-Control or siRNA-ATP6V0e, as indicated, normalized to GAPDH. N=6. **** indicates P value <.0001. ** indicates P value <.001.

There are no antibodies available against ATP6V0e1. I was able to obtain an antibody for western blot specific for ATP6V0A1 that is in development at Cell Signaling Technology through a work contact. The A1 protein is part of the V1 subunit of the V-type ATPase (Figure 6), which can be found in the cytoplasm or can assemble with the V0 subunit, which is embedded in the plasma membrane. While theoretically, the V1 and V0 subunits may be stable in the absence of each other, I observed a slight reduction in ATP6V0A1 in cells transfected with miR-BART10 (Figure 6, left). Interestingly, siRNA directed against ATP6V0e did not have this effect.

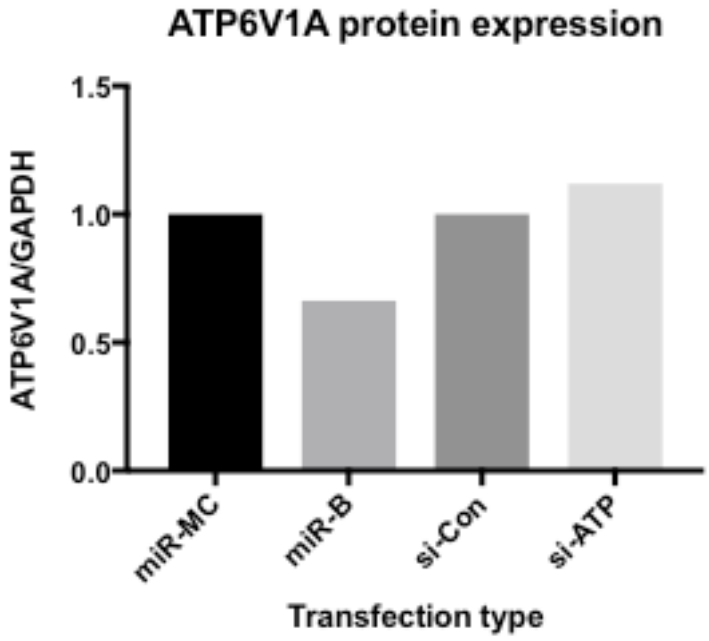

FIGURE 3.6. **Quantification of western blot using antibody against ATP6V1A.** (Cell Signaling Technology, in development). Lysates were transfected using Xtreme gene siRNA transfection reagent (Roche) with microRNA mimic control (A) or mature microRNA BART 10 (B) (ambion). N=1.

To inquire whether mIR-BART10 directly targets ATP6V0e1 in my experimental system, I utilized a luciferase-based luminescence assay in HEK293T cells. I generated vectors carrying a luciferase reporter downstream of each of the following experimental sequences taken from ATP6V0e1 mRNA: 3'UTR, 5'UTR, Coding Region or 3'UTR with the predicted seed region mutated to prevent binding of miRNA (figure 7, B). I co-transfected cells with vectors and miR-BART10 or the validated siRNA against ATP6V0e used in the previous experiments. As shown in figure 7, the luciferase activity was significantly downregulated in the cells transfected with the unmuated 3'UTR-containing vector, while all other conditions were unimpacted (figure 7, C). This implies that miR-BART10 directly targets ATP6V0e in vitro.

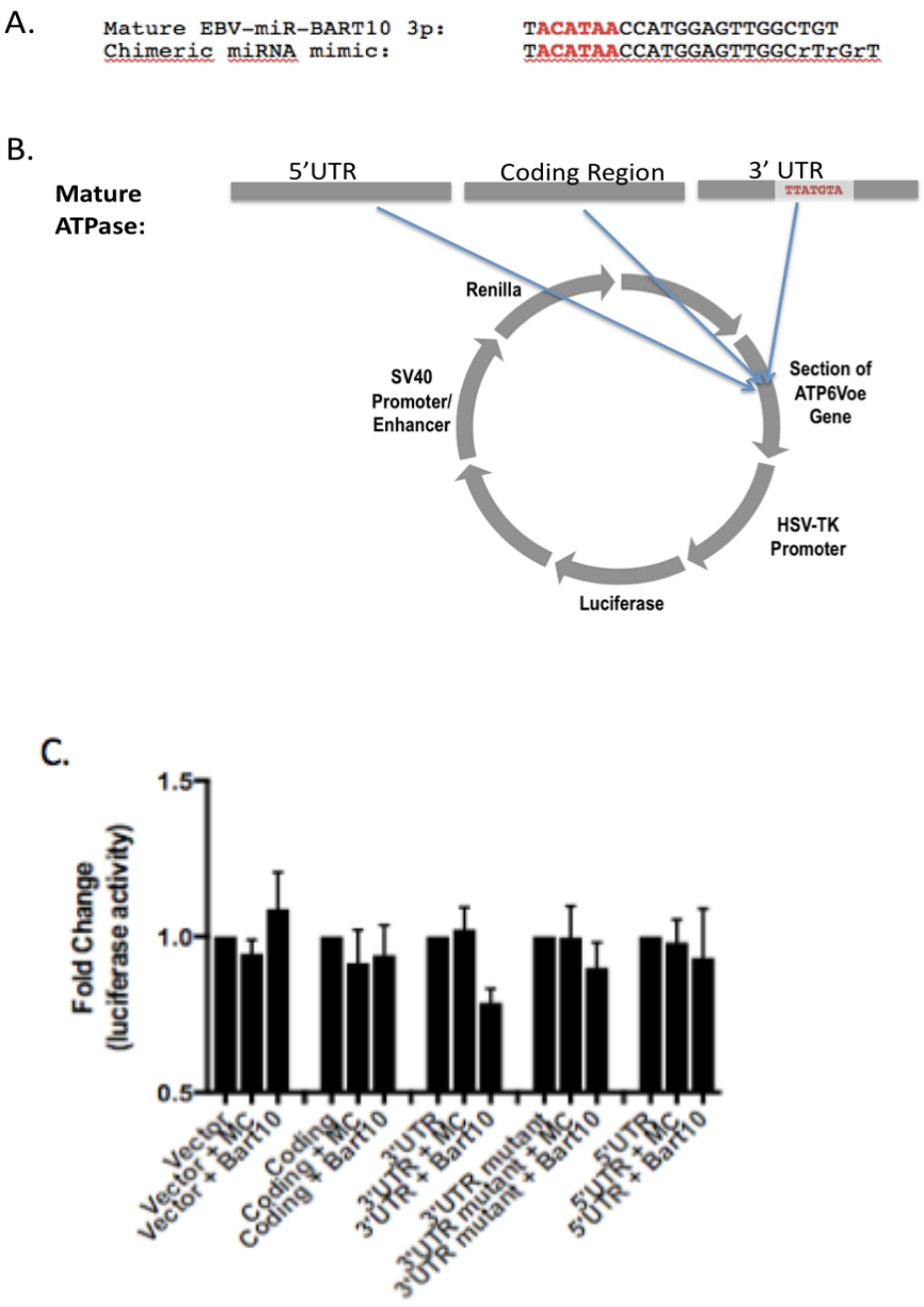

FIGURE 3.7. **Luciferase assay confirms miR-BART10 direct targeting of ATP6V0e mRNA.** A.) sequence of mature EBV-miR-BART10 and chimeric miR-BART10 mimic used in experiments. B.) Schematic of ATP6V0e gene, broken into sections that were separately cloned into vector, also shown. C.) Results of luciferase assay with transfections indicated on x-axis. N=1.

3.2 Transfection of miR-BART 10 increases rate of proliferation in vitro.

In addition to finding a target for miR-BART10, I wanted to investigate what impacts expression of the microRNA have on host cells. Previous work in our lab had lead us to characterize a number of EBV encoded microRNAs, including miR-BART10, as potentially pro-proliferative (section 1.3.2), so I decided to begin explorations by determining if exogenous expression of miR-BART10 would impact proliferation in trasfected cells *in vitro*. I performed an assay to measure proliferation of transfected cells using Cell Trace Violet (Invitrogen). This reagent is a cytoplasmic dye similar to CSFE that is diluted as cells divide during proliferation. I first transfected HEK293 cells with the same irrelevant control microRNA and BART10 microRNA as well as the siRNA control and validated siRNA against ATP6V0e (Ambion) used in the transfection experiments described in section 3.1. For these cells, the transfections were done using a chemotransfectant (X-treme gene siRNA transfection reagent - Roche) instead of nucleofection. Approximately 12 hours after transfection, I stained the cells with cell trace violet and 6 hours later measured the fluorescence intensity by FACS on a sample of the cells. This first timepoint is “Day 1”, the next is “Day 2”, the next “Day 3” and two days later “Day 5”. I then compared the proliferation rates (Representative experiment for MC and B10 transfected cells shown in figure 8; Representative experiment for siRNA Control and siRNA ATP6V0e transfected cells shown in figure 9).

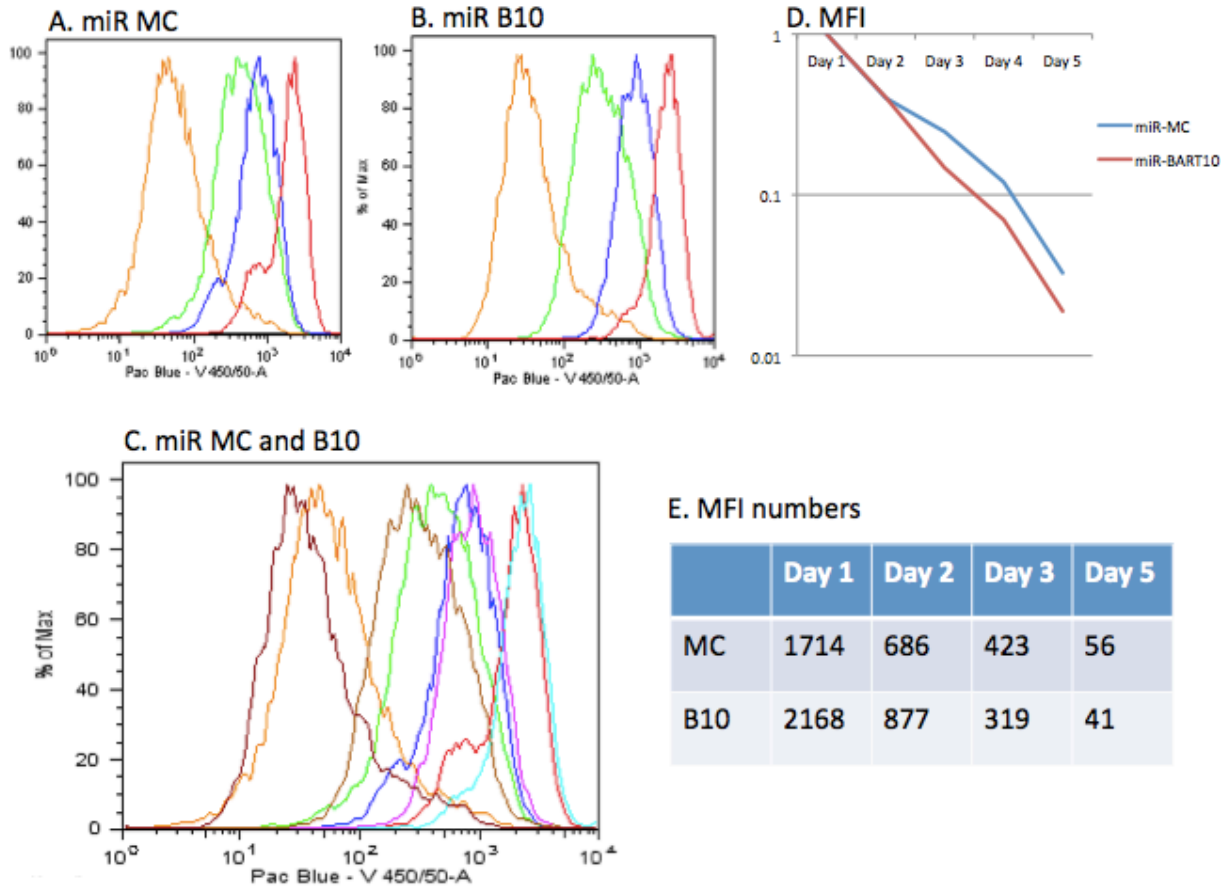

E. MFI numbers

	Day 1	Day 2	Day 3	Day 5
MC	1714	686	423	56
B10	2168	877	319	41

FIGURE 3.8. **HEK293 cells transfected with miR-BART10 proliferate more rapidly than control transfected cells.** HEK293 cells were transfected using Xtreme gene siRNA transfection reagent (Roche) with microRNA mimic control (A) or mature microRNA BART 10 (B) (ambion). Day 1 is shown in red, day 2 in blue, day 3 in green, and day 5 in orange. C. Histograms for microRNA mimic control transfected cells and microRNA BART10 transfected cells are shown together. Mimic control shown in red (day 1), blue (day 2), green (day 3) and orange (day 5) while BART10 shown in teal (day 1), purple (day 2), light brown (day 3), and dark brown (day 5). D. MFI values normalized to day 1 and shown on a log scale. E. Raw numbers of MFI values on each day. N=3

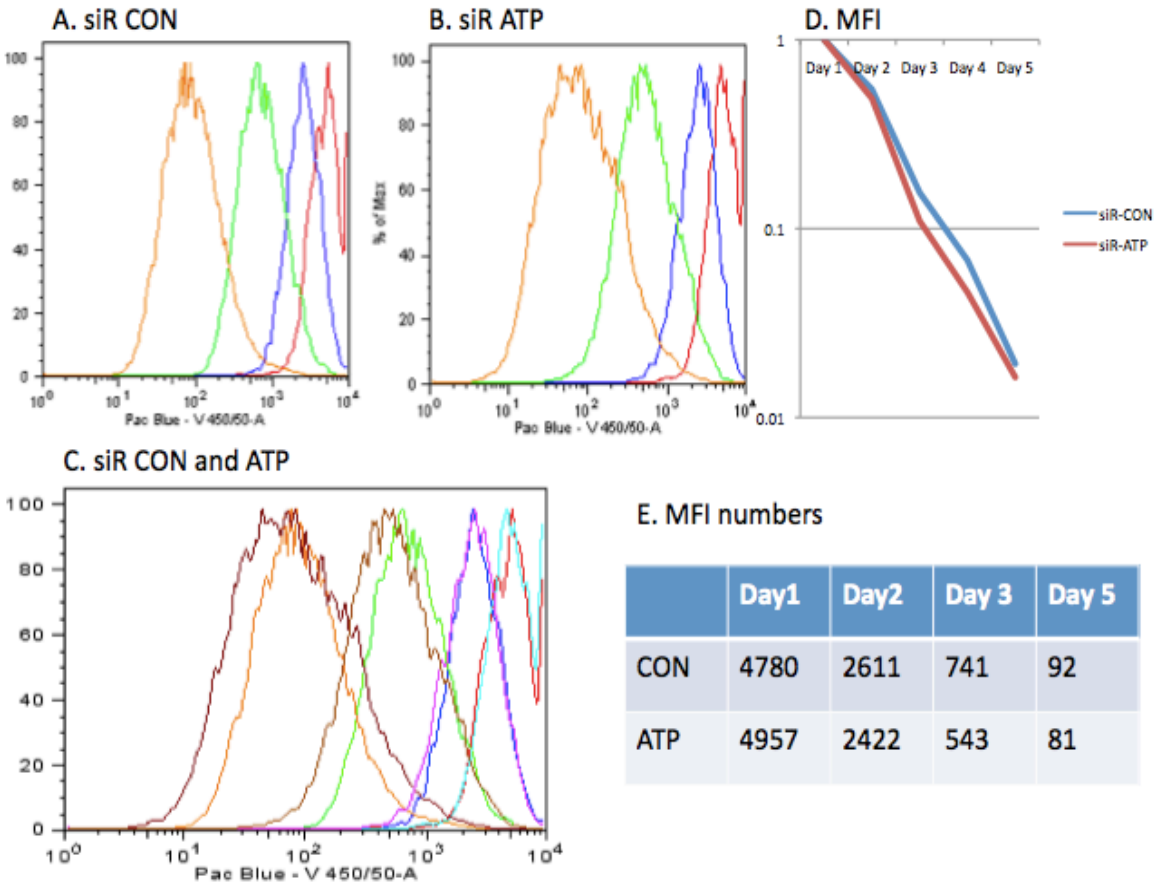

	Day1	Day2	Day 3	Day 5
CON	4780	2611	741	92
ATP	4957	2422	543	81

FIGURE 3.9. **HEK293 cells transfected with siRNA-ATP6V0e proliferate more rapidly than control transfected cells.** HEK293 cells were transfected using Xtreme gene siRNA transfection reagent (Roche) with siRNA control (A) or validated siRNA against ATP6V0e (B) (ambion). Day 1 is shown in red, day 2 in blue, day 3 in green, and day 5 in orange. C. Histograms for siRNA control transfected cells and siRNA ATP transfected cells are shown together. Control shown in red (day 1), blue (day 2), green (day 3) and orange (day 5) while ATP shown in teal (day 1), purple (day 2), light brown (day 3), and dark brown (day 5). D. MFI values normalized to day 1 and shown on a log scale. E. Raw numbers of MFI values on each day. N=3

The cells transfected with mature microRNA BART10 consistently proliferate ~15%+ faster than control cells transfected with a microRNA mimic control. To further confirm this observation, I employed a second technique for measuring population growth. I transfected HEK293 cells (figure 10) and AGS cells (figure 11) with mi/siRNA as before and calculated the total number of cells on days following transfection. The AGS cell line is derived from an EBV + adenocarcinoma cell line, although it has lost the virus through passage in vitro.

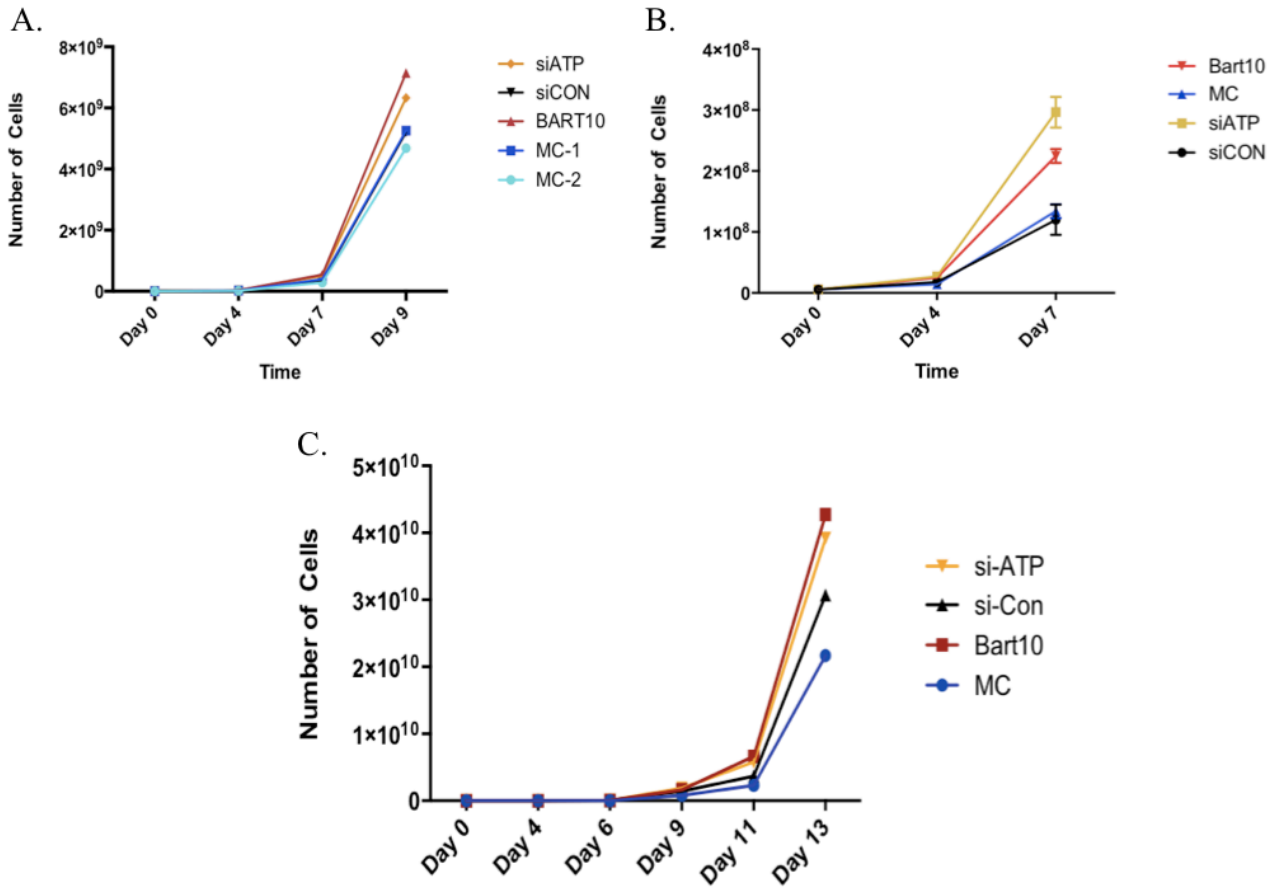

FIGURE 3.10. **HEK293 cells transfected with miR-BART10 or siRNA-ATP6V0e proliferate more rapidly than control transfected cells.** HEK293 cells were transfected using Xtreme gene siRNA transfection reagent (Roche) with mi/siRNA as in figures 10 and 11. Cells were counted using millipore scepter automated cell counter on days indicated. A, B, and C, represent three separate transfection episodes, performed on different dates. In A, a second control microRNA was used to confirm that the first control was not negatively impacting cell growth.

STATISTICAL ANALYSIS	miR-BART10 to miR-MC	siR-ATP to siR-Con
P value (unpaired t-test)	0.0199 (*)	0.720 (ns)

TABLE 3.1. **Statistical analysis of change in proliferation rate in transfected HEK293 cells**. Unpaired two tailed T test was used to calculate the statistical significant in the percent change in proliferation rate between control transfected cells and miR-Bart10 or si-ATP cells. Data from three separate experiments (biological replicates) was used to calculate statistics.

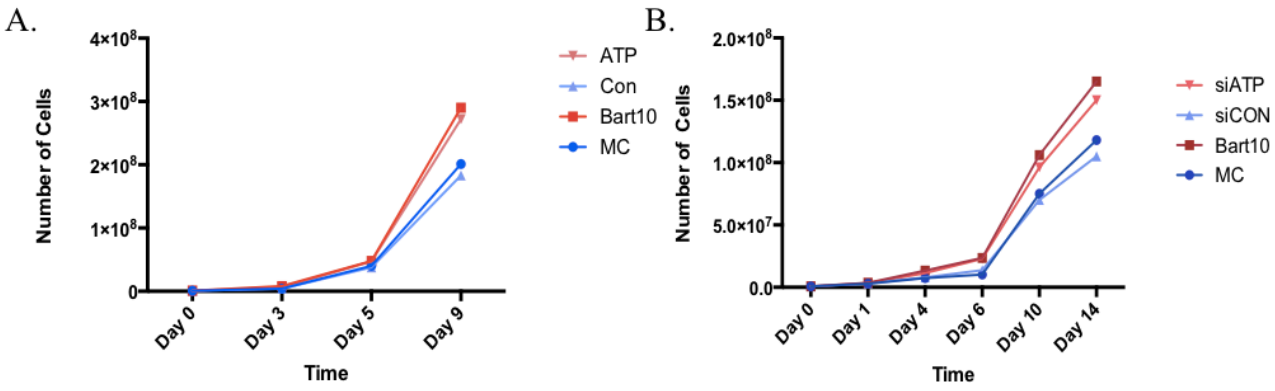

FIGURE 3.11. **AGS cells transfected with miR-BART10 or siRNA-ATP6V0e proliferate more rapidly than control transfected cells.** AGS cells were transfected using Xtreme gene siRNA transfection reagent (Roche) with mi/siRNA as in figures 10 and 11. Cells were counted using millipore scepter automated cell counter on days indicated. A and B represent two separate transfection episodes, performed on different dates.

STATISTICAL ANALYSIS	miR-BART10 to miR-MC	siR-ATP to siR-Con
P value (unpaired t-test)	0.0023 (**)	0.003 (**)

TABLE 3.2. **Statistical analysis of change in proliferation rate in transfected AGS cells**. Unpaired two tailed T test was used to calculate the statistical significant in the percent change in proliferation rate between control transfected cells and miR-Bart10 or si-ATP cells. Data from two separate experiments (biological replicates) was used to calculate statistics.

Across multiple transfection episodes and employing two different techniques for measuring proliferation rate, I have observed a reproducible growth advantage in cells transfected with miR-BART10. Statstical analysis on three biological replicate cells counting experiments confirm the results are significant with a P value < 0.05 for HEK293 cells (table 1) and for AGS cells (table 2). This finding is consistent with previous observations (introductory figures 4 and 6) that EBV-encoded BART microRNAs may be associated with proliferation, and increase malignancy, growth, and survival of tumors.

3.3. Transfection of other proliferation associated BARTS, including miR-BART10, increases rate of proliferation in vitro.

I also investigated whether other Bart microRNAs together might increase proliferation. BARTS 14* and 15 are also highly expressed in LCL and tumor cells so I began by combining 14*, 15, and 10 together and observing effects on proliferation. I performed

the proliferation experiment with Cell Trace as in figures 10 and 11, this time transfecting in all 3 microRNAs together (figure 12). The results show a prolonged increase in proliferation lasting the duration of the experiment (6 days), similar to that seen with miR-BART10 alone. I also observed that the media in the wells containing cells transfected with BARTs was notably more acidic, indicating greater proliferation, compared to the media in the wells containing cells transfected with a control and indicated by the pH indicator that is part of complete media, which I also observed in cells transfected with miR-BART10 alone (appendix figure 2). A higher density of cells is also observable by microscope in the wells containing cells transfected with BARTs or miR-BART10 compared to cells transfected with a control.

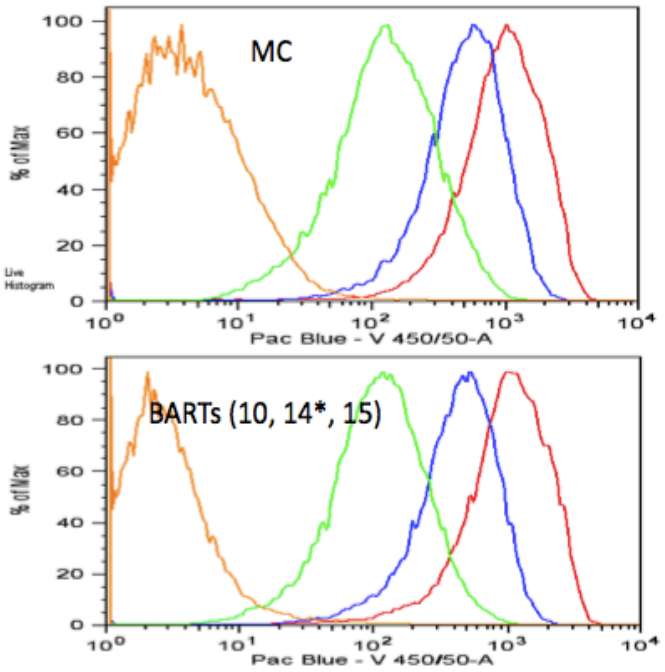

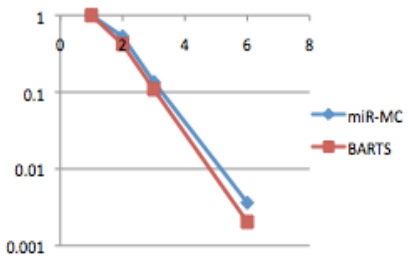

	Day 1	Day 2	Day 3	Day 6
MC	911	483	124	3.37
BARTS	982	413	107	2.27

FIGURE 3.12. **HEK293 cells transfected with miR-BARTs proliferate more rapidly than control transfected cells.** HEK293 cells were transfected using Xtreme gene siRNA transfection reagent (Roche) with microRNA mimic control (A) or mature microRNA BART 10, 14*, and 15 (B) (ambion). Day 1 is shown in red, day 2 in blue, day 3 in green, and day 5 in orange. C. Histograms for microRNA mimic control transfected cells and microRNA BART10 transfected cells are shown together. Mimic control shown in red (day 1), blue (day 2), green (day 3) and orange (day 5) while BARTs shown in teal (day 1), purple (day 2), light brown (day 3), and dark brown (day 5). D. MFI values normalized to day 1 and shown on a log scale. E. Raw numbers of MFI values on each day. N=3

This experiment prompted us to begin investigating proliferation phenotypes with other BART microRNAs individually. For this experiment I employed a second technique for measuring population growth. I transfected HEK293 cells (figure 13) with mi/siRNA as before and calculated the total number of cells on days following transfection. I transfected in 5 BART microRNAs individually in addition to BART10 and a control.

After transfection, I split the cells into three separate dishes in order to get technical triplicates (figure 13, A). I observed a similar increase in proliferation in all conditions except those cells which had been transfected with miR-BART15, which grew at the same rate as control cells (figure 13). To confirm this finding, I repeated the individual transfections with 4 of the microRNAs (including BART10) and an additional microRNA (figure 13, B and D) to ensure the specific control microRNA used in the previous experiment was not having a negative impact on proliferation.

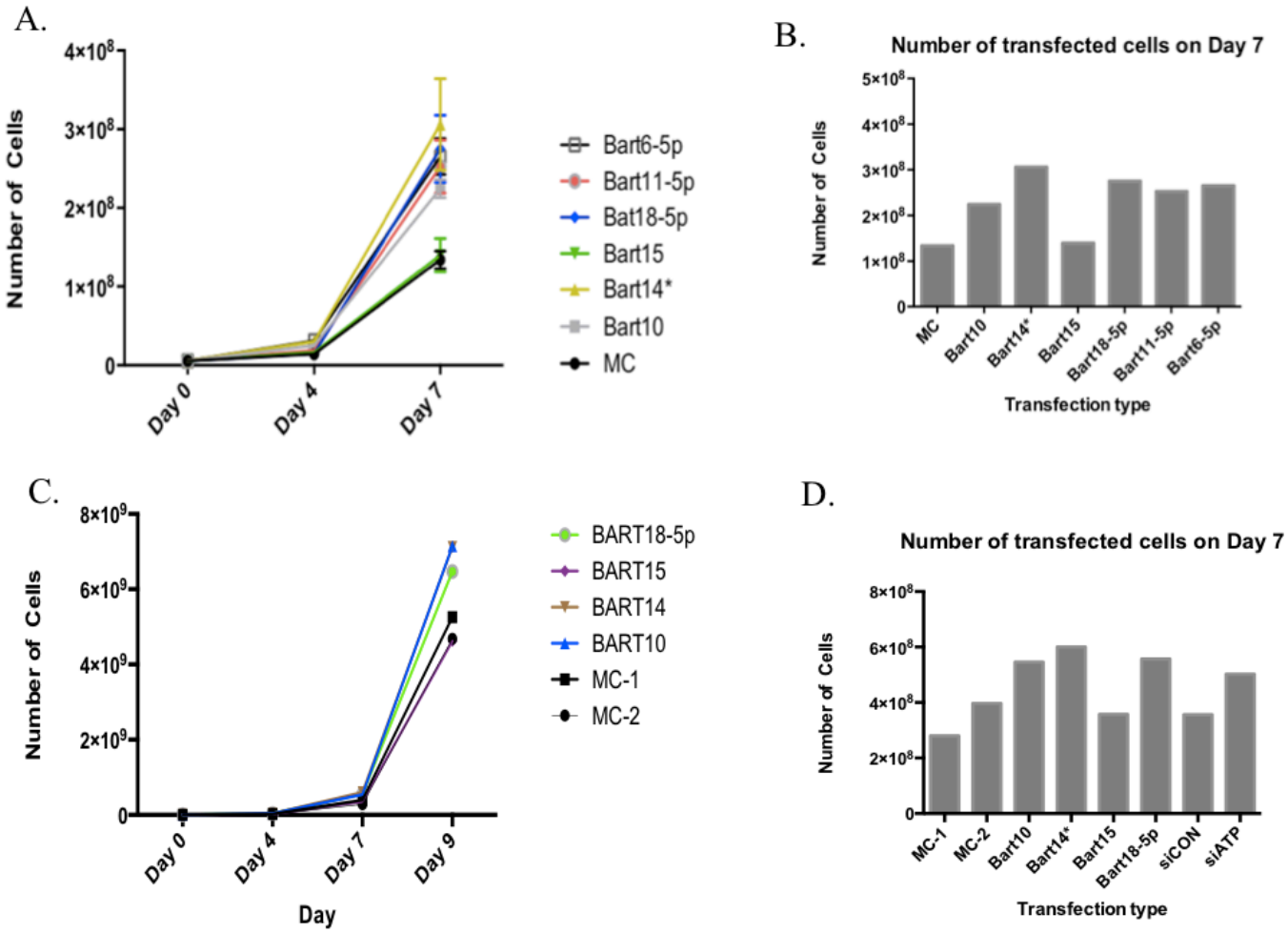

FIGURE 3.13. **HEK293 cells transfected with miR-BARTs proliferate more rapidly than control transfected cells except miR-BART15.** HEK293 cells were transfected using Xtreme gene siRNA transfection reagent (Roche) with miRNAs as in figures 10 and 11. Cells were counted using millipore scepter automated cell counter on days indicated. A and C represent two separate transfection episodes, performed on different dates. B repesents data from the same experiment as A, and D represents data from the same experiment as B.

Therefore, I have established that in addition to miR-BART10, other EBV-miRNAs including 18-5p, 14*, and other, increase proliferation while miR-BART15 does not. Interestingly, BART15 is one of the microRNAs found to be highly expressed in LCL and dysregulated in tumor samples. However, it does not increase rate of proliferation.

3.4. Transfection of miR-BART10 increases presence of acidic vessicles, implying reduction in autophagic flux.

In addition to effects on proliferation, we hypothesized that reduction in ATP6V0e would also have impacts on maintenance of organelle pH or autophagy, two processes that depend heavily on functional V-ATPases. Autophagy is upregulated in vivo in response to stressors such as rapid proliferation, infection with virus (specifically in response to IFN-y), or cellular damage. While excessive autophagy results in cell death, it is usually characterized as a pro-survival adaptation to stress (Xie WY, et al, 2015). Therefore, the relationship between autophagy and cell survival is complicated and not well understood. In contrast, the role of autophagy in cellular defense against pathogens is well characterized. Invading bacteria and viruses, which stimulate autophagy by competing for nutrients and/or binding to TLRs, are ingested and degraded via the autophagic pathway in a process called xenophagy (Tattoli I, et al, 2012; Shelly S, et al, 2009). Autophagy can also deliver cytoplasmic pathogen-associated molecular patterns (PAMPs) to endocytic TLRs and can stimulate their activity through this process (Shi C. et al, 2010). MHC class II antigen presentation of viral antigens is augmented by autophagy, through the same mechanism by which self-antigens are processed (Paludan, et al, 2005). Therefore, it is logical that a pathogen might evolve to downregulate autophagy

as a strategy for immune evasion. In fact, numerous viruses of the Herpesviridae family have been shown to inhibit autophagy. Herpes simplex virus (HSV-1) encodes a virulence protein ICP34.5 which has been shown to inhibit autophagy through interactions with Beclin-1, and HSV-1 mutants lacking this protein are substantially attenuated (Lieb D, et al, 2009). Viral homologues of Bcl-2 encoded by Kaposi sarcoma virus (HHV8), murine gammaherpesvirus 68 (γHV-68), and EBV (HHV-4) have also been shown to inhibit autophagy through interactions with Beclin 1 (Orvedahl A, et al, 2007; Pattingre S , et al, 2005; Sinha S, et al, 2008; Kelly GL, et al, 2009). With regards to EBV, previous work has shown that autophagic vessicles are stabilized during lytic EBV replication and that these autophagic membranes become incorporated into EBV viral envelopes, suggesting that EBV subverts antiviral xenophagy processes and recruits autophagic membranes to its viral envelope for efficient viral packaging during lytic infection (Nowag H, et al, 2013). Others have shown that inhibition of autophagy by Bafilomycin A1 increased EBV lytic genes expression and viral progeny yield, and furthermore observed a decrease in autophagy correlating with increased expression of EBV early antigens, suggesting that EBV inhibits autophagy early after reactivation from latency (De Leo A, et al, 2015)

In order to investigate the impact of miR-BART10 on autophagy, I utilized two assays to look at accumulation of acidic vessicles and accumulation of autophagosomes (LCB-II) separately. HEK293 cells were transfected using lipofectamine reagent (Roche) with miR-BART10, miR-MC, siRNA-control, or siRNA-ATP6V0e1. 36 hours later, the cells were stained with Lysosensor dye (life technologies), which specifically stains acidic organelles such as lysosomes, but is non-fluorescent in neutral pH conditions in the cytoplasm.

Experimental control cells were treated for 1.5 hr with 0.5uM Bafilomycin A1, an established inhibitor of V-type ATPase activity, prior to staining. As seen in Figure 16A (top panel), the cells treated with Bafilomycin A1 exhibited an increase in average fluorescence intensity, indicating an increase in acidity/acidic vessicles in the cell. This observation is consistent with findings in the literature, in which inhibition of the V-type ATPase H+ pump by Bafilomycin A1 reduces the functionality of autolysosomes because they cannot become sufficiently acidic to activate proteasomes, resulting in their accumulation. Bafilomycin also inhibits the step in autophagy where lysosomes and phagosomes fuse due to targeting of CA-P60A/SERCA, which also causes an accumulation of acidic lysosomes (Kallifatidis G, et al, 2013; Mauvezin et al, 2015). Both HEK293 and AGS cells transfected with miR-BART10 also exhibited an increase in median fluorescence intensity, indicating an accumulation of acidic vessicles and implying that rate of autophagy may have been reduced due to reduced expression of ATP6V0e1 (figures 14 and 15). Transfection of both cell lines with the siRNA against ATP6V0e1 also caused an increase in MFI, which is consistent with the observations in miR-BART10 transfected cells (figures 14 and 15).

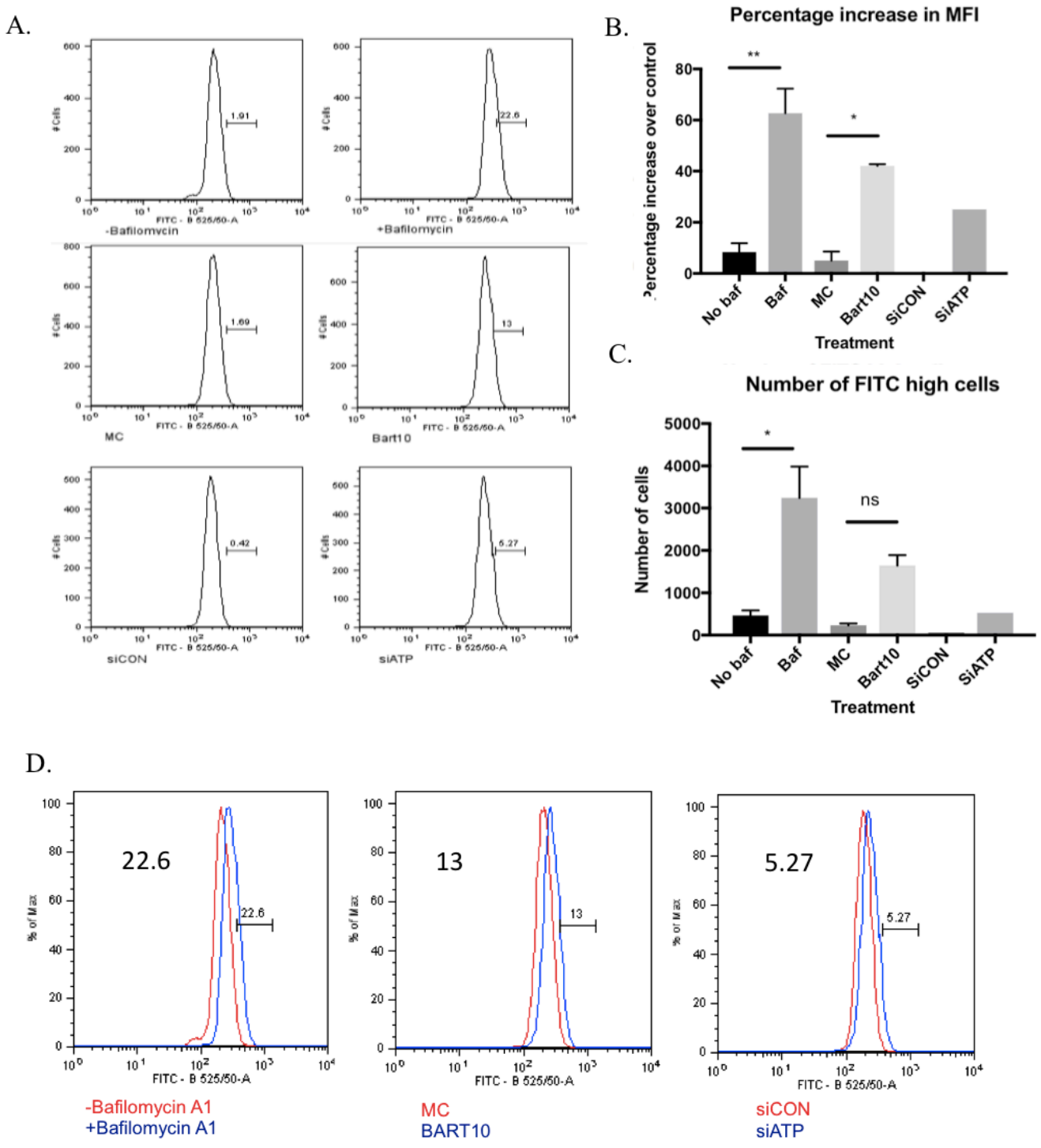

FIGURE 3.14. **Acidic vessicles/lysosomes accumulate in HEK293 cells treated with Bafilomycin A1, or transfected with miR-BART10 or siRNA-ATP6V0e**. A. HEK293 cells were treated with 60uM Bafilomycin A1 for 1.5 hours, or transfected with microRNAs or siRNAs as labeled below the histograms ~36 hours, before being stained

with Lysosensor Green DND-189 (Life technologies) which indicates lower pH with higher intensity of flourescence. Cells were analyzed immediately following staining by flow cytometry. Representative experiment shown, N=3. B. Average MFI of live HEK293 cells for 3 experiments. Calculation was normalized based on lowest MFI value, and percent increase for each condition for each of 3 biological replicate experiments used to get average and standard deviation values. Error bars represent standard deviation. C. Number of cells falling into the "FIT-C high gate, per every 10,000 cells. Average number of cells in FITC high gate per every 10,000 cells for each condition shown for 3 biological replicate experiments. Error bars represent standard deviation. D. Overlay of histograms shown in A.
** indicates $P<0.01$. * indicates $P<0.05$. ns indicates $P>0.05$.

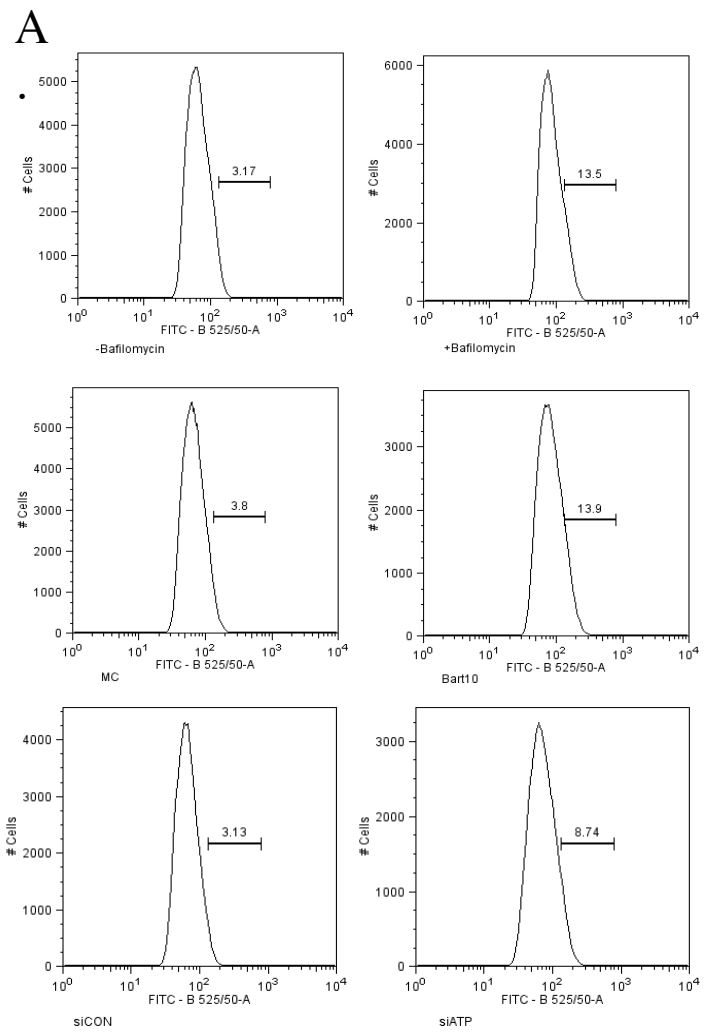
A
3.17
-Bafilomycin
13.5
+Bafilomycin
3.8
MC
13.9
Bart10
3.13
siCON
8.74
siATP
Cells
FITC - B 525/50-A

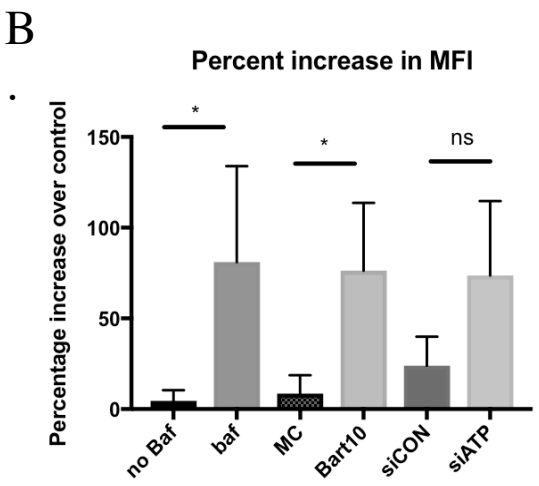
B
Percent increase in MFI
Percentage increase over control
*
*
ns
no Baf
baf
MC
Bart10
siCON
siATP

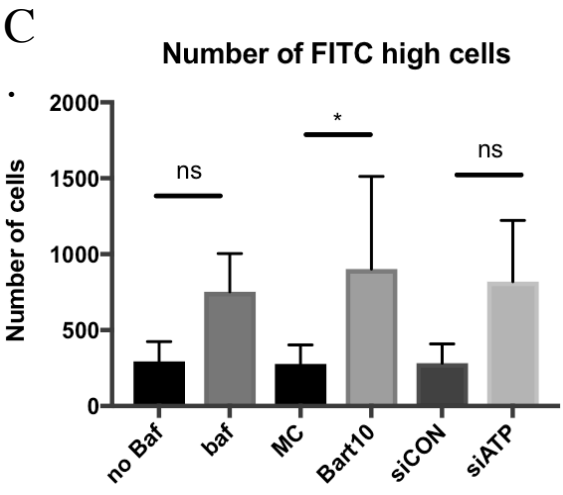
C
Number of FITC high cells
Number of cells
ns
*
ns
no Baf
baf
MC
Bart10
siCON
siATP

D.

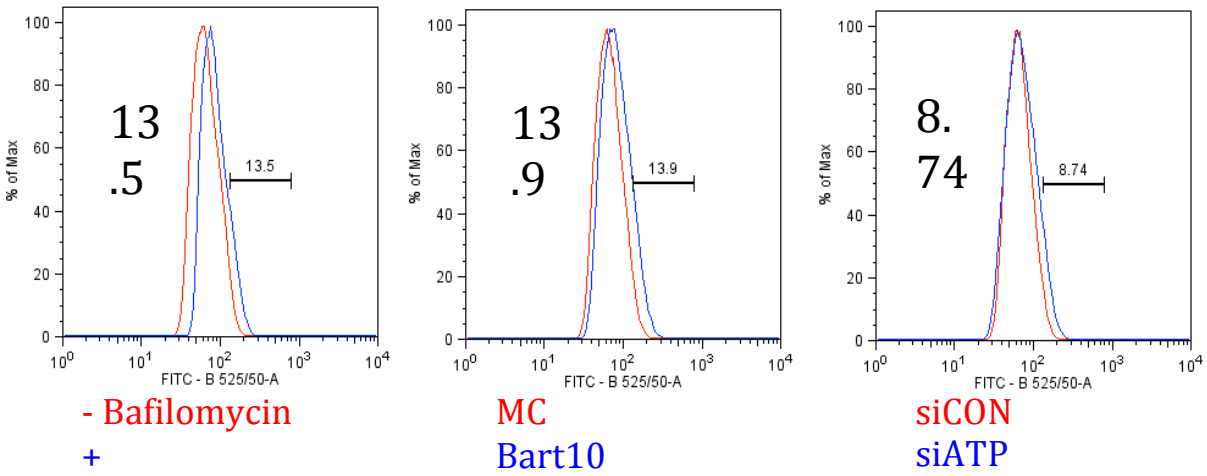

FIGURE 3.15. **Acidic vessicles/lysosomes accumulate in AGS cells treated with Bafilomycin A1, or transfected with miR-BART10 or siRNA-ATP6V0e.** A. AGS cells were treated with 60uM Bafilomycin A1 for 1.5 hours, or transfected with microRNAs or siRNAs as labelled below the histograms ~36 hours, before being stained with Lysosensor Green DND-189 (Life technologies) which indicates lower pH with higher intensity of flourescence. Cells were analyzed immediately following staining by flow cytometry. Representative experiment shown, N=4. B. Average MFI of live HEK293 cells for 4 experiments. Calculation was normalized based on lowest MFI value, and percent increase for each condition for each of 4 biological replicate experiments used to get average and standard deviation values. Error bars represent standard deviation. C. Number of cells falling into the "FIT-C high gate, per every 10,000 cells. Average number of cells in FITC high gate per every 10,000 cells for each condition shown for 4 biological replicate experiments. Error bars represent standard deviation. D. Overlay of histograms shown in A.

** indicates $P<0.01$. * indicates $P<0.05$. ns indicates $P>0.05$.

3.5. Transfection of miR-BART10 increases accumulation of LCB3, a marker for autophagosomes.

Next, to assess whether autolysosomes remain functional upon transfection with miR-BART10, I have performed a western blot with lysates made from transfected cells to determine protein level of LC3B-II. During autophagosome formation, cellular membranes engulf intracellular debris targeted for autophagic degradation. During this step, cytoplasmic LC3B-I is processed to LC3B-II and becomes bound to membranes of autophagosomes. Therefore, LC3B-II is a widely accepted marker for autophagosomes (Mizushima N, et al, 2007). Subsequent to fusion of autophagosomes and lysosomes, the LCB3-II is degraded if conditions are sufficiently acidic and lysosomal proteases are functional. However, in the absence of functional V-ATPases, the autolysosomes abilty to reach sufficiently low pH required for functional autolysosomes may be impaired, and LCB3-II degradation will be reduced. HEK293 cells exhibited detectable levels of LC3B-I at baseline, while LCB3-I was undetectable in AGS cells. Transfection with miR-BART10 or siRNA against ATP6V0e also increased expression of LC3B-I and –II in HEK293 and LCB3-II in AGS cells compared to control microRNA transfected cells after 48 hours, indicating a prolonged downregulation of autophagic flux (figures 16 and 17). This effect could also been seen in cells transfected with siRNA against ATP6V0e compared to control transfected cells (figures 16 and 17). I also observed an increase in LC3B-II protein expression in both HEK293 and AGS cells treated with our control, Bafilomycin A1 (figures 16 and 17). Because the accumulation of LCB3 protein

observed in the western blot was not extreme, I wanted to ensure the result was consistent and reproducible. Therefore, I repeated the transfections and western blot analysis multiple times (figures 18, 19, 20, and 21) and found that the accumulation of LCB3 was consistent each time. The consistency of the results indicates that also the effect is small (as is common for microRNA-induced effects), it is likely due to the expression of miR-BART10 or siRNA-ATP6V0e, and not experimental error or random chance.

Recent work shows that Bafilomycin A1 strongly inhibits ATP6V0e1, and also moderately inhibits CA-P60A/SERCA (Mauvezin et al, 2015). Inhibition of ATP6V0e results in accumulation of non-functional autolysosomes, similarly to our miRNA-BART10 transfected cells, while inhibition of CA-P60A/SERCA prevents fusion of autophagosomes and lysosomes. Therefore, I was able to see a greater accumulation of LC3B-II in a short time (3 hrs) with treatment of Bafilomycin A1 (figures 16, A and 17, A). These results are consistent with the observations in figures 14 and 15 that imply the presence of accumulated acidic autolysosomes.

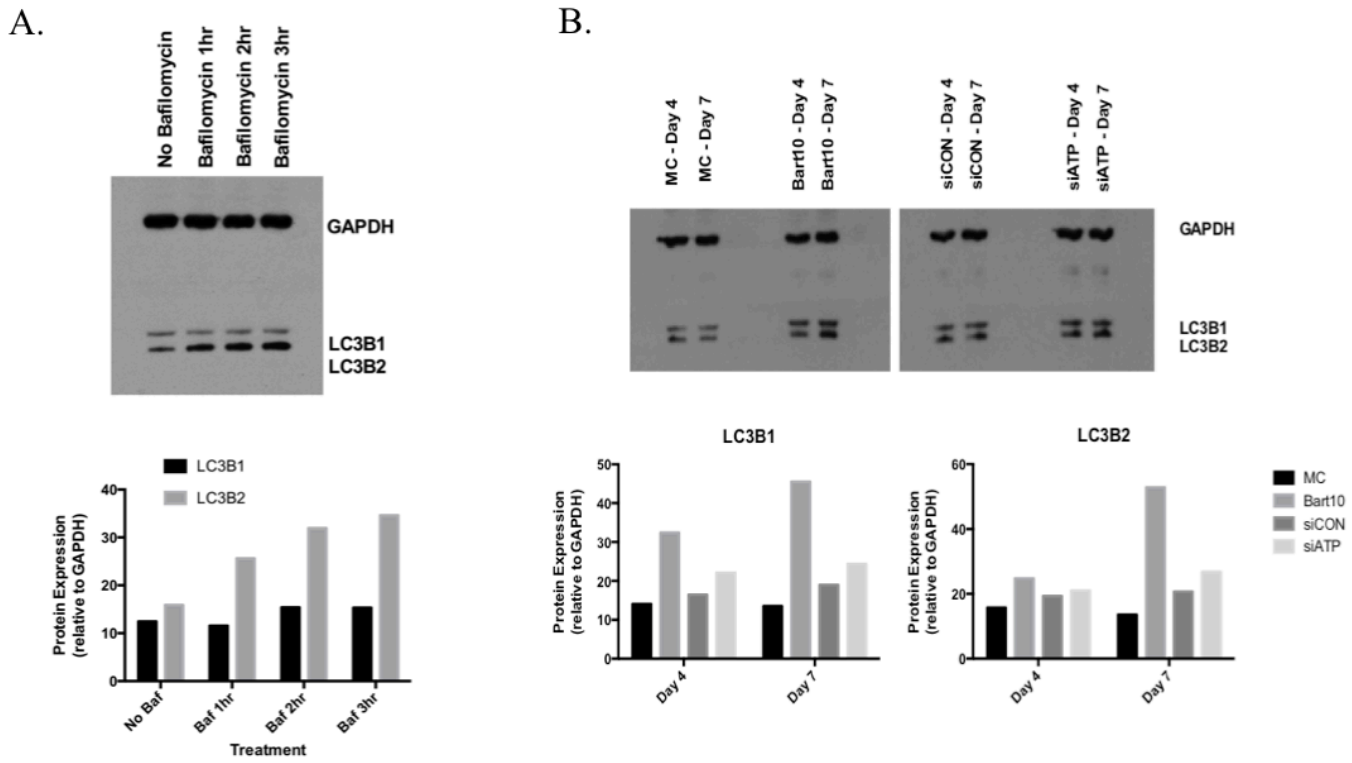

FIGURE 3.16. **HEK293 cells transfected with miR-BART10 or siRNA against ATP6V0e accumulate LCB3**. HEK293 (A,B) cells were treated with 60uM Bafilomycin A1 (A, C) or transfected with indicated mi/siRNA (B, D) 36 hours prior to being lysed at indicated time points. Western Blot was probed with both GapDH (1:10,000) and LCB3 (1:1000) antibodies as indicated.

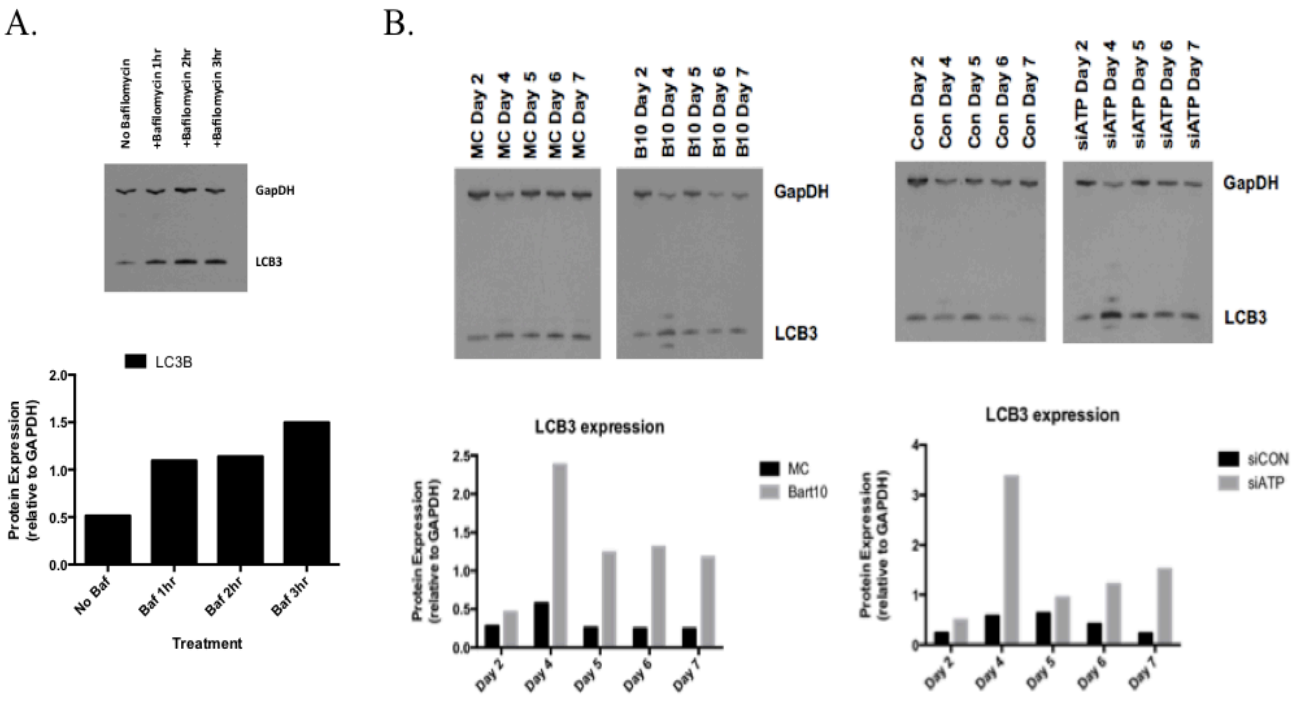

FIGURE 3.17. **AGS cells transfected with miR-BART10 or siRNA against ATP6V0e accumulate LCB3**. AGS cells were treated with 60uM Bafilomycin A1 (A) or transfected with indicated mi/siRNA (B) 36 hours prior to being lysed at indicated time points. Western Blot was probed with both GapDH (1:10,000) and LCB3 (1:1000) antibodies as indicated.

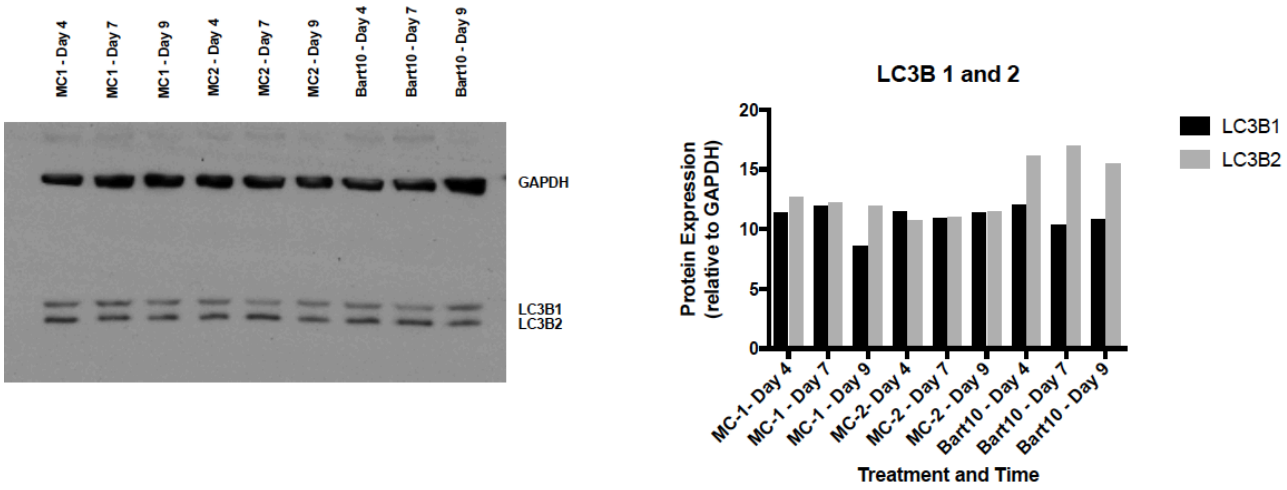

FIGURE 3.18. **HEK293 cells transfected with miR-BART10 or siRNA against ATP6V0e accumulate LCB3**. HEK293 cells were transfected with indicated mi/siRNA (A, B) 36 hours prior to being lysed at indicated time points. Western Blot was probed with both GapDH (1:10,000) and LCB3 (1:1000) antibodies as indicated. (Transfections were repeated to confirm findings).

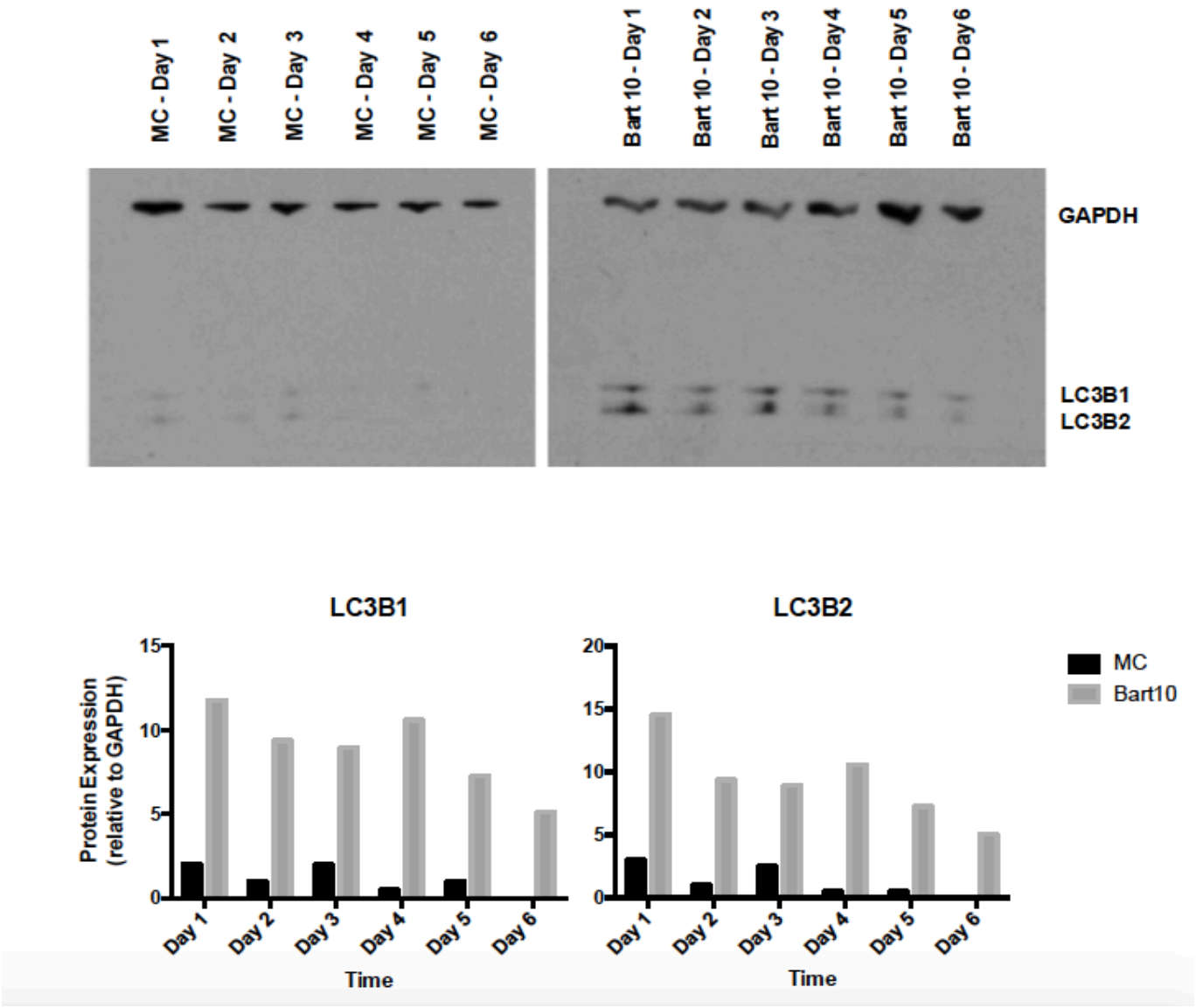

FIGURE 3.19. **HEK293 cells transfected with miR-BART10 or siRNA against ATP6V0e accumulate LCB3**. HEK293 cells were transfected with indicated mi/siRNA (A, B) 36 hours prior to being lysed at indicated time points. Western Blot was probed with both GapDH (1:10,000) and LCB3 (1:1000) antibodies as indicated. (Transfections were repeated to confirm findings).

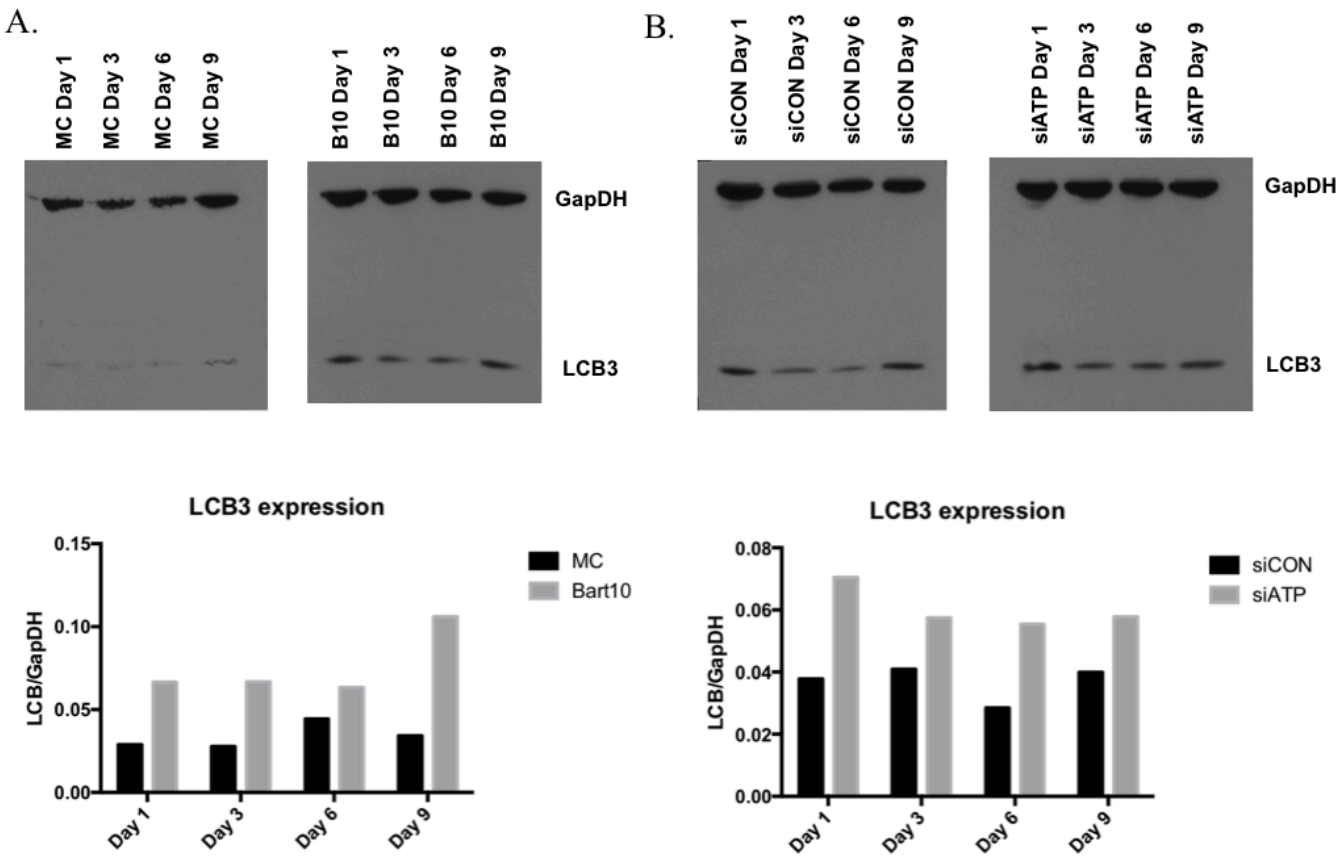

FIGURE 3.20. **AGS cells transfected with miR-BART10 or siRNA against ATP6V0e accumulate LCB3**. AGS cells were transfected with indicated mi/siRNA (A, B) 36 hours prior to being lysed at indicated time points. Western Blot was probed with both GapDH (1:10,000) and LCB3 (1:1000) antibodies as indicated. (Transfections were repeated to confirm findings).

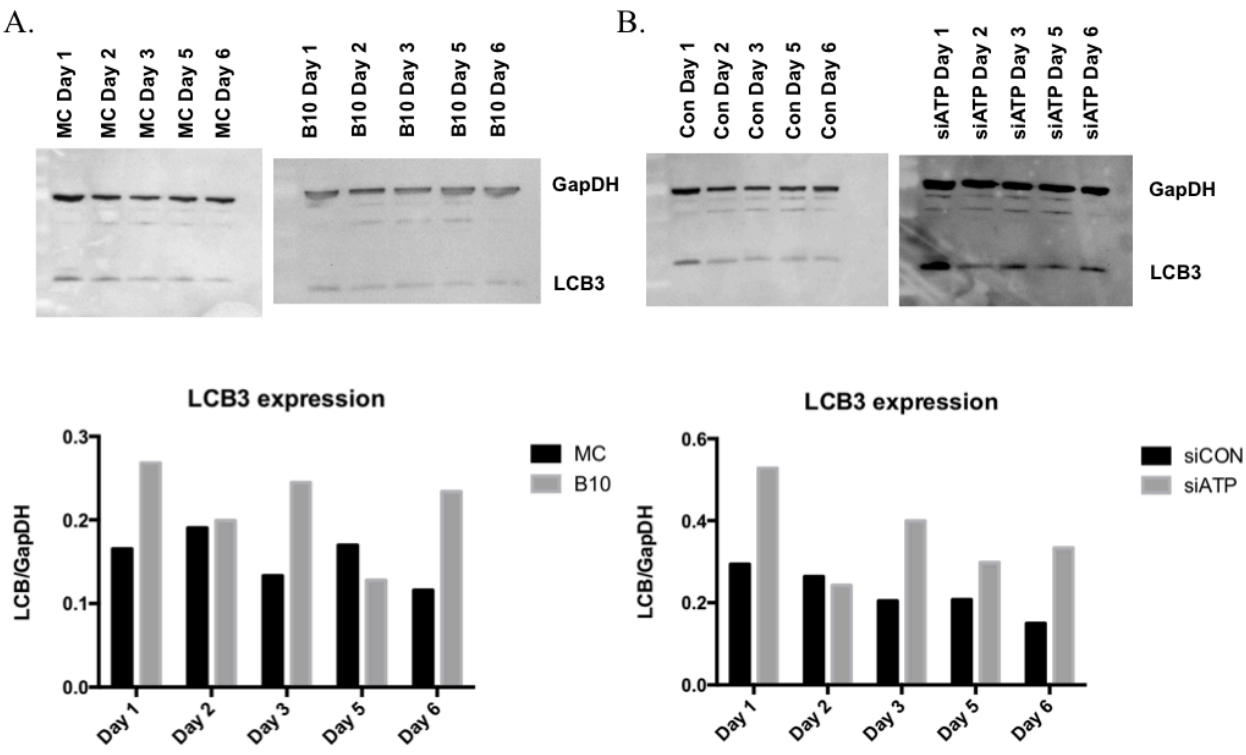

FIGURE 3.21. **AGS cells transfected with miR-BART10 or siRNA against ATP6V0e accumulate LCB3**. AGS cells were transfected with indicated mi/siRNA (A, B) 36 hours prior to being lysed at indicated time points. Western Blot was probed with both GapDH (1:10,000) and LCB3 (1:1000) antibodies as indicated. (Transfections were repeated to confirm findings).

3.6. Accumulation of acidic vessicles and LCB3 is also observable in EBV infected cells compared to control cells

In order to begin to address the question of whether miR-BART10 might be reducing rate of autophagy within the context of EBV infection, we decided to compare AGS.BX1 cells to AGS cells using the same assays as in Aim 2.1.2. AGS.BX1 is a wild-type EBV positive counterpart cell line to AGS cells and therefore provides a very good model for comparison of infected and uninfected cells. AGS.BX1 cells are also one of the few cell lines which express wild type EBV, in contrast to the mutant strain B95.8 commonly expressed in vitro and which is missing many BART microRNAs due to a genetic deletion.

AGS.BX1 cells express latency II transcription program, but have dysregulated BART microRNAs similar to tissue samples shown in introductory figure 4. AGS and AGS.BX1 cells were stained with the Lysosensor dye used in figures 10 and 11. AGS.BX1 cells exhibited a significant increase in average fluorescence intensity, indicating an increase in acidity/acidic vessicles in the cell (figure 22). I also observed an increase in LCB3 in AGS.BX1 cells compared to AGS cells, suggesting that autolysosomes are also accumulated in the infected cell line (figure 22). These observations suggest that AGS cells infected with EBV have a lower rate of autophagy than uninfected AGS cells. Therefore, the phenotype observed in cells transfected with miR-BART10 alone is recapitulated in cells infected with wild type virus. Together with our finding that miR-

BART10 reduces the rate of autophagy, we hypothesize that miR-BART10 may contribute to reducing autophagic flux in the context of EBV infection. Previous work has already suggested that during the lytic phase of infection, EBV inhibits autophagy in order to increase virion production (Nowag H, et al, 2013; De Leo A, et al, 2015), so miR-BART10 expression may be one of a number of strategies employed by EBV to reduce rate of autophagic flux at various stages of infection.

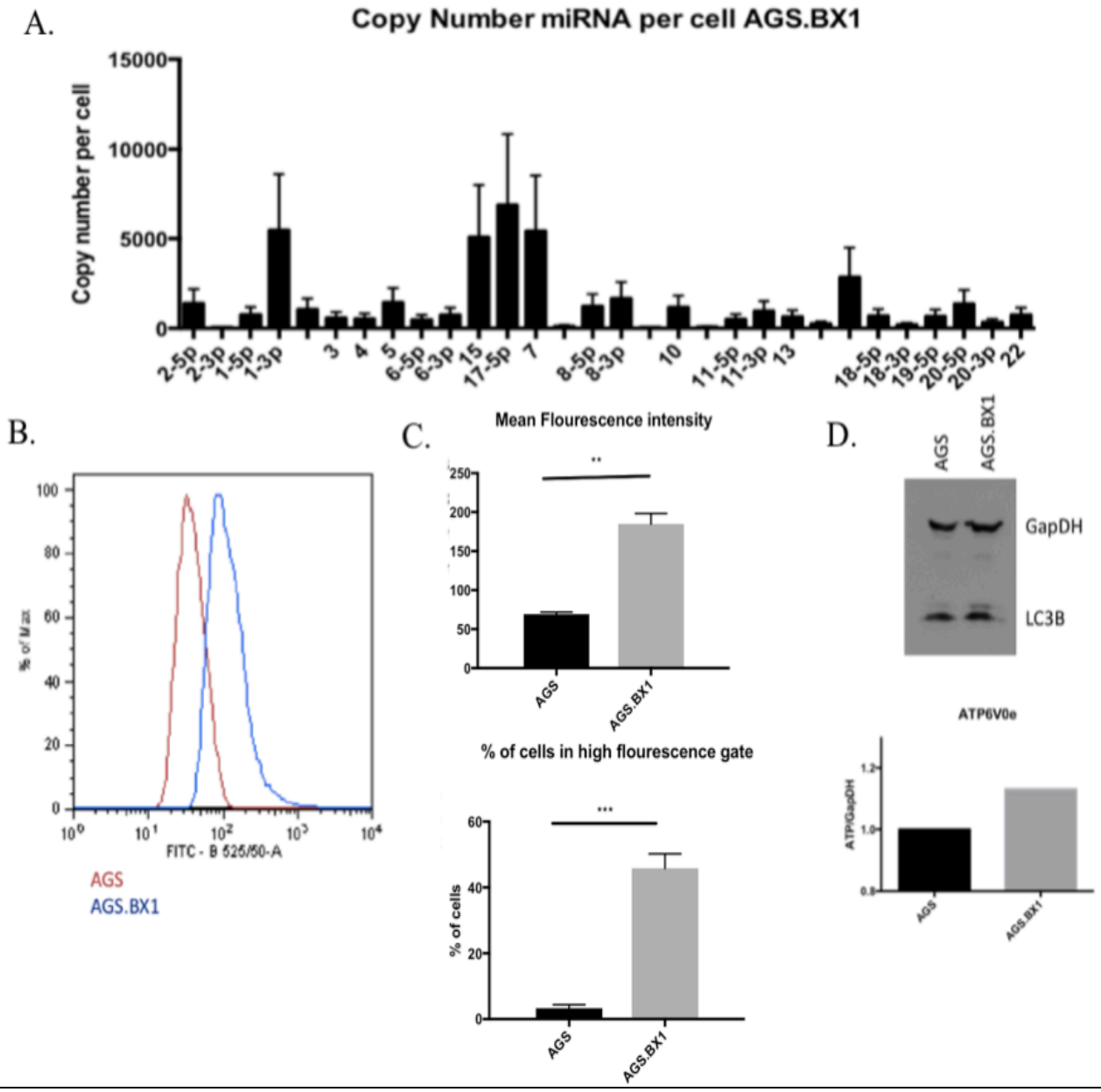

FIGURE 3.22. **AGS.BX1 cells (infected with EBV) accumulate lysosomes and autophagosomes compared to uninfected counterpart (AGS cells).** A. EBV-BART microRNAs in AGS.BX1 cells expressed as copy number per cell. Data generated by Jin Qiu. B. AGS.BX1 AGS and AGS.BX1 cells were stained with Lysosensor DND-189 and analyzed by flow cytometry . C. Quanitifcation from 3 separate experiments of mean flourescence intensity of indicated cells (upper panel) and % of cells in FITC-high gate shown on histogram for indicated cells (lower panel). D. Western blot (top) and quantification of western blot (bottom). *** indicates P<0.001. ** indicates P<0.01

3.7. Conclusions

In this project, I have begun investigating the individual impact of BART microRNAs on proliferation, in order to follow up on observations made in the lab by a previous student that suggested they may promote tumor growth in vivo. With regards to miR-BART10 specifically, I have identified ATP6V0e as a target for BART10 using transient transfections coupled with qRT-PCR and am hoping to confirm the targeting is direct via luciferase assays. ATP6V0e is a crucial gene for V-type H+ ATPases, which are involved in cellular trafficking, maintaining organelle pH, zymogen activation, and receptor mediated endocytosis, among others. I have observed that miR-BART10 promotes accumulation of acidic autolysosomes, suggesting that rate of autophagy is being reduced. I also observed accumulation of LCB3-II, suggesting that degradation autophagosomal cargo in autolysosomes is reduced. I observed a similar effect upon treatment with Bafilomycin A1, an inhibitor of V-type ATPases, and a well-established inhibitor of autophagy. I also observed similar phenotypes in a cell line infected with EBV, compared to its uninfected counterpart. These observations suggest that, in the context of EBV infection, miR-BART10 may contribute to reducing the rate of autophagy by downregulating ATP6V0e mRNA.

Previous work in the literature has shown that gamma herpesviruses including Kaposi sarcoma virus (HSV-8), Herpes simplex virus (HSV-1), Human cytomegalovirus (HCMV), murine gammaherpesvirus 68 (γHV-68), and EBV (HHV-4) inhibit autophagy through interactions of their respective Bcl2 homologues with endogenous Beclin-1 (Leib

D, et al, 2009; Orvedahl A, et al, 2007; Pattingre S , et al, 2005; Sinha S, et al, 2008; English D, et al, 2007). This inhibition promotes immune evasion and in the context of HSV-1 and γHV-68 significantly increases virulence (Leib D, et al, 2009). This project contributes to the existing body of evidence that gammaherpesviruses target autophagy by showing that an EBV encoded microRNA reduces autphagic flux in vitro. Further work is necessary to definitively characterize the impact of this microRNA in the context of an in-vivo EBV infection.

Chapter 4. Discussion

4.1. Evidence that numerous Herpes viruses may inhibit autophagy.

Numerous viruses of the *Herpesviridae* family have been shown to inhibit autophagy. The process of autophagy is important for numerous cellular processes including tissue homeostasis and development, as well as immune control of pathogens and host response to disease in general. Autophagy is therefore carefully regulated by a number of mechanisms. Crucial for this regulation is the evolutionarily conserved pro-autophagy protein, Beclin-1, as well as the anti-autophagy protein Bcl-2, which has been shown to downregulate autophagy through binding to Beclin-1 (Pattingre S , et al, 2005; Maiuri MC, et al, 2007).

Herpes simplex virus (HSV-1) encodes a virulence protein ICP34.5 which acts as a homolouge to Bcl-2 - it has been shown to inhibit autophagy through interactions with Beclin-1, and evidence in the literature shows that HSV-1 mutants lacking this protein are substantially attenuated. The Thomas Ferguson lab created a mutant HSV-1 strain with the Beclin binding domain of ICP34.5 mutated so it would not bind host Beclin-1. This strain was able to replicate as a similar rate to wild type strains at early time points in mice, but was more rapidly cleared and severity of diesase was attenuated. Therefore, the mutant strain's reduced pathengenicity was due to failure to evade adaptive, rather than innate, immunity (Leib D, et al, 2009). Kaposi sarcoma virus has been shown to evade the immune system through targeting of autophagy at every step. Kaposi sarcoma virus encodes homologues of Bcl-2 to inhibit vessicle nucleation (E X, et al, 2009), FLIP to inhibit vessicle elongation (Lee JS, et al, 2009), and K7 to inhibit autophagosome maturation (Liang Q, et al, 2013). These inhibitors of autophagy allow the virus to

sucessfully propegate in host cells, and research has shown that in particular, KHSV's homologue of Bcl-2 (viral Bcl-2, vBcl-2) is required for lytic replication in vitro (Liang Q, et al, 2015). Murine gammaherpesvirus 68 (γHV-68) has also been shown to encode a Bcl-2 homologue, M11 (Wang G, et al, 1999).

4.2. Previous work shows that EBV modulates autophagy through a number of mechanisms.

With regards to EBV, previous work has shown that autophagic vessicles are stabilized during lytic EBV replication and that these autophagic membranes become incorporated into EBV viral envelopes, suggesting that EBV subverts antiviral xenophagy processes and recruits autophagic membranes to its viral envelope for efficient viral packaging during lytic infection (Nowag H, et al, 2013). Others have shown that inhibtion of autophagy by Bafilomycin A1 increased EBV lytic genes expression and viral progeny yield, and furthermore observed a decrease in autophagy correlating with increased expression of EBV early antigens, suggesting that EBV inhibits autophagy early after reactivation from latency (De Leo A, et al, 2015). Expression of EBV lytic genes in vitro has also been shown to block autophagic flux. In this study, the early lytic gene ZEBRA did not inhibit autophagy, but rather autophagy was blocked during the later stage of lytic cycle where viral replication is occurring rapidly. The authors further hypothesized that by blocking the elongation step of autophagy, the virus is able to exploit the autophagic pathway by repurposing the autophagic vesicles for viral transportation into the cell cytoplasm and furthermore avoid viral degradation into the lysosomes (Granato M, et al,

2014). Interestingly, other studies have found that exposure to EBV, at least acutely, induces autophagy. Plasmacytoid dendritic cells were found to release type-1 interferons (IFN) after infection with EBV by a mechanism that requires a functional autophagic pathway (Severa M, et al, 2012). The studies mentioned here and others clearly indicate that EBV has the ability to modulate the autophagic process, potentially contributing to it's ability to evade the immune system as well as its propensity for malignant tranformation of infected cells.

4.3. Evidence that EBV benefits from inhibition of autophagy.

The inhibition of autophagy can benefit EBV during latent infection. As mentioned previously, Epstein Barr Virus Nuclear Antigen 1 (EBNA-1), the sole protein antigen expressed during latency and the dominant CD4+ T cell antigen, has been shown to be digested and presented on MHC-II through a proces that requires autophagy and that inhibition of autophagy decreases it's presentation in vitro (Paludan, et al, 2005). Response to this antigen is paramout for the host's immune system to be able to control the infection (Moorman AM, et al, 2007). Therefore, during latent infection, EBV may subvert the adaptive immune response by downregulating autophagy through expression of miR-BART10, reducing expression of EBNA-1 on MHC molecules on the surface of the host cell. Interestingly, during malignant transformation, autophagy seems to suppress tumor formation by neutralizing damaged oxidative organelles, thereby reducing accumulation of reactive oxygen radicals and preventing genome instability (Matthew R, et al, 2007). Therefore, while the virus may have evolved the ability to suppress

autophagy during latency in order to evade recognition by immune cells, it may also predispose latently infected cells to become malignant.

4.4. Deregulation of Proliferation and cell death in cancer.

The common denominator in all tumors is abnormal (increased) proliferation of malignant cells. Therefore, oncogenes (or, in the normal state, proto-oncogenes) are frequently involved in cell cycle and cellular metabolism. Examples include myc, Ras, Wnt, Erk and Trk. However, genes involved in autophagy and/or apoptosis are also common oncogenes. One of the most famous oncogenes, p53 (Vousden, K and Lu, X, 2002), has been found to be involved in regulation of autophagy. Recent work has shown that mutant p53 inhibits autophagy, but interestingly, functional autophagic flux can degrade mutant p53, in what amounts to a complicated interplay that can drastically impact tumor progression (Moorseli E, et al, 2008). It is well established that autophagy is a crucial mechanism for regulation of cancer cell proliferation and is frequently disregulated especially in therapuetic-resistant cancers (Henson, E. et al, 2017; Zambrano, J. et al, 2016), although apoptosis is frequently involved as well. The interaction between autophagy and proliferation is complex and not fully described, and furthermore is likely impacted by environmental factors within the cell. Investigations into both autophagy and proliferation are therefore very compelling fields of inquiry for advancing scientific understanding of EBV-associated cancers.

4.5. Importance of this work.

The studies referenced above in sections 4.2 and 4.3 contribute to the large body of work that exists linking EBV to modulation of autophagy. The evidence in the literature indicates that EBV encodes elements with the ability to influence rate of autophagy in host cells during infection. Much focus has been on EBV's impact on autophagy during the lytic phase of infection -- however, investigations into the virus' impact on autophagy during the latent phases of infection are needed in order to determine how latent infection with EBV may be contributing to EBV-associated cancers. In this study, I was able to show evidence that suggests that an EBV encoded microRNA, which is highly expressed during the lymphoblastoid (latency III) phase of infection as well as in EBV positive tumors, might be able to reduce the rate of autophagy. I was also able to show that the microRNA, miR-BART10, directly targets the ATP6V0e gene. Furthermore, I have showed that the same microRNA, as well as a number of other EBV encoded microRNAs, are able to reproducibly increase proliferation in vitro. A brief schematic of these finds are represented in figure 4.1. Both proliferation and autophagy are tightly controlled processes within the host cell, and both are disregulated in cancer always or most of the time, respectively. This finding is important to improving our understanding of how infection with EBV can be playing a role in so many disparate types of cancer. These "common denominator" processes being impacted by EBV is a logical and concise answer to the question, what about infection with EBV promotes malignant transformation? This work shows a novel target for EBV encoded microRNA BART10,

ATP6V0e, and furthermore begins investigations into characterizing the functional significance of this targeting.

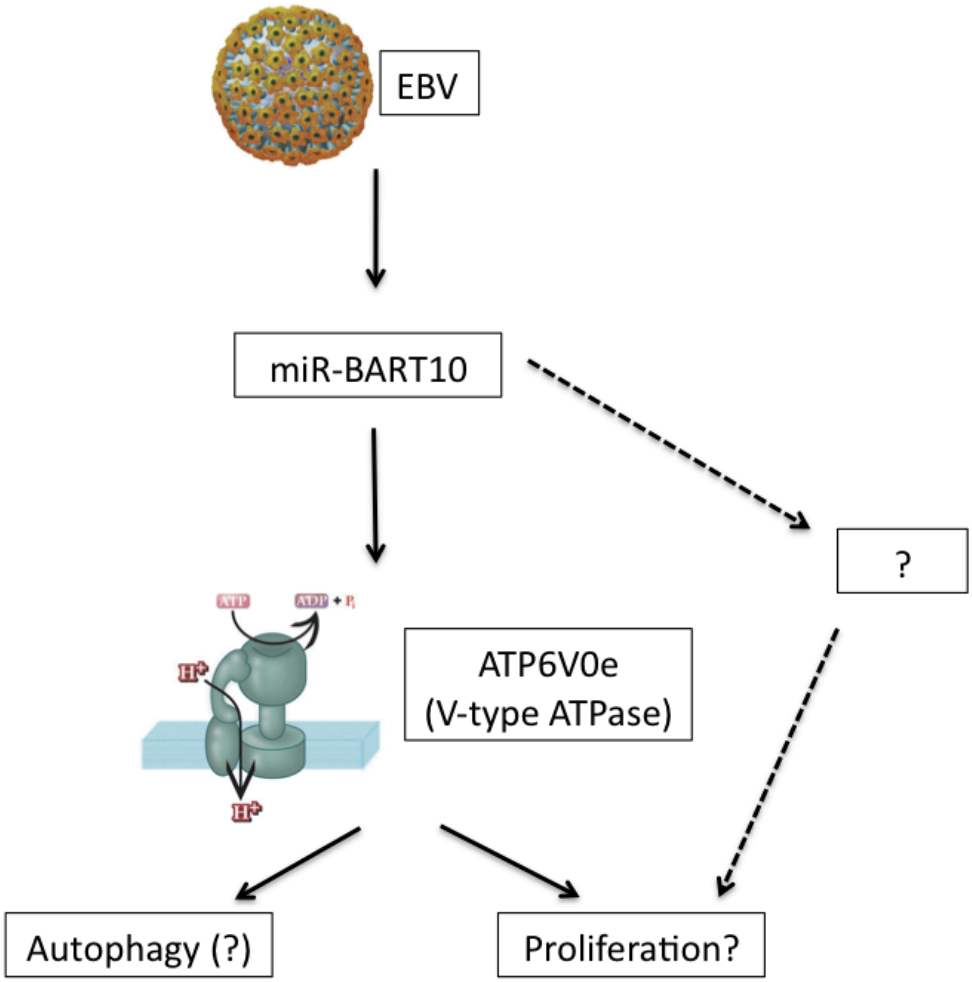

Figure 4.1. **Brief Schematic illustrating the main findings of this project.** In this project I was able to show that EBV encoded microRNA, miR-BART10, directly targets the gene encoded a subunit of the host's V-type ATPase. This would cause instability in the assembled V-ATPase unit, and therefore it could not function normally. V-Type ATPases play a known role in autophagy, and my studies suggest that through ATP6V0e, mir-BART10 may be impacting autophagy. My studies also suggest that through the same target, miR-BART10 may also impact proliferaion, although the effect on proliferation may be through other, as yes unknown, targets as well.

4.6. Future Directions.

In the short term, further explorations into proliferation associated BART microRNAs, and miR-BART10 specifically, could focus on inducing the observed phenotypes in pursuit of observing a more conclusive and exaggerated phenotype. For example, INF-y or rapamycin could be used to induce autophagy in miR-BART10 transfected cells and the same assays could be performed to determine if miR-BART10 significantly reduces induction of autophagy. Depending on the type of cell, primary cells can be induced to proliferate by stimulation by signaling molecules that bind receptors on the surface of the cells. Inducing proliferation in cell lines can be difficult due to the fact that cell lines are generally derived from cancers and are thus rapidly proliferating already.

It would also be interesting to investigate other EBV-encoded microRNA targets, with the eventual goal of teasing out the ways in which multiple microRNAs may be acting together by targeting multiple factors in a single signaling cascade. Current technologies may not exist to allow for expeditious experiments to address this question, however it could be addressed in the future as more and more tools become available to researchers.

Future work could also attempt to connect the proliferation phenotype to the reduction in V-ATPase activity. An increase in proliferation was observed in cells transfected with siRNA against ATP6V0e, which suggests reducing ATP6V0e mRNA increases rate of proliferation in vitro. A simple test to determine whether reducing autophagy increases proliferation in vitro would be to transfect cells with siRNA against another protein that is essential for autophagy, and observe if proliferation is similarly increased. If we observe an increase in proliferation, this would provide evidence that the increase in

proliferation in miR-BART10 transfected cells observed previously is due to reduced rate of autophagy due to downregulation of ATP6V0e mRNA. This would not explain the mechanism of how autophagy and proliferation are connected, however. More sophisticated experimental techniques would likely be necessary in order to uncover the exact process that occurs when proliferation is increased in vitro due to a decrease in rate of autophagy.

Chapter 5. Appendix

5.1. Optimization of Electroporation:

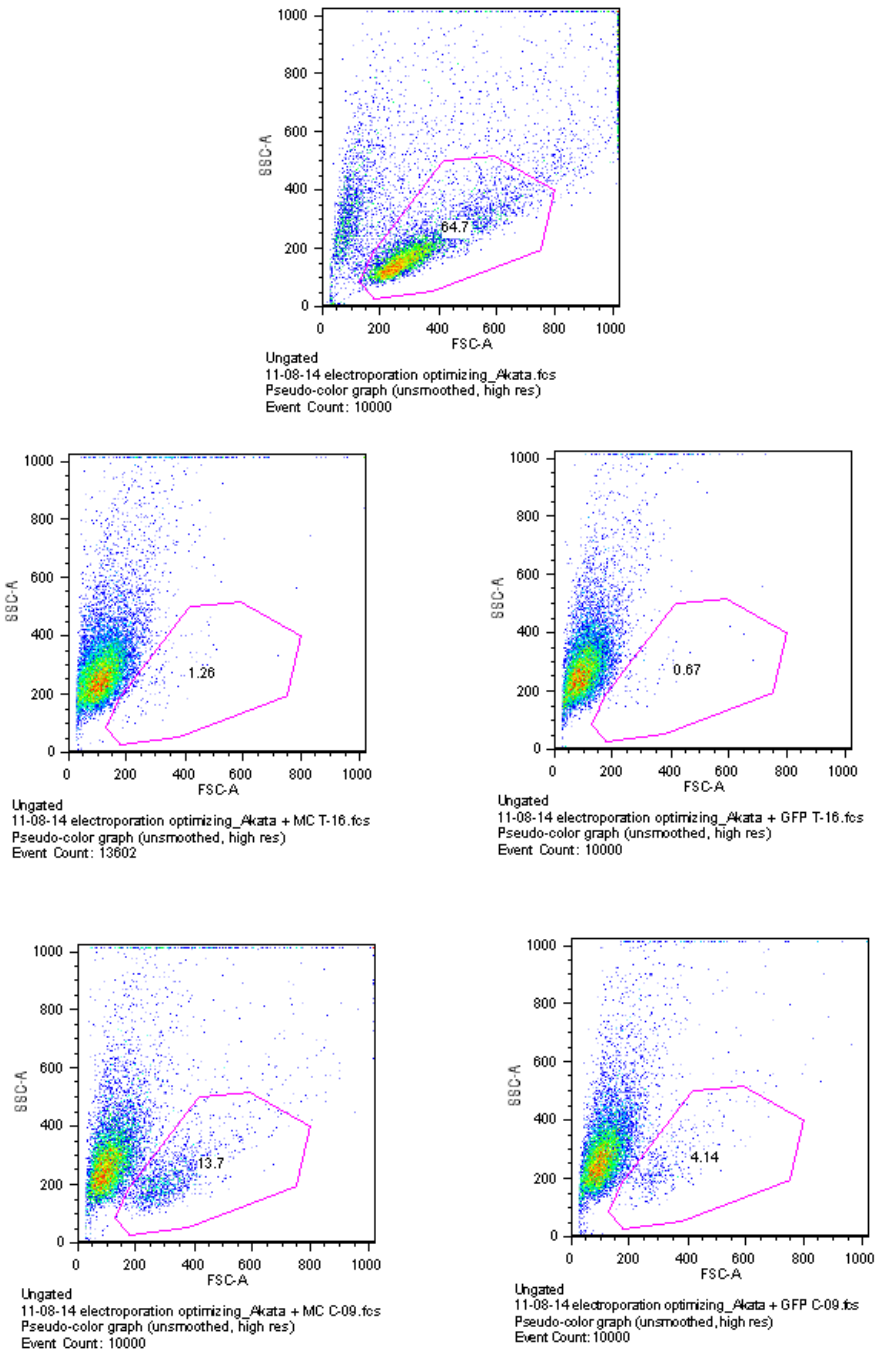

FIGURE 5.1. Flow Cytometry Plots. These flow cytometry plots are annotated at bottom left with the condition used on the AMAXA nucleofector for the transfection of GFP for optimization purproses. Different electroporation programs using the Nucleofector (Lonza) were used to transfect cells with GFP, and analyzed by FACS for viability and tranfection efficiency.

FIGURE 5.2. Sequences of oligos that were inserted into the Pcheck2 Vector for the Luciferase Assay.

Oligos were synthesized by Integrated DNA Technologies, Inc. and sequences were as follows:

5' UTR:
AATTCGTTTAAACCTAGAGCAGGCGGGGCTTGCACACGCTGGTCACGCGGTC
AGCTATTGACACTTCCTGGTGGGATCCGAGTGAGGCGACGGGGTAGGGGTTG
GCGCTCAGGCGGCGACCATGGCGTATCACGGCCTCACTGTGCCTCTCATTGTG
ATGAGCGTGTTCTGGGGCTTCGTCGGCTTCTTGGTGCCTTGGTTCATCCCTAA
GGGTCCTAACCGGGGAGTTAGGCCGCTGGCCGCAATAAAA
Coding Region:
AATTCGTTTAAACCTAGAGCATGGCGTATCACGGCCTCACTGTGCCTCTCATT
GTGATGAGCGTGTTCTGGGGCTTCGTCGGCTTCTTGGTGCCTTGGTTCATCCC
TAAGGGTCCTAACCGGGGAGTTATCATTACCATGTTGGTGACCTGTTCAGTTT
GCTGCTATCTCTTTTGGCTGATTGCAATTCTGGCCCAACTCAACCCTCTCTTTG
GACCGCAATTGAAAAATGAAACCATCTGGTATCTGAAGTATCATTGGCCTTG
AGGCCGCTGGCCGCAATAAAA
3'UTR:
AATTCGTTTAAACCTAGAGCGGAAGAAGACATGCTCTACAGTGCTCAGTCTTT
GAGGTCACGAGAAGAGAATGCCTTCTAGATGCAAAATCACCTCCAAACCAGA
CCACTTTTCTTGACTTGCCTGTTTTGGCCATTAGCTGCCTTAAACGTTAACAGC
ACATTTGAATGCCTTATTCTACAATGCAGCGTGTTTTCCTTTGCCTTTTTTGCA
CTTTGGTGAATTACGTGCCTCCATAACCTGAACTGTGCCGACTCCACAAAACG
ATTATGTACTCTTCTGAGATAGAAGATGCTGTTCTTCTGAGAGATACGTTACT
CTCTCCTTGGAATCTGTGGATTTGAAGATGGCTCCTGCCTTCTCACGTGGGAA
TCAGTGAAGTGTTTAGAAACTGCTGCAAGACAAACAAGACTCCAGTGGGGTG
GTCAGTAGGAGAGCACGTTCAGAGGGAAGAGCCATCTCAACAGAATCGCAC
CAAACTATACTTTCAGGATGAATTTCTTCTTTCTGCCATCTTTTGGAATAAATA
TTTTCCTCCTTTCTATGGAAATCTGGAAAAAAAAAAAA
GGCCGCTGGCCGCAATAAAA

FIGURE 5.3. PSIcheck2 Vector Sequence.

AGATCTGCGCAGCACCATGGCCTGAAATAACCTCTGAAAGAGGAACTTGGTT
AGGTACCTTCTGAGGCGGAAAGAACCAGCTGTGGAATGTGTGTCAGTTAGGG
TGTGGAAAGTCCCCAGGCTCCCCAGCAGGCAGAAGTATGCAAAGCATGCATC
TCAATTAGTCAGCAACCAGGTGTGGAAAGTCCCCAGGCTCCCCAGCAGGCAG
AAGTATGCAAAGCATGCATCTCAATTAGTCAGCAACCATAGTCCCGCCCCTA

ACTCCGCCCATCCCGCCCCTAACTCCGCCCAGTTCCGCCCATTCTCCGCCCCA
TGGCTGACTAATTTTTTTTATTTATGCAGAGGCCGAGGCCGCCTCGGCCTCTG
AGCTATTCCAGAAGTAGTGAGGAGGCTTTTTTGGAGGCCTAGGCTTTTGCAA
AAAGCTTGATTCTTCTGACACAACAGTCTCGAACTTAAGCTGCAGAAGTTGGT
CGTGAGGCACTGGGCAGGTAAGTATCAAGGTTACAAGACAGGTTTAAGGAG
ACCAATAGAAACTGGGCTTGTCGAGACAGAGAAGACTCTTGCGTTTCTGATA
GGCACCTATTGGTCTTACTGACATCCACTTTGCCTTTCTCTCCACAGGTGTCCA
CTCCCAGTTCAATTACAGCTCTTAAGGCTAGAGTACTTAATACGACTCACTAT
AGGCTAGCCACCATGGCTTCCAAGGTGTACGACCCCGAGCAACGCAAACGCA
TGATCACTGGGCCTCAGTGGTGGGCTCGCTGCAAGCAAATGAACGTGCTGGA
CTCCTTCATCAACTACTATGATTCCGAGAAGCACGCCGAGAACGCCGTGATTT
TTCTGCATGGTAACGCTGCCTCCAGCTACCTGTGGAGGCACGTCGTGCCTCAC
ATCGAGCCCGTGGCTAGATGCATCATCCCTGATCTGATCGGAATGGGTAAGT
CCGGCAAGAGCGGGAATGGCTCATATCGCCTCCTGGATCACTACAAGTACCT
CACCGCTTGGTTCGAGCTGCTGAACCTTCCAAAGAAAATCATCTTTGTGGGCC
ACGACTGGGGGGCTTGTCTGGCCTTTCACTACTCCTACGAGCACCAAGACAA
GATCAAGGCCATCGTCCATGCTGAGAGTGTCGTGGACGTGATCGAGTCCTGG
GACGAGTGGCCTGACATCGAGGAGGATATCGCCCTGATCAAGAGCGAAGAG
GGCGAGAAAATGGTGCTTGAGAATAACTTCTTCGTCGAGACCATGCTCCCAA
GCAAGATCATGCGGAAACTGGAGCCTGAGGAGTTCGCTGCCTACCTGGAGCC
ATTCAAGGAGAAGGGCGAGGTTAGACGGCCTACCCTCTCCTGGCCTCGCGAG
ATCCCTCTCGTTAAGGGAGGCAAGCCCGACGTCGTCCAGATTGTCCGCAACT
ACAACGCCTACCTTCGGGCCAGCGACGATCTGCCTAAGATGTTCATCGAGTC
CGACCCTGGGTTCTTTTCCAACGCTATTGTCGAGGGAGCTAAGAAGTTCCCTA
ACACCGAGTTCGTGAAGGTGAAGGGCCTCCACTTCAGCCAGGAGGACGCTCC
AGATGAAATGGGTAAGTACATCAAGAGCTTCGTGGAGCGCGTGCTGAAGAAC
GAGCAGTAATTCTAGGCGATCGCTCGAGCCCGGGAATTCGTTTAAACCTAGA
GC/GGCCGCTGGCCGCAATAAAATATCTTTATTTTCATTACATCTGTGTGTTGG
TTTTTTGTGTGAGGATCTAAATGAGTCTTCGGACCTCGCGGGGGCCGCTTAAG
CGGTGGTTAGGGTTTGTCTGACGCGGGGGGAGGGGGAAGGAACGAAACACT
CTCATTCGGAGGCGGCTCGGGGTTTGGTCTTGGTGGCCACGGGCACGCAGAA
GAGCGCCGCGATCCTCTTAAGCACCCCCCCGCCCTCCGTGGAGGCGGGGGTT
TGGTCGGCGGGTGGTAACTGGCGGGCCGCTGACTCGGGCGGGTCGCGCGCCC
CAGAGTGTGACCTTTTCGGTCTGCTCGCAGACCCCCGGGCGGCGCCGCCGCG
GCGGCGACGGGCTCGCTGGGTCCTAGGCTCCATGGGGACCGTATACGTGGAC
AGGCTCTGGAGCATCCGCACGACTGCGGTGATATTACCGGAGACCTTCTGCG
GGACGAGCCGGGTCACGCGGCTGACGCGGAGCGTCCGTTGGGCGACAAACA
CCAGGACGGGGCACAGGTACACTATCTTGTCACCCGGAGGCGCGAGGGACTG
CAGGAGCTTCAGGGAGTGGCGCAGCTGCTTCATCCCCGTGGCCCGTTGCTCG
CGTTTGCTGGCGGTGTCCCCGGAAGAAATATATTTGCATGTCTTTAGTTCTAT
GATGACACAAACCCCGCCCAGCGTCTTGTCATTGGCGAATTCGAACACGCAG
ATGCAGTCGGGGCGGCGCGGTCCCAGGTCCACTTCGCATATTAAGGTGACGC
GTGTGGCCTCGAACACCGAGCGACCCTGCAGCGACCCGCTTAAAAGCTTGGC
ATTCCGGTACTGTTGGTAAAGCCACCATGGCCGATGCTAAGAACATTAAGAA
GGGCCCTGCTCCCTTCTACCCTCTGGAGGATGGCACCGCTGGCGAGCAGCTG
CACAAGGCCATGAAGAGGTATGCCCTGGTGCCTGGCACCATTGCCTTCACCG

ATGCCCACATTGAGGTGGACATCACCTATGCCGAGTACTTCGAGATGTCTGTG
CGCCTGGCCGAGGCCATGAAGAGGTACGGCCTGAACACCAACCACCGCATCG
TGGTGTGCTCTGAGAACTCTCTGCAGTTCTTCATGCCAGTGCTGGGCGCCCTG
TTCATCGGAGTGGCCGTGGCCCCTGCTAACGACATTTACAACGAGCGCGAGC
TGCTGAACAGCATGGGCATTTCTCAGCCTACCGTGGTGTTCGTGTCTAAGAAG
GGCCTGCAGAAGATCCTGAACGTGCAGAAGAAGCTGCCTATCATCCAGAAGA
TCATCATCATGGACTCTAAGACCGACTACCAGGGCTTCCAGAGCATGTACAC
ATTCGTGACATCTCATCTGCCTCCTGGCTTCAACGAGTACGACTTCGTGCCAG
AGTCTTTCGACAGGGACAAAACCATTGCCCTGATCATGAACAGCTCTGGGTC
TACCGGCCTGCCTAAGGGCGTGGCCCTGCCTCATCGCACCGCCTGTGTGCGCT
TCTCTCACGCCCGCGACCCTATTTTCGGCAACCAGATCATCCCCGACACCGCT
ATTCTGAGCGTGGTGCCATTCCACCACGGCTTCGGCATGTTCACCACCCTGGG
CTACCTGATTTGCGGCTTTCGGGTGGTGCTGATGTACCGCTTCGAGGAGGAGC
TGTTCCTGCGCAGCCTGCAAGACTACAAAATTCAGTCTGCCCTGCTGGTGCCA
ACCCTGTTCAGCTTCTTCGCTAAGAGCACCCTGATCGACAAGTACGACCTGTC
TAACCTGCACGAGATTGCCTCTGGCGGCGCCCCACTGTCTAAGGAGGTGGGC
GAAGCCGTGGCCAAGCGCTTTCATCTGCCAGGCATCCGCCAGGGCTACGGCC
TGACCGAGACAACCAGCGCCATTCTGATTACCCCAGAGGGCGACGACAAGCC
TGGCGCCGTGGGCAAGGTGGTGCCATTCTTCGAGGCCAAGGTGGTGGACCTG
GACACCGGCAAGACCCTGGGAGTGAACCAGCGCGGCGAGCTGTGTGTGCGC
GGCCCTATGATTATGTCCGGCTACGTGAATAACCCTGAGGCCACAAACGCCC
TGATCGACAAGGACGGCTGGCTGCACTCTGGCGACATTGCCTACTGGGACGA
GGACGAGCACTTCTTCATCGTGGACCGCCTGAAGTCTCTGATCAAGTACAAG
GGCTACCAGGTGGCCCCAGCCGAGCTGGAGTCTATCCTGCTGCAGCACCCTA
ACATTTTCGACGCCGGAGTGGCCGGCCTGCCCGACGACGATGCCGGCGAGCT
GCCTGCCGCCGTCGTCGTGCTGGAACACGGCAAGACCATGACCGAGAAGGA
GATCGTGGACTATGTGGCCAGCCAGGTGACAACCGCCAAGAAGCTGCGCGGC
GGAGTGGTGTTCGTGGACGAGGTGCCCAAGGGCCTGACCGGCAAGCTGGACG
CCCGCAAGATCCGCGAGATCCTGATCAAGGCTAAGAAAGGCGGCAAGATCG
CCGTGTAATAATTCTAGAGTCGGGGCGGCCGGCCGCTTCGAGCAGACATGAT
AAGATACATTGATGAGTTTGGACAAACCACAACTAGAATGCAGTGAAAAAA
ATGCTTTATTTGTGAAATTTGTGATGCTATTGCTTTATTTGTAACCATTATAAG
CTGCAATAAACAAGTTAACAACAACAATTGCATTCATTTTATGTTTCAGGTTC
AGGGGGAGGTGTGGGAGGTTTTTTAAAGCAAGTAAAACCTCTACAAATGTGG
TAAAATCGATAAGGATCCAGGTGGCACTTTTCGGGGAAATGTGCGCGGAACC
CCTATTTGTTTATTTTTCTAAATACATTCAAATATGTATCCGCTCATGAGACAA
TAACCCTGATAAATGCTTCAATAATATTGAAAAAGGAAGAGTATGAGTATTC
AACATTTCCGTGTCGCCCTTATTCCCTTTTTTGCGGCATTTTGCCTTCCTGTTTT
TGCTCACCCAGAAACGCTGGTGAAAGTAAAAGATGCTGAAGATCAGTTGGGT
GCACGAGTGGGTTACATCGAACTGGATCTCAACAGCGGTAAGATCCTTGAGA
GTTTTCGCCCCGAAGAACGTTTTCCAATGATGAGCACTTTTAAAGTTCTGCTA
TGTGGCGCGGTATTATCCCGTATTGACGCCGGGCAAGAGCAACTCGGTCGCC
GCATACACTATTCTCAGAATGACTTGGTTGAGTACTCACCAGTCACAGAAAA
GCATCTTACGGATGGCATGACAGTAAGAGAATTATGCAGTGCTGCCATAACC
ATGAGTGATAACACTGCGGCCAACTTACTTCTGACAACGATCGGAGGACCGA
AGGAGCTAACCGCTTTTTTGCACAACATGGGGGATCATGTAACTCGCCTTGAT

CGTTGGGAACCGGAGCTGAATGAAGCCATACCAAACGACGAGCGTGACACC
ACGATGCCTGTAGCAATGGCAACAACGTTGCGCAAACTATTAACTGGCGAAC
TACTTACTCTAGCTTCCCGGCAACAATTAATAGACTGGATGGAGGCGGATAA
AGTTGCAGGACCACTTCTGCGCTCGGCCCTTCCGGCTGGCTGGTTTATTGCTG
ATAAATCTGGAGCCGGTGAGCGTGGGTCTCGCGGTATCATTGCAGCACTGGG
GCCAGATGGTAAGCCCTCCCGTATCGTAGTTATCTACACGACGGGGAGTCAG
GCAACTATGGATGAACGAAATAGACAGATCGCTGAGATAGGTGCCTCACTGA
TTAAGCATTGGTAACTGTCAGACCAAGTTTACTCATATATACTTTAGATTGAT
TTAAAACTTCATTTTTAATTTAAAAGGATCTAGGTGAAGATCCTTTTTGATAA
TCTCATGACCAAAATCCCTTAACGTGAGTTTTCGTTCCACTGAGCGTCAGACC
CCGTAGAAAAGATCAAAGGATCTTCTTGAGATCCTTTTTTTCTGCGCGTAATC
TGCTGCTTGCAAACAAAAAAACCACCGCTACCAGCGGTGGTTTGTTTGCCGG
ATCAAGAGCTACCAACTCTTTTTCCGAAGGTAACTGGCTTCAGCAGAGCGCA
GATACCAAATACTGTTCTTCTAGTGTAGCCGTAGTTAGGCCACCACTTCAAGA
ACTCTGTAGCACCGCCTACATACCTCGCTCTGCTAATCCTGTTACCAGTGGCT
GCTGCCAGTGGCGATAAGTCGTGTCTTACCGGGTTGGACTCAAGACGATAGT
TACCGGATAAGGCGCAGCGGTCGGGCTGAACGGGGGGTTCGTGCACACAGC
CCAGCTTGGAGCGAACGACCTACACCGAACTGAGATACCTACAGCGTGAGCT
ATGAGAAAGCGCCACGCTTCCCGAAGGGAGAAAGGCGGACAGGTATCCGGT
AAGCGGCAGGGTCGGAACAGGAGAGCGCACGAGGGAGCTTCCAGGGGGAAA
CGCCTGGTATCTTTATAGTCCTGTCGGGTTTCGCCACCTCTGACTTGAGCGTC
GATTTTTGTGATGCTCGTCAGGGGGGCGGAGCCTATGGAAAAACGCCAGCAA
CGCGGCCTTTTTACGGTTCCTGGCCTTTTGCTGGCCTTTTGCTCACATGGCTCG
AC

FIGURE 5.4. Primer Sequences.

Human GAPDH (PrimerBank ID 7669492a3):

F: CATGAGAAGTATGACAACAGCCT

R: AGTCCTTCCACGATACCAAAGT

Human FBXW7:

F: CGACGCCGAATTACATCTGTC

R: CGTTGAAACTGGGGTTCTATCA

Human ATP6V0e

F: GGTGACCTGTTCAGTTTGCTG

R: AAAGAGAGGGTTGAGTTGGGC

siRNA against ATP6V0e:

5’-GACCGCAAUUGAAAAAUGAtt-3’

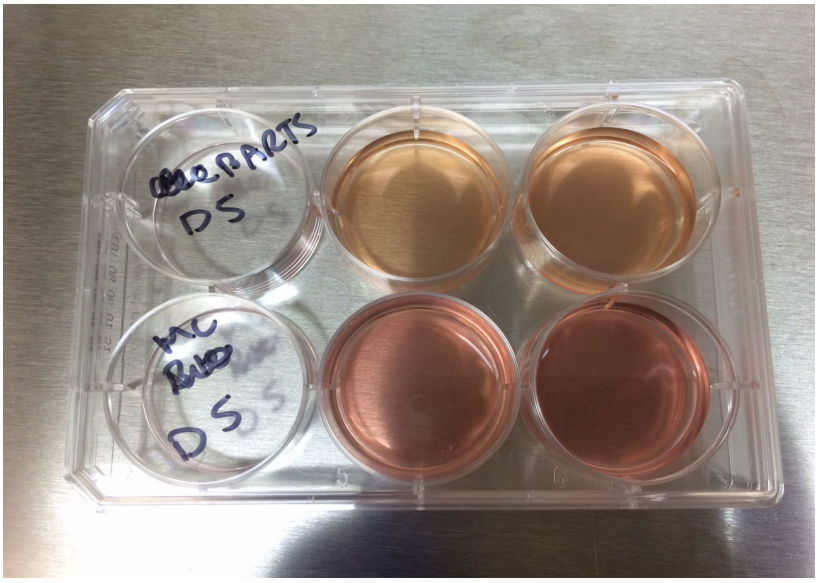

FIGURE 5.5. Picture of transfected cells. Photograph of transfected cells on day 7, showing faster proliferation in BART transfected cells (upper row) as indicated by the pH color indicator (phenol red) that is part of the media the cells are grown in. More orange color indicates lower pH, as a result of more cells in the media (more metabolites).

Chapter 6. Bibliography

Adamson, A.L., N. Wright, and D.R. LaJeunesse, Modeling early Epstein-Barr virus infection in Drosophila melanogaster: the BZLF1 protein. Genetics, 2005. 171(3): p. 1125-35.

Amoroso R, Fitzsimmons L, Thomas WA, Kelly GL, Rowe M, Bell AI. Quantitative studies of Epstein-Barr virus-encoded microRNAs provide novel insights into their regulation. J Virol. 2011;85(2):996-1010.

Andersson-anvret M, Forsby N, Klein G, Henle W. Relationship between the Epstein-Barr virus and undifferentiated nasopharyngeal carcinoma: correlated nucleic acid hybridization and histopathological examination. Int J Cancer. 1977;20(4):486-94.

Aravin AA, Lagos-quintana M, Yalcin A, et al. The small RNA profile during Drosophila melanogaster development. Dev Cell. 2003;5(2):337-50.

Arroyo, J.D., Chevillet, J.R., Kroh, E.M., Ruf, I.K., Pritchard, C.C., Gibson, D.F., et al. (2011). Argonaute2 complexes carry a population of circulating microRNAs independent of vesicles in human plasma. Proc Natl Acad Sci U S A 108, 5003–5008.

Asaga, S., Kuo, C., Nguyen, T., Terpenning, M., Giuliano, A.E., and Hoon, D.S. (2011). Direct serum assay for microRNA-21 concentrations in early and advanced breast cancer. Clin Chem 57, 84–91.

Babcock GJ, Decker LL, Volk M, Thorley-lawson DA. EBV persistence in memory B cells in vivo. Immunity. 1998;9(3):395-404.

Bahrami A, Aledavoud SA, Anvari K, et al. The Prognostic and Therapeutic Application of microRNAs in Breast Cancer: Tissue and Circulating microRNAs. J Cell Physiol. 2017;

Banerjee S, Lu J, Cai Q, Sun Z, Jha HC, Robertson ES. EBNA3C augments Pim-1 mediated phosphorylation and degradation of p21 to promote B-cell proliferation. PLoS Pathog. 2014;10(8):e1004304.

Bryant, R.J., Pawlowski, T., Catto, J.W., Marsden, G., Vessella, R.L., Rhees, B., et al. (2012). Changes in circulating microRNA levels associated with prostate cancer. Br J Cancer 106, 768– 774.

Cahir-McFarland ED, Carter K, Rosenwald A, Giltnane JM, Henrickson SE, Staudt LM, Kieff E. 2004. Role of NF-kappa B in cell survival and transcription of latent membrane protein 1-expressing or Epstein-Barr virus latency III-infected cells. J Virol 78:4108-4119

Cai L, Li J, Zhang X, et al. Gold nano-particles (AuNPs) carrying anti-EBV-miR-BART7-3p inhibit growth of EBV-positive nasopharyngeal carcinoma. Oncotarget. 2015;

Capello D, Cerri M, Muti G, et al. Analysis of immunoglobulin heavy and light chain variable genes in post-transplant lymphoproliferative disorders. Hematol Oncol. 2006;24(4):212-9.

Cesarman E. 2011. Gammaherpesvirus and lymphoproliferative disorders in immunocompromised patients.Cancer Letters. 305: 163-174.

Chan, M., Liaw, C.S., Ji, S.M., Tan, H.H., Wong, C.Y., Thike, A.A., et al. (2013). Identification of circulating microRNA signatures for breast cancer detection. Clin Cancer Res 19, 4477–4487.

Chen J, Jardetzky TS, Longnecker R. The Cytoplasmic Tail Domain of Epstein-Barr Virus gH Regulates Membrane Fusion Activity through Altering gH Binding to gp42 and Epithelial Cell Attachment. MBio. 2016;7(6)

Chen S, Wang Z, Dai X, et al. Re-expression of microRNA-150 induces EBV-positive Burkitt lymphoma differentiation by modulating c-Myb in vitro. Cancer Sci. 2013;104(7):826-34.

Chen, W., Cai, F., Zhang, B., Barekati, Z., and Zhong, X.Y. (2013). The level of circulating miRNA-10b and miRNA-373 in detecting lymph node metastasis of breast cancer: potential biomarkers. Tumour Biol 34, 455–462.

Cui, E.H., Li, H.J., Hua, F., Wang, B., Mao, W., Feng, X.R., et al. (2013). Serum microRNA 125b as a diagnostic or prognostic biomarker for advanced NSCLC patients receiving cisplatinbased chemotherapy. Acta Pharmacol Sin 34, 309–313

Cuk, K., Zucknick, M., Heil, J., Madhavan, D., Schott, S., Turchinovich, A., et al. (2013). Circulating microRNAs in plasma as early detection markers for breast cancer. Int J Cancer 132, 1602–1612.

De leo A, Colavita F, Ciccosanti F, Fimia GM, Lieberman PM, Mattia E. Inhibition of autophagy in EBV-positive Burkitt's lymphoma cells enhances EBV lytic genes expression and replication. Cell Death Dis. 2015;6:e1876.

Deiuliis JA, Syed R, Duggineni D, et al. Visceral Adipose MicroRNA 223 Is

Upregulated in Human and Murine Obesity and Modulates the Inflammatory Phenotype of Macrophages. PLoS ONE. 2016;11(11):e0165962.

Donati D, Espmark E, Kironde F, et al. Clearance of circulating Epstein-Barr virus DNA in children with acute malaria after antimalaria treatment. J Infect Dis. 2006;193(7):971-7.

E X, Hwang S, Oh S, et al. Viral Bcl-2-mediated evasion of autophagy aids chronic infection of gammaherpesvirus 68. PLoS Pathog. 2009;5(10):e1000609.

Epstein MA, Achong BG, Barr YM. Virus particles in cultured lymphoblasts from Burkitt's lymphoma. Lancet. 1964;1(7335):702-3.

Espert L, Denizot M, Grimaldi M, et al. Autophagy is involved in T cell death after binding of HIV-1 envelope proteins to CXCR4. J Clin Invest. 2006;116(8):2161-72.

Feng, S., G. Zhu, M. McConnell, L. Deng, Q. Zhao, M. Wu, Q. Zhou, J. Wang, J. Qi, Y. P. Li and W. Chen (2013). "Silencing of atp6v1c1 prevents breast cancer growth and bone metastasis." Int J Biol Sci 9(8): 853-862.

Fernandes Q. MicroRNA: Defining a new niche in Leukemia. Blood Rev. 2016;

Fingeroth JD, Weis JJ, Tedder TF, Strominger JL, Biro PA, Fearon DT. Epstein-Barr virus receptor of human B lymphocytes is the C3d receptor CR2. Proc Natl Acad Sci USA. 1984;81(14):4510-4.

Fish K, Chen J, Longnecker R. Epstein-Barr virus latent membrane protein 2A enhances MYC-driven cell cycle progression in a mouse model of B lymphoma. Blood. 2014;123(4):530-40.

Flügel D, Görlach A, Kietzmann T. GSK-3β regulates cell growth, migration, and angiogenesis via Fbw7 and USP28-dependent degradation of HIF-1α. Blood. 2012;119(5):1292-301.

Forgac M. Vacuolar ATPases: rotary proton pumps in physiology and pathophysiology. Nat Rev Mol Cell Biol. 2007;8(11):917-29.

Franchina, T., Amodeo, V., Bronte, G., Savio, G., Ricciardi, G.R., Picciotto, M., et al. (2014). Circulating miR-22, miR-24 and miR-34a as novel predictive biomarkers to pemetrexed based chemotherapy in advanced non-small cell lung cancer. J Cell Physiol 229, 97–99.

Gartel AL, Radhakrishnan SK. Lost in transcription: p21 repression, mechanisms, and consequences. Cancer Res. 2005;65(10):3980-5.

Gires O, Zimber-Strobl U, Gonnella R, Ueffing M, Marschall G, Zeidler R, Pich D, Hammerschmidt W. 1997.Latent membrane protein 1 of Epstein–Barr virus mimics a constitutively active receptor molecule. The EMBO Journal. 16(20): 6131–6140.

Given D, Yee D, Griem K, Kieff E. DNA of Epstein-Barr virus. V. Direct repeats of the ends of Epstein-Barr virus DNA. J Virol. 1979;30(3):852-62.

Granato M, Santarelli R, Farina A, et al. Epstein-barr virus blocks the autophagic flux and appropriates the autophagic machinery to enhance viral replication. J Virol. 2014;88(21):12715-26.

Gruhne B, Sompallae R, Marescotti D, et al. The Epstein–Barr virus nuclear antigen-1 promotes genomic instability via induction of reactive oxygen species. Proc Natl Acad Sci USA 2009;106:2313–2318.

Gupta-rossi N, Le bail O, Gonen H, et al. Functional interaction between SEL-10, an F-box protein, and the nuclear form of activated Notch1 receptor. J Biol Chem. 2001;276(37):34371-8.

Hammond SM, Bernstein E, Beach D, Hannon GJ. An RNA-directed nuclease mediates post-transcriptional gene silencing in Drosophila cells. Nature. 2000;404(6775):293-6.

Hao B, Oehlmann S, Sowa ME, Harper JW, Pavletich NP. Structure of a Fbw7-Skp1-cyclin E complex: multisite-phosphorylated substrate recognition by SCF ubiquitin ligases. Mol Cell. 2007;26(1):131-43.

Henson E, Chen Y, Gibson S. EGFR Family Members' Regulation of Autophagy Is at a Crossroads of Cell Survival and Death in Cancer. Cancers (Basel). 2017;9(4)

Horenkamp FA, Kauffman KJ, Kohler LJ, et al. The Legionella Anti-autophagy Effector RavZ Targets the Autophagosome via PI3P- and Curvature-Sensing Motifs. Dev Cell. 2015;34(5):569-76.

Houbaviy HB, Murray MF, Sharp PA. Embryonic stem cell-specific MicroRNAs. Dev Cell. 2003;5(2):351-8.

Hsu CY, Yi YH, Chang KP, Chang YS, Chen SJ, Chen HC. The Epstein-Barr virus-encoded microRNA MiR-BART9 promotes tumor metastasis by targeting E-cadherin in nasopharyngeal carcinoma. PLoS Pathog. 2014;10(2):e1003974.

Huang WT, Lin CW. EBV-encoded miR-BART20-5p and miR-BART8 inhibit the IFN-γ-STAT1 pathway associated with disease progression in nasal NK-cell lymphoma. Am J Pathol. 2014;184(4):1185-97.

Joseph, A. M., Babcock, G. J., & Thorley-Lawson, D. A. Cells Expressing the

Epstein-Barr Virus Growth Program Are Present in and Restricted to the Naive B-Cell Subset of Healthy Tonsils. Journal of Virology. 2000; 74(21), 9964–9971.

Kallifatidis G, Hoepfner D, Jaeg T, Guzmán EA, Wright AE. The marine natural product manzamine A targets vacuolar ATPases and inhibits autophagy in pancreatic cancer cells. Mar Drugs. 2013;11(9):3500-12.

Kieff E, Rickinson AB. 2007. Epstein-Barr virus and Its Replication, p 1225–2654. In Knipe DM, Howley PM, Griffin DE, Lamb RA, Martin MA, Roizman B, Straus SE (ed), Fields virology, 5th ed. Lippincott Williams & Wilkins, Philadelphia, PA.

Kilger E, Kieser A, Baumann M, et al. Epstein–Barr virus mediated B-cell proliferation is dependent upon latent membrane protein 1, which simulates an activated CD40 receptor. EMBO J 1998;17:1700–1709.

Kjersem, J.B., Ikdahl, T., Lingjaerde, O.C., Guren, T., Tveit, K.M., and Kure, E.H. (2014). Plasma microRNAs predicting clinical outcome in metastatic colorectal cancer patients receiving firstline oxaliplatin-based treatment. Mol Oncol 8, 59–67.

Kubisch R, Fröhlich T, Arnold GJ, et al. V-ATPase inhibition by archazolid leads to lysosomal dysfunction resulting in impaired cathepsin B activation in vivo. Int J Cancer. 2014;134(10):2478-88.

Lagos-quintana M, Rauhut R, Meyer J, Borkhardt A, Tuschl T. New microRNAs from mouse and human. RNA. 2003;9(2):175-9.

Lagos-quintana M, Rauhut R, Yalcin A, Meyer J, Lendeckel W, Tuschl T. Identification of tissue-specific microRNAs from mouse. Curr Biol. 2002;12(9):735-9.

Lawrie, C.H., Gal, S., Dunlop, H.M., Pushkaran, B., Liggins, A.P., Pulford, K., et al. (2008). Detection of elevated levels of tumour-associated microRNAs in serum of patients with diffuse large B-cell lymphoma. Br J Haematol 141, 672–675

Lee JS, Li Q, Lee JY, et al. FLIP-mediated autophagy regulation in cell death control. Nat Cell Biol. 2009;11(11):1355-62.

Lee Y, Ahn C, Han J, et al. The nuclear RNase III Drosha initiates microRNA processing. Nature. 2003;425(6956):415-9.

Leib DA, Alexander DE, Cox D, Yin J, Ferguson TA. Interaction of ICP34.5 with Beclin 1 Modulates Herpes Simplex Virus Type 1 Pathogenesis through Control of CD4+ T-Cell Responses . Journal of Virology. 2009;83(23):12164-12171. doi:10.1128/JVI.01676-09.

Lemon, S.M., et al., Replication of EBV in epithelial cells during infectious

Lemon, S.M., et al., Replication of EBV in epithelial cells during infectious mononucleosis. Nature, 1977. 268(5617):268-70.

Lemon, S.M., et al., Replication of Epstein-Barr virus DNA in epithelial cells in vivo. IARC scientific publications, 1978(24 Pt 2):739-44.

Leoncini L, Raphael M, Stein H, Harris NL, Jaffe E, Kluin PM (eds). Burkitt Lymphoma. IARC: Lyon, France, 2008.

Li Q, Spriggs MK, Kovats S, et al. Epstein-Barr virus uses HLA class II as a cofactor for infection of B lymphocytes. J Virol. 1997;71(6):4657-62.

Li Y, Long X, Huang L, et al. Epstein-Barr Virus BZLF1-Mediated Downregulation of Proinflammatory Factors Is Essential for Optimal Lytic Viral Replication. J Virol. 2015;90(2):887-903.

Liang Q, Chang B, Brulois KF, et al. Kaposi's sarcoma-associated herpesvirus K7 modulates Rubicon-mediated inhibition of autophagosome maturation. J Virol. 2013;87(22):12499-503.

Liang Q, Chang B, Lee P, et al. Identification of the Essential Role of Viral Bcl-2 for Kaposi's Sarcoma-Associated Herpesvirus Lytic Replication. J Virol. 2015;89(10):5308-17.

Liang XH, Kleeman LK, Jiang HH, et al. Protection against fatal Sindbis virus encephalitis by beclin, a novel Bcl-2-interacting protein. J Virol. 1998;72(11):8586-96.

Lund E, Güttinger S, Calado A, Dahlberg JE, Kutay U. Nuclear export of microRNA precursors. Science. 2004;303(5654):95-8.

Luzuriaga K, Sullivan JL. Infectious mononucleosis. N Engl J Med. 2010;362(21):1993-2000.

Maiuri MC, Le toumelin G, Criollo A, et al. Functional and physical interaction between Bcl-X(L) and a BH3-like domain in Beclin-1. EMBO J. 2007;26(10):2527-39.

Mancao C, Hammerschmidt W. 2007. Epstein-Barr virus latent membrane protein 2A is a B cell receptor mimic and essential for B cell survival. Blood 110:3715-3721.

Mao JH, Kim IJ, Wu D, et al. FBXW7 targets mTOR for degradation and cooperates with PTEN in tumor suppression. Science. 2008;321(5895):1499-502.

Mathew R, Kongara S, Beaudoin B, et al. Autophagy suppresses tumor progression by limiting chromosomal instability. Genes Dev. 2007;21(11):1367-81.

Mauvezin C, Nagy P, Juhász G, Neufeld TP. Autophagosome-lysosome fusion is independent of V-ATPase-mediated acidification. Nat Commun. 2015;6:7007.

Mauvezin C, Neufeld TP. Bafilomycin A1 disrupts autophagic flux by inhibiting both V-ATPase-dependent acidification and Ca-P60A/SERCA-dependent autophagosome-lysosome fusion. Autophagy. 2015;11(8):1437-8.

Ménard F, Besson C, Rincé P, et al. Hodgkin lymphoma-associated hemophagocytic syndrome: a disorder strongly correlated with Epstein-Barr virus. Clin Infect Dis. 2008;47(4):531-4.

Meo-evoli N, Almacellas E, Massucci FA, et al. V-ATPase: a master effector of E2F1-mediated lysosomal trafficking, mTORC1 activation and autophagy. Oncotarget. 2015;6(29):28057-70.

Mitchell, P.S., Parkin, R.K., Kroh, E.M., Fritz, B.R., Wyman, S.K., Pogosova-Agadjanyan, E.L., et al. (2008). Circulating microRNAs as stable blood-based markers for cancer detection. Proc Natl Acad Sci U S A 105, 10513–10518.

Miyashita EM, Yang B, Babcock GJ, Thorley-Lawson DA. J Virol. 1997 Jul; 71(7):4882-91.

Mizushima N, Yoshimori T. How to interpret LC3 immunoblotting. Autophagy. 2007;3(6):542-5.

Molina-Privado I, Rodriguez-Martinez M, Rebollo P, Martin-Perez D, Artiga MJ, Menarguez J, Flemington EK, Piris MA, Campanero MR. E2F1 expression is deregulated and plays an oncogenic role in sporadic Burkitt's lymphoma. Cancer research. 2009; 69:4052–4058.

Moormann AM, Heller KN, Chelimo K, et al. Children with endemic Burkitt lymphoma are deficient in EBNA1-specific IFN-gamma T cell responses. Int J Cancer. 2009;124(7):1721-6.

Moridikia A, Mirzaei H, Sahebkar A, Salimian J. MicroRNAs: Potential Candidates for Diagnosis and Treatment of Colorectal Cancer. J Cell Physiol. 2017.

Morselli E, Tasdemir E, Maiuri MC, et al. Mutant p53 protein localized in the cytoplasm inhibits autophagy. Cell Cycle. 2008;7(19):3056-61.

Mosialos G, Birkenbacht M, Yalamanchill R, et al. The Epstein-Barr virus transforming protein LMP1 engages signaling proteins for the tumor necrosis factor

receptor family. Cell 1995;80:389–399.

Mourelatos Z, Dostie J, Paushkin S, et al. miRNPs: a novel class of ribonucleoproteins containing numerous microRNAs. Genes Dev. 2002;16(6):720-8.

Münz C. Enhancing immunity through autophagy. Annu Rev Immunol. 2009;27:423-49.

Nakahira K, Choi AM. Autophagy: a potential therapeutic target in lung diseases. Am J Physiol Lung Cell Mol Physiol. 2013;305(2):L93-107.

Nateri AS, Riera-sans L, Da costa C, Behrens A. The ubiquitin ligase SCFFbw7 antagonizes apoptotic JNK signaling. Science. 2004;303(5662):1374-8.

Neri A, Barriga F, Inghirami G, et al. Epstein-Barr virus infection precedes clonal expansion in Burkitt's and acquired immunodeficiency syndrome-associated lymphoma. Blood. 1991;77(5):1092-5.

Ng, E.K., Chong, W.W., Jin, H., Lam, E.K., Shin, V.Y., Yu, J., et al. (2009). Differential expression of microRNAs in plasma of patients with colorectal cancer: a potential marker for colorectal cancer screening. Gut 58, 1375–1381

Nowag H, Guhl B, Thriene K, et al. Macroautophagy Proteins Assist Epstein Barr Virus Production and Get Incorporated Into the Virus Particles. EBioMedicine. 2014;1(2-3):116-25.

Oberg C, Li J, Pauley A, Wolf E, Gurney M, Lendahl U. The Notch intracellular domain is ubiquitinated and negatively regulated by the mammalian Sel-10 homolog. J Biol Chem. 2001;276(38):35847-53.

Ogembo JG, Kannan L, Ghiran I, et al. Human complement receptor type 1/CD35 is an Epstein-Barr Virus receptor. Cell Rep. 2013;3(2):371-85.

Ok CY, Li L, Young KH. EBV-driven B-cell lymphoproliferative disorders: from biology, classification and differential diagnosis to clinical management. Exp Mol Med. 2015;47:e132.

Paludan C, Schmid D, Landthaler M, et al. Endogenous MHC class II processing of a viral nuclear antigen after autophagy. Science. 2005;307(5709):593-6.

Pattingre S, Tassa A, Qu X, et al. Bcl-2 antiapoptotic proteins inhibit Beclin 1-dependent autophagy. Cell. 2005;122(6):927-39.

Paulson EJ, Speck SH. Differential methylation of Epstein-Barr virus latency promoters facilitates viral persistence in healthy seropositive individuals. J Virol.

1999;73(12):9959-68.

Price AM, Luftig MA. Dynamic Epstein-Barr virus gene expression on the path to B-cell transformation. Adv Virus Res. 2014;88:279-313.

Qiu, J. Epstein-Barr Virus microRNA Expression and Function in Persistent Infection and Oncogenesis, Doctor of Philosophy, 2014, Tufts University Sackler School of Graduate Biomedical Sciences, Boston, Massachusetts.

Qiu J, Cosmopoulos K, Pegtel M, et al. A novel persistence associated EBV miRNA expression profile is disrupted in neoplasia. PLoS Pathog. 2011;7(8):e1002193.

Qiu J, Thorley-lawson DA. EBV microRNA BART 18-5p targets MAP3K2 to facilitate persistence in vivo by inhibiting viral replication in B cells. Proc Natl Acad Sci USA. 2014;111(30):11157-62.

Ren H, Koo J, Guan B, et al. The E3 ubiquitin ligases β-TrCP and FBXW7 cooperatively mediates GSK3-dependent Mcl-1 degradation induced by the Akt inhibitor API-1, resulting in apoptosis. Mol Cancer. 2013;12:146.

Rich KA, Burkett C, Webster P. Cytoplasmic bacteria can be targets for autophagy. Cell Microbiol. 2003;5(7):455-68.

Rickinson A B, Kieff E. Epstein-Barr virus. In: Fields B N, Knipe D M, Howley P M, editors. Fields virology. 3rd ed. Vol. 2. New York, N.Y: Raven Press; 1996. pp. 2397–2446.

Rickinson AB, Kieff E. 2007. Epsetin-Barr virus, p 2655–2700. In Knipe DM, Howley PM, Griffin DE, Lamb RA, Martin MA, Roizman B, Straus SE (ed), Fields virology, 5th ed. Lippincott Williams & Wilkins, Philadelphia, PA.

Saridakis V, Sheng Y, Sarkari F, et al. Structure of the p53 binding domain of HAUSP/USP7 bound to Epstein-Barr nuclear antigen 1 implications for EBV-mediated immortalization. Mol Cell. 2005;18(1):25-36.

Sennoune SR, Bakunts K, Martínez GM, et al. Vacuolar H+-ATPase in human breast cancer cells with distinct metastatic potential: distribution and functional activity. Am J Physiol, Cell Physiol. 2004;286(6):C1443-52.

Severa M, Giacomini E, Gafa V, et al. EBV stimulates TLR- and autophagy-dependent pathways and impairs maturation in plasmacytoid dendritic cells: implications for viral immune escape. Eur J Immunol. 2013;43(1):147-58.

Shimizu N, Takada K. Analysis of the BZLF1 promoter of Epstein-Barr virus: identification of an anti-immunoglobulin response sequence. Journal of Virology.

1993;67(6):3240-3245.

Sinha S, Colbert CL, Becker N, Wei Y, Levine B. Molecular basis of the regulation of Beclin 1-dependent autophagy by the gamma-herpesvirus 68 Bcl-2 homolog M11. Autophagy. 2008;4(8):989-97.

Sixbey, J.W., et al., Epstein-Barr virus replication in oropharyngeal epithelial cells. The New England journal of medicine, 1984. 310(19):1225-30.

Skalsky RL, Cullen BR. EBV Noncoding RNAs. Curr Top Microbiol Immunol. 2015;391:181-217.

Soni V, Cahir-McFarland E, Kieff E. LMP1 TRAFficking activates growth and survival pathways. Adv Exp Med Biol. 2007; 597():173-87.

Sourvinou, I.S., Markou, A., and Lianidou, E.S. (2013). Quantification of circulating miRNAs in plasma: effect of preanalytical and analytical parameters on their isolation and stability. J Mol Diagn 15, 827–834.

Spruck CH, Strohmaier H, Sangfelt O, et al. hCDC4 gene mutations in endometrial cancer. Cancer Res. 2002;62(16):4535-9.

Sun CC, Thorley-Lawson DA. Plasma cell-specific transcription factor XBP-1s binds to and transactivates the Epstein-Barr virus BZLF1 promoter. J Virol. 2007 Dec; 81(24):13566-77.

Sun XF, Sun JP, Hou HT, Li K, Liu X, Ge QX. MicroRNA-27b exerts an oncogenic function by targeting Fbxw7 in human hepatocellular carcinoma. Tumour Biol. 2016;37(11):15325-15332.

Sundqvist A, Bengoechea-alonso MT, Ye X, et al. Control of lipid metabolism by phosphorylation-dependent degradation of the SREBP family of transcription factors by SCF(Fbw7). Cell Metab. 2005;1(6):379-91.

Tang B, Lei B, Qi G, et al. MicroRNA-155-3p promotes hepatocellular carcinoma formation by suppressing FBXW7 expression. J Exp Clin Cancer Res. 2016;35(1):93

Uchida J, Yasui T, Takaoka-Shichijo Y, Muraoka M, Kulwichit W, Raab-Traub N, Kikutani H. 1999. Mimicry of CD40 signals by Epstein-Barr virus LMP1 in B lymphocyte responses. Science 286:300-303

Vousden KH, Lu X. Live or let die: the cell's response to p53. Nat Rev Cancer. 2002;2(8):594-604.

Walker DH, Popov VL, Crocquet-valdes PA, Welsh CJ, Feng HM. Cytokine-

induced, nitric oxide-dependent, intracellular antirickettsial activity of mouse endothelial cells. Lab Invest. 1997;76(1):129-38.

Wang GH, Garvey TL, Cohen JI. The murine gammaherpesvirus-68 M11 protein inhibits Fas- and TNF-induced apoptosis. J Gen Virol. 1999;80 (Pt 10):2737-40.

Wang, S., Xiang, J., Li, Z., Lu, S., Hu, J., Gao, X., et al. (2015). A plasma microRNA panel for early detection of colorectal cancer. Int J Cancer 136, 152–161.

Welcker M, Clurman BE. FBW7 ubiquitin ligase: a tumour suppressor at the crossroads of cell division, growth and differentiation. Nat Rev Cancer. 2008;8(2):83-93.

Welcker M, Orian A, Jin J, et al. The Fbw7 tumor suppressor regulates glycogen synthase kinase 3 phosphorylation-dependent c-Myc protein degradation. Proc Natl Acad Sci USA. 2004;101(24):9085-90.

Wong AM, Kong KL, Tsang JW, Kwong DL, Guan XY. Profiling of Epstein-Barr virus-encoded microRNAs in nasopharyngeal carcinoma reveals potential biomarkers and oncomirs. Cancer. 2012;118(3):698-710.

Wong AM, Kong KL, Tsang JW, Kwong DL, Guan XY. Profiling of Epstein-Barr virus-encoded microRNAs in nasopharyngeal carcinoma reveals potential biomarkers and oncomirs. Cancer. 2012;118(3):698-710.

Wu G, Lyapina S, Das I, et al. SEL-10 is an inhibitor of notch signaling that targets notch for ubiquitin-mediated protein degradation. Mol Cell Biol. 2001;21(21):7403-15.

Xia W, Zhou J, Luo H, et al. MicroRNA-32 promotes cell proliferation, migration and suppresses apoptosis in breast cancer cells by targeting FBXW7. Cancer Cell Int. 2017;17:14.

Xiao L, Hu ZY, Dong X, et al. Targeting Epstein-Barr virus oncoprotein LMP1-mediated glycolysis sensitizes nasopharyngeal carcinoma to radiation therapy. Oncogene. 2014;33(37):4568-78.

Xie WY, Zhou XD, Li Q, Chen LX, Ran DH. Acid-induced autophagy protects human lung cancer cells from apoptosis by activating ER stress. Exp Cell Res. 2015;

Yada M, Hatakeyama S, Kamura T, et al. Phosphorylation-dependent degradation of c-Myc is mediated by the F-box protein Fbw7. EMBO J. 2004;23(10):2116-25.

Yang JY, Park MY, Park SY, et al. Nitric Oxide-Induced Autophagy in MC3T3-E1

Yang JY, Park MY, Park SY, et al. Nitric Oxide-Induced Autophagy in MC3T3-E1 Cells is Associated with Cytoprotection via AMPK Activation. Korean J Physiol Pharmacol. 2015;19(6):507-14.

Yi R, Qin Y, Macara IG, Cullen BR. Exportin-5 mediates the nuclear export of pre-microRNAs and short hairpin RNAs. Genes Dev. 2003;17(24):3011-6.

Yuxia, M., Zhennan, T., and Wei, Z. (2012). Circulating miR-125b is a novel biomarker for screening non-small-cell lung cancer and predicts poor prognosis. J Cancer Res Clin Oncol 138, 2045–2050.

Zambrano J, Yeh ES. Autophagy and Apoptotic Crosstalk: Mechanism of Therapeutic Resistance in HER2-Positive Breast Cancer. Breast Cancer (Auckl). 2016;10:13-23

Zhang Y, Peng Z, Zhao Y, Chen L. microRNA-25 Inhibits Cell Apoptosis of